New isotope search experiments at the FRS for FAIR phase-0

S. Pietri[1], A.M. Bruce[2], T. Grahn[3,4], W.R. Plass[1,5], C. Scheidenberger[1,5], T. Dickel[1,5], A. Kelić-Heil[1], H. Geissel[1,5], H. Weick[1], F. Ameil[1], L. Audouin[6], J. Aysto[3,4], S. Bagchi[1,5,7], M. Bai[1], J. Benlliure[8], G. Benzoni[9], C. Bruno[10], D. Cortina[8], T. Davisson[10], J. Gerl[1], M. Gorska[1], E. Haettner[1], O. Hall[10], L. Harkness-Brennan[11], A. Heinz[12], A. Helert[13], J.P. Hucka[1,14], A. Jokinen[3,4], A. Kankainen[4], D. Kahl[10], B. Kindler[1], I. Kojuharov[1], D. Kostyleva[1,5], N. Kuzminchuk[1], M. Labiche[15], C. Lederer-Woods[11], B. Lommel[1], G. Matinez-Pinedo[14], G. Münzenberg[1], I. Mukha[1], R. Page[12], M. Pfutzner[16], Zs. Podolyak[17], A. Prochazka[1], S. Purushotaman[1], C. Rappold[1,5], P. Regan[17], M.V. Ricciardi[1], S. Rinta-Antila[4], S. Saha[1], T. Saito[1,5,18], H. Schaffner[1], F. Schirru[1], J. Simpson[15], H. Simon[1], P. Spiller[1], J. Stadlmann[1], J. Taieb[19], Y. Tanaka[1], I. Tanihata[20,21], J. Vesic[1], B. Voss[1], P.M. Walker[17], P.J. Woods[10], J. Winfield[1], M. Winkler[1].

for the Super-FRS Experiment Collaboration, in collaboration with the DESPEC Collaboration

[1]GSI Helmholzzentrum für Schwerionenforschung GmbH, Darmstadt, Germany ;[2]University of Brighton, UK;[3]Helsinki institute of Physics, Finland;[4]University of Jyväskylä, Finland;[5]Justus-Liebig-Universität Gießen, Germany; [6]IPNO, Université de Paris-Saclay, CNRS/IN2P3, Orsay, France; [7]St Mary's University, Halifax, Canada;[8]Universidad de Santiago de Compostela, Spain;[9]INFN sezione di Milano, Italy;[10]University of Edinbourg, UK;[11]University of Liverpool, UK;[12]Chalmers University of Technology, Göteborg, Sweden;[13]FAIR Darmstadt, Germany ;[14]Technische Universität Darmstadt, Germany;[15]SFTC Daresbury Laboratory, UK;[16]University of Warsaw, Poland;[17]University of Surrey, UK;[18]Iwate University Morioka ;[19]CEA DAM Bruyères-le-Châtel;[20]Beihang University, Beijing, China;[21]Osaka University, Japan

The region "south" of ^{208}Pb nuclei along the N=126 line has been identified as a region of key interest for the NUSTAR Collaboration at GSI/FAIR; generally it is of high interest for nuclear structure studies and nuclear astrophysics applications. A proposal has been submitted and accepted to the GSI PAC to perform an exploratory study; it aims to extend the frontiers of known isotopes and to obtain nuclear structure data on gross properties. It is expected to simultaneously identify over 28 new isotopes. Using new detector equipment from different NUSTAR sub-collaborations jointly and using the same FRS settings that are used very successfully in the identification of new isotopes permits to obtain 26 news masses and 47 new lifetimes together with spectroscopic investigations on isomeric decay properties. Furthermore, the experiment will study the production of (new) isotopes "south" of the primary-beam isotones, i.e., measure their production cross sections and momentum distributions.

Today this region can best be studied at "FAIR phase-0" using fragmentation of the intense ^{208}Pb beam and in-flight separation of the neutron-rich projectile fragments. The crossing of the N=126 line "south" of ^{201}Re will be accomplished by the higher intensities of ^{238}U beam and the Super-FRS beams at "FAIR phase-1".

The current experiment is, moreover, presented as a benchmark of the NUSTAR "FAIR phase-0" facility proving the worldwide competitiveness of the current facility in this mass region, it will help planning further other NUSTAR "FAIR phase-0" experiments and serve for testing of new NUSTAR devices (AIDA, Cryogenic Stopping Cell….) and data acquisition together.

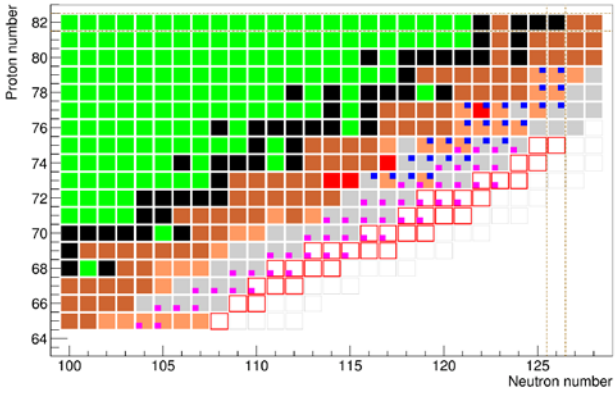

Figure 1: The region of interest in the chart of nuclei for the coming experiment. Black: stable nuclei; green: neutron deficient nuclei; dark brown: isotopes with known half-lives and masses; salmon: nuclei with known half-lives; red: nuclei with known mass; grey: already discovered isotopes; red borders: new isotopes from this proposal; pink square: proposed halve-lives measurements; blue squares: proposed masses measurements.

This will be achieved by extraction of a 1000 A·MeV ^{208}Pb^{67+} primary beam from the SIS-18 and focusing it on the production target at the entrance of the FRS. A target of 2.5 g/cm^2 Be with a 223 mg/cm^2 Nb backing will be used to produce the isotopes of interest via projectile fragmentation. The thickness of the target was estimated as an optimum between the number of produced isotopes (which would call for a thicker target) and transmission through the separator (which suffers when target thickness and momentum spread are too large). The high beam energy, together with the Nb backing, assures that more than 90% of the ions emerging from the target will be

fully stripped, which is important for high transmission and unambiguous identification by the Bρ-ΔE-ToF method. In order to optimize the efficient use of the beam time overall, only one target will be used for all settings.

The FRS is equipped with its standard instrumentation for beam tracking, separation and particle identification. Some of the MUSIC or TPC detectors will be replaced by their upgraded versions planned for the Super-FRS when available.

The 1000 A·MeV primary beam assures that all fragments penetrate the MUSIC detectors at the final focus of the FRS with at least 600 A·MeV. At this energy for the worst case (Re) a 13% chance exists to pick up an electron inside the active volume of the MUSIC detector. Using two MUSICs and a stripper foil in between means incorrectly identified elements are in the 1.6% range. As mentioned earlier the higher energy primary beam assures a more forward focus of the fragments thus a higher transmission. Aluminum degraders at the first focal plane and in the middle focal plane will assure separation of the ions of interest and eliminate unwanted contaminants.

The mean energy loss in the degrader is independent of the ionic charge state of the emerging fragments. This information can help in addition to identify the element number and the few-electron ions.

New NUSTAR equipment, constructed for FAIR, and already available – at least as prototypes or "start versions" – for experiments in phase-0, will be used. In the FRS, new TPC- and MUSIC-detectors will be used for beam monitoring and particle identification. At the final focus (F4 area), the FRS Ion Catcher and detectors of the DESPEC collaboration (AIDA, FATIMA) will be used for the first time for experiments. It is the combined use of these novel instruments, which allows for these pioneering studies and the rich nuclear data harvest in short time. The overall experimental setup is shown in figure 2.

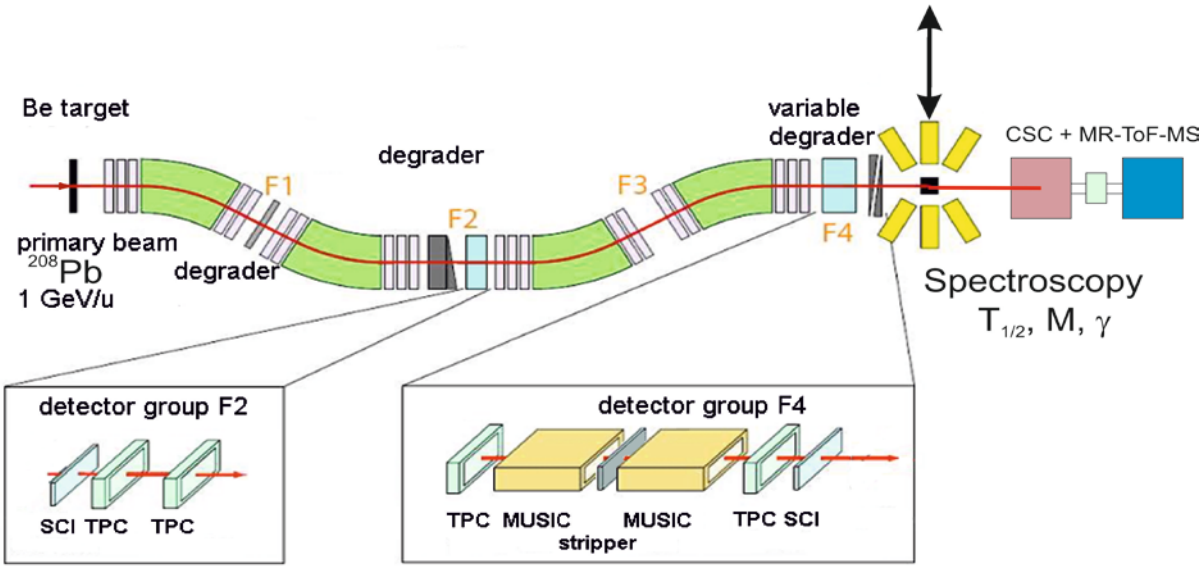

Figure 2: Schematic view of the two FRS final focal-plane setups planned for this experiment. The FRS detectors for particle identification in-flight are indicated. At the final focal plane F4 two experimental setups can be used alternatively (black arrow), a spectroscopy setup with LaBr3 gamma detectors viewing the silicon implantation detector and the cryogenic stopping cell (CSC) coupled to the multiple reflection time-of-flight mass spectrometer (MR-ToF-MS).

Outlook

The project presented here is part of the topic 1 of the Super-FRS Experiment Collaboration (SEC), which aims at similar experiment in phase 1 looking for new isotopes and studying their gross properties. In parallel to this the topic 1 of SEC together with performing nuclear reaction studies using the combination of the FRS Ion Catcher with standard DESPEC equipment to perform isomeric ratio measurements over a wide life time range[1].

Experiment beamline: FRS
Experiment collaboration: NUSTAR-SuperFRS-Experiments/ NUSTAR-DESPEC-HISPEC
Experiment proposal: S468
Accelerator infrastructure: UNILAC / SIS18 / FRS /
Strategic university co-operation with: Giessen, Darmstadt

References

[1] Ubbi Sauerwine, summer student report 2015

 DOI:10.15120/GR-2018-1

Development of new ion-optical modes for NUSTAR FAIR Phase-0 experiments at the FRS

E. Haettner[1], T. Dickel[1,2], K. Dort[2], H.Geissel[1,2], N. Iwasa[3], W. R. Plaß[1,2], C. Scheidenberger[1,2], Y. Tanaka[1], S. Terashima[4], H. Weick[1], J. S. Winfield[1], M. Winkler[1], M. Yavor[5], and the Super-FRS Experiment collaboration

[1]GSI, Darmstadt, Germany; [2]University of Giessen, Giessen, Germany; [3]Tohoku University, Sendai, Japan; [4]Beihang University, Beijing, China; [5]Institute of Analytical Instrumentation, Russian Academy of Science, St Petersburg, Russia

The in-flight separator and spectrometer for short-lived exotic nuclei Fragment Separator FRS [1,2] is a central instrument in the NUSTAR collaboration. The FRS consists of four stages with various diagnostic equipment and shaped matter in between. This makes the FRS flexible; transmission, resolution, separation, focal plane conditions, achromatism are example of properties that have to be optimized for each category of experiments.

Experiments and tests with the FRS Ion Catcher [3] have so far used an ion-optical mode [4] with a monoenergetic degrader [1,5,6] installed at the mid-focal plane. In principle, this particular experiment setup can, because of its own mass tagging capabilities [7] and separation by range selection, tolerate less identification and separation quality of the FRS. However, the resolving power also determines the energy bunching quality, thus it should not be reduced below approximately 800 (ε_x=13.5 π mm mrad, x_0=1.5 mm). Furthermore, the degrader itself, even without presence of possible inhomogenities, limits the achievable resolution to the order of 0.1%, due to unavoidable energy loss straggling. Figure 1 shows the optical transmission of the mode used so far in these experiments as well as of two modified optic settings with lower resolving power. The transmission (evaluated with a phase space filling an ellipsoid with parameters as indicated in the figure) can be improved by about a factor of 2-3. The development is of advantage for all NUSTAR experiments that do not need the ion optical resolution of the mode used so far, either because the nuclide of interest is still separated and identified, or the experiment provides its own identification and/or benefits from a cocktail beam.

Similarly, other experiments need optimization and development of ion-optical modes. An example is an experiment that investigates the influence of the tensor force as a part of the nuclear force [8]. In a pilot experiment the population of ground and excited states in the ^{16}O(p,d) reaction for various beam energies was measured. This only possible due to the development of an ion optical mode where the resolving powers of the four dispersive dipole magnet stages were added such that a momentum resolving power of 16,500 (x_0=0.5mm, realized by sharp focusing, $B\rho_{max}$=13.8 Tm) was achieved.

A third example is the atomic collision experiment [9], where precise heavy ion energy-loss measurements as well as charge-state distributions behind different targets will be measured. The atomic-collision target is placed at the dispersive mid-focal plane of the FRS. The charge-state distribution will be measured via position sensitive detectors at the subsequent focal plane and the energy-loss distribution at the final focal plane which is achromatic with respect to the entrance of the FRS. The optics has been adapted to the requirement of the mounted setups of other NUSTAR experiments and the need to minimize the matter thickness.

These described new ion-optical developments are essential for successful completion of the FAIR phase-0 experiments of the NUSTAR collaboration.

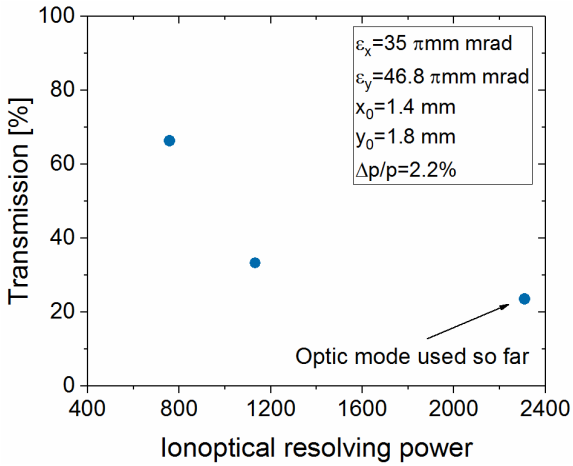

Figure 1: Simulated transmission as a function of resolving power (see text for details) of three different ion-optical modes.

References

[1] H. Geissel et al., Nucl. Inst. Meth. A 282 (1989) 247.
[2] H. Geissel et al., Nucl. Inst. Meth. B 70 (1992) 286.
[3] W. R. Plaß et al., Nucl. Inst. Meth. B 317 (2013) 457.
[4] H. Irnich, PhD Thesis, JLU Giessen (1995).
[5] H. Weick et al., Nucl. Inst. Meth. B 164-165 (2000) 168.
[6] Ch. Scheidenberger et al., Nucl. Inst. Meth. B 204 (2003) 119.
[7] C. Hornung et al., GSI Sci. Rep. 2016 (2017) p. 175.
[8] H. J. Ong et al., Phys. Lett. B 725 (2013) 277.
[9] S. Purushothaman et al., GSI Sci. Rep. 2017, this issue.

Experiment beamline FRS
Experiment collaboration: NUSTAR-SuperFRS-Experiments
Experiment proposal: S436, S469, S474
Accelerator infrastructure: UNILAC / SIS18
PSP codes: none
Grants: BMBF (05P16RGFN1), HMWK (LOEWE Center HICforFAIR)
Strategic university co-operation with: Gießen

New opportunities at the border of nuclear and hadron physics using WASA at FRS: a status report

K.-H. Behr[1], J. Benlliure[2], T. Blatz[1], H. Calen[3], M. Gleim[1], F. Goldenbaum[4], K. Itahashi[5], C. Rappold[1,6], J. Ritman[4], J.L. Rodrigues-Sanchez[1,2], T.R. Saito[1,7], V. Serdyuk[4], S. Schadmand[4], C. Scheidenberger[1,6], B. Szczepanczyk[1], Y. Tanaka[1,6], M. Wolke[3], for the WASA-at-FRS collaboration, the S447 collaboration, the S457 collaboration, the S463 collaboration, and the Super-FRS Experiment collaboration

[1]GSI, Darmstadt, Germany; [2]USC, Santiago de Compostela, Spain; [3]Uppsala Univ., Uppsala, Sweden; [4]Forschungszentrum Juelich, Juelich, Germmany; [5]RIKEN, Wako, Japan; [6]Giessen Univ, Giessen, Germany; [7]HIM, Mainz, Germany

Introduction

Study of the nature of hadrons inside sub-atomic nuclear systems has recently become more important in the fields of nuclear and hadron physics. In particular, with heavy ion- and proton-beams at GSI, several results on light Λ-hypernuclei, η'-nucleus and baryon resonances in nuclei have recently revealed. These experiments have revealed interesting phenomenon as discussed in the following sections in this report. However, the results have also shown that resolution and sensitivity of these experiment were not yet sufficient for the results to be conclusive. Therefore, we are introducing a new technique at GSI.

To improve resolution and sensitivity, we have proposed a novel technique for measuring light charged particles and photons from exotic nuclei at the mid-focal plane of the FRS, S2, in coincidence with decay residues detected by the second half of the FRS. As a target spectrometer at S2, the WASA central detector (WASA CD), currently at COSY in Juelich, will be implemented. With the setup of WASA CD at FRS, as shown in Figure 1, three experimental programs on hypernuclear spectroscopy, η'-nucleus and baryon resonances in nuclei have been proposed, as discussed below.

Figure 1: Layout of the FRS. The WASA CD will be mounted at the mid-focal plane S2.

The WASA central detector at FRS

The 4π detector WASA (Wide Angle Shower Apparatus) was designed for studies of production and decays of light mesons at CELSIUS in Uppsala, Sweden. Pions and η-mesons were produced in proton-proton and proton-deuteron interactions. In 2005, WASA was moved to the Cooler Synchrotron COSY at Juelich, Germany, where the forward detection and the data acquisition were upgraded. A detailed description of the WASA is found in [1].

The WASA central detector consists of an inner mini-drift chamber (MDC) of straw tubes, thin plastic scintillators in a cylinder geometry (PS), a super-conducting solenoid, and a CsI calorimeter. The general idea is to use WASA for measuring light particles from the decay of exotic nuclei produced in front of or inside the WASA CD with a large acceptance, while decay residues are measured by the second half of the FRS with an excellent momentum resolution. Figure 2 shows a side view of the WASA CD at S2 of FRS. The production target of nuclei of interest for experiments of hypernuclei and baryon resonances in nuclei will be in front of the WASA CD, while that for the η'-nucleus experiment will be mounted behind the MDC.

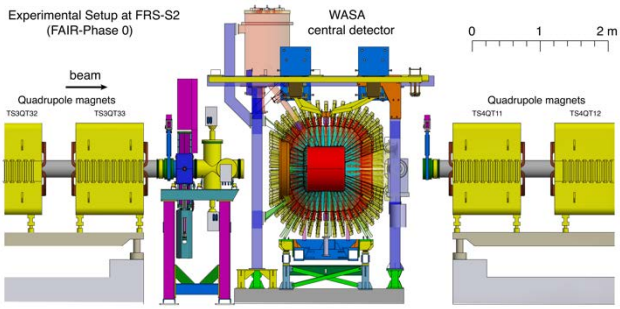

Figure 2: A side view of the WASA CD installed at S2 of FRS.

Physics case

Three projects are in preparation; S447 for hypernuclei, S457 for η'-mesic nucleus and S463 for baryon resonances in nuclei. These proposals were discussed in the G-PAC at GSI in 2017. Other new experiments are also under preparation.

Hypernuclei

Hypernuclei, subatomic nuclei with strange quark(s), have been studied in order to understand baryon interactions under the flavored-SU(3) symmetry. Conventional ways to produce hypernuclei are with the use of secondary meson- and primary electron beams, mainly with the missing mass spectroscopy or/and emulsion techniques. Ultra-relativistic heavy ion collisions at RHIC and LHC have also been employed to study light hypernuclei with mass values of A<4. Recently, the hypernuclear physics has entered a new era by the success of the HypHI Phase 0 experiment at GSI [2]. It has demonstrated feasibility of hypernuclear spectroscopy with heavy ion beams bombarding a fixed target by employing invariant mass tech-

 DOI:10.15120/GR-2018-1

nique. The HypHI Phase 0 experiment was performed with ^{6}Li beams at 2 A GeV and the graphite target, and it successfully produced and identified hypernuclei with A=3 and 4 [2].

One of the striking but also surprising results of HypHI Phase 0 is the observation of signals that may be related to the existence of an extremely exotic neutral hypernucleus, two neutrons together with a Λ-hyperon, (nnΛ), which has been observed in the d+π^- and t+π^- invariant mass distributions [3]. However, there are no theoretical calculations that can reproduce such a bound state [4,5,6,7]. Therefore, the existence of the nnΛ bound state is under debate and will be studied in forthcoming experiments.

Another striking result of the HypHI Phase 0 experiment is the observation of unexpected short lifetime of $^{3}_{\Lambda}$H, 183^{+42}_{-32} ps, for the first time, which is significantly shorter than that of the free Λ-hyperon (263.2 ps) [2]. This contradicts the current understanding of the structure of the lightest hypernucleus $^{3}_{\Lambda}$H, which is understood as Λ attached to a deuteron core with a binding energy of only 130 keV. With such a small binding energy, the lifetime of $^{3}_{\Lambda}$H has been expected to be similar to that of free Λ-hyperons. So far, none of the theoretical calculations can reproduce such short lifetime of $^{3}_{\Lambda}$H. Very recently, the STAR and ALICE collaborations also observed significantly shorter lifetime of $^{3}_{\Lambda}$H than Λ respectively to be 155^{+25}_{-22} ps [8] and 181^{+54}_{-39} ps [9].

Though the results of the HypHI Phase 0 experiment have revealed interesting and new mysterious observations, the achieved sensitivity and resolution of the hypernuclear spectroscopy with heavy-ion beams does not allow for detailed conclusions. Also, with the previous setup, further studies on unknown and exotic hypernuclei will not be feasible.

In contrast to the results of the HypHI experiment, with the proposed experiment with WASA at FRS, negative charged pions will be measured with a large angular and momentum coverage, therefore, observed signals will be well separated by a broad background distribution. The invariant mass resolution will be improved due to the excellent momentum resolution of FRS. Furthermore, the statistics will be largely increased due to the large acceptance of the WASA detector for measuring negative charged pions and the new possibility to simplify the trigger to the DAQ system because of reasonably small geometrical and momentum acceptance of FRS.

Additional detectors for measuring decay vertexes of hypernuclei and position and time information of decay residues will be installed in front of and behind the WASA CD. According to Monte Carlo simulations, the resolutions and statistics will be improved by factors of approximately 3 and 10, respectively. Therefore, the results of the proposed experiments will contribute further to solve the two puzzles discussed above. Furthermore, $^{4}_{\Lambda}$H will also be studied in the same experiment.

η'-mesic nuclear bound state

The possible existence of η'-mesic nuclei, i.e., bound states of an η' meson in nuclei, has recently attracted strong interests related to UA(1) quantum anomaly and partial restoration of chiral symmetry in QCD. The η' meson has an exceptionally large mass of 958 MeV/c^2, which is considered as a consequence of the anomaly effect under presence of spontaneous breaking of chiral symmetry [10]. In finite nuclear density, where chiral symmetry is partially restored, reduction of the η' mass is predicted [11, 12]. Such an in-medium mass reduction would induce an attractive potential between an η' meson and a nucleus, suggesting the possible existence of η'-mesic nuclei [13].

The first experiment to search for η'-mesic nuclei was performed with the FRS at GSI in 2014 by missing mass spectroscopy of the ^{12}C(p,d) reaction at an incident proton energy of 2.5 GeV [14, 15]. The proton beam extracted from SIS-18 impinged on a carbon target installed at the target area of the FRS. The momentum of the ejected deuterons at forward 0 degrees was analyzed by the FRS, operated as a high-resolution spectrometer.

High statistical sensitivity was achieved in the measured spectra to search for relatively narrow and small peak structures in the continuous background due to quasi-free meson production processes. However, no significant peak structure related to the formation of the η'-mesic states was observed, and thus upper limits on the formation cross section of the bound states as well as constraints on the η'-nucleus interaction were deduced [14, 15]. The experimental sensitivity was limited mainly by the continuous background, which had in total >100 times larger cross section than expected formation cross sections of the bound states.

For FAIR Phase 0, a semi-exclusive measurement of the ^{12}C(p,dp) reaction is planned to aim at increasing the experimental sensitivity [16]. In coincidence with the ejected deuteron from the (p,d) reaction, decay particles from η'-mesic nuclei are detected and identified for event selection. The continuous background dominating the spectra of the previous experiment can be suppressed by tagging the decay particles. Expected major decay modes of the η'-mesic nuclei are one- and two-nucleon absorption processes: η'N → η'N, η'N → π'N, and η'NN → NN [17]. In particular, the two-nucleon absorption process emits a proton (or neutron) with relatively high kinetic energy of about 500 MeV [18].

The experimental setup with the WASA-CD at FRS-S2 is an ideal configuration for the planned measurement. The carbon target will be installed at the downstream side of the WASA-CD to maximize the angular acceptance for the detection of the backward emitted proton. The ejectile deuteron will be measured with the S2-S4 section of the FRS, and the decay proton with the WASA-CD. By tagging high-energy protons in the backward angular range (θ lab > 90deg) by WASA-CD, we expect that the signal-to-background ratio will be improved by two orders of magnitude compared to the previous experiment [18].

S463: Baryon resonances in nuclei

Resonances are largely produced in relativistic heavy-ion collisions and could appear in the core of neutron stars at densities around 2 or 3 times the nuclear matter saturation density [19]. Nucleon resonances also play a

significant role in the understanding of three-body nuclear forces or the quenching of the Gamow-Teller strength [20]. For instance, the Δ-resonance is a ΔS =1; ΔI =1 spin- and isospin-flip intrinsic excitation of the nucleon. As such it is a partner of the corresponding ΔS=1; ΔI=1 excitation of the nuclear medium, known as the Gamow-Teller resonance.

Studies with the Super-FRS present unique possibilities to study the Delta(Δ)- and other baryon resonances in stable and in exotic nuclei by using isobaric charge-exchange reactions in relativistic heavy-ion collisions. Pilot experiments have already been performed with the FRS and reveal that the high resolution of the spectrometer makes it possible to identify in the missing energy spectra of the forward-emitted ejectiles the in-medium excitation of Delta and Roper resonances [21].

These measurements are expected to contribute to open up a new field linking subnucleonic and nucleonic degrees of freedom through the production of resonant nuclear matter. In particular, these experiments will help to constrain the in-medium NΔ and NR potentials above the 400 MeV range covered by electron-nucleus and pion-nucleus scattering experiments and to address the possible in-medium mass modification of nuclear resonances. These reactions may also provide an opportunity to study two Δ's in nuclei and provide a chance to study ΔΔ interactions and the recently observed d*(2380) resonance. Moreover, the use of relativistic nuclei far off stability will allow exploring the isospin degree of freedom enlarging in this way our present knowledge of the properties of isospin-rich nuclear systems. Particularly, one could also take advantage of the peripheral character of these reactions to probe the relative abundances of protons and neutrons at the nuclear periphery and constraint the density derivative of the symmetry energy.

The proposed experiments can be realized by using the FRS with its standard tracking detector systems measuring the momentum distribution of the isobaric projectile residues created via charge-exchange reactions. In addition, measuring the charged pions emitted in the decay of the nucleon resonances in coincidence with the WASA CD detector will allow to separate resonance excitations in the projectile and target nuclei remnants. The use of a liquid hydrogen target will also contribute to isolate the excitation of particular resonances.

Status of the project

Green light from the WASA-at-COSY collaboration to transport the WASA CD to GSI was given in August 2017. In November 2017, the Joint Scientific Council of GSI/FAIR approved the WASA-at-GSI project, stating the goodness of the physics cases. Three experimental proposals have been discussed with the G-PAC in 2017, and two of them, S447 and S457, have been approved. Allocated shifts will be 27 shifts for S447 and 18 shifts for S457, with 18 parasitic shifts for commissioning the detectors. Preparations are on-going to perform the two experiments in the second half of 2019.

Design work for the holding structure of the WASA CD at S2 of FRS is in progress and manufacturing will begin in 2018. The MDC together with electronics, slow control and gas controlling systems have been transported to GSI. Currently, we are preparing laboratory space for WASA CD and the superconducting magnet with its cryogenic system. Subdetectors of the WASA CD will be tested and commissioned with cosmic rays and radioactive sources by the end of 2018. In the beginning of 2019, the WASA CD will be mounted at S2 of FRS to be ready for commissioning.

In the meantime, Monte Carlo simulations for the optimization of the detection and analysis methods are in progress. Furthermore, the development of the online/offline analysis software is to be completed.

References

[1] nucl-ex/0411038.
[2] C. Rappold et al., Nucl. Phys. A 913 170 (2013).
[3] C. Rappold et al., Phys. Rev. C 88 041001(R) (2013).
[4] A. Gal and H. Garcilazo, Phys. Lett. B 736 93 (2014).
[5] E. Hiyama et al., Phys. Rev. C 89 061302R (2014).
[6] H. Garcilazo and A. Valcarce, Phys. Rev. C 89 057001 (2014).
[7] J.M. Richard et al., Phys. Rev. C 91 014003 (2015).
[8] STAR Collaboration, Proc. 12th Int. Conf. on Hypernuclear and Strange Particle Physics (HYP2015) JPS Conf. Proc. 021005 (2017).
[9] ALICE Collaboration, Phys. Lett. B 754 360 (2016).
[10] D. Jido et al., Phys. Rev. C85,032201(R) (2012).
[11] P. Costa, M. C. Ruivo, C. A. de Sousa, and Y. L. Kalinovsky, Phys. Rev. D 71, 116002 (2005).
[12] H. Nagahiro, M. Takizawa, and S. Hirenzaki, Phys. Rev. C 74, 045203 (2006).
[13] H. Nagahiro and S. Hirenzaki, Phys. Rev. Lett. 94, 232503 (2005).
[14] Y. K. Tanaka et al., Phys. Rev. Lett. 117, 202501 (2016).
[15] Y. K. Tanaka et al., Phys. Rev. C97, 015202 (2018).
[16] K. Itahashi et al., Experimental Proposal for FAIR Phase 0, S457 (2017).
[17] H. Nagahiro, Nucl. Phys. A 914, 360 (2013).
[18] Y. Higashi, Master's thesis, Nara Women's University (2015).
[19] A. Drago et al., Phys. Rev. C 90, 065809 (2014).
[20] H. Lenske et al. Prog. Nucl. Part. Phys. 98, 118 (2018).
[21] J. Vargas et al., Nucl. Instrum. Methods A 707, 16 (2013).

 DOI:10.15120/GR-2018-1

Experiment beamline: FRS
Experiment collaboration: NUSTAR-SuperFRS-Experiments
Experiment proposal: S447, S457, S463
Accelerator infrastructure: SIS18

Search for η′-mesic nuclei with the ^{12}C(*p*,*d*) reaction

Y. K. Tanaka[1], K. Itahashi[2], H. Fujioka[3] for the η-PRiME/Super-FRS Experiment collaboration

[1]GSI, Darmstadt, Germany; [2]RIKEN, Wako, Japan; [3]Kyoto University, Kyoto, Japan.

We investigate η′-meson nucleus bound states (η′-mesic nuclei) by missing-mass spectroscopy of the ^{12}C(*p*,*d*) reaction [1]. Such bound states are expected to provide a unique and direct probe for studying in-medium properties of the η′ meson, which are closely related to chiral symmetry and axial $U_A(1)$ anomaly in QCD [2].

In 2014, we performed an inclusive measurement of the ^{12}C(*p*,*d*) reaction to measure the excitation spectrum of ^{11}C near the η′-meson production threshold. A carbon target was irradiated with a 2.5 GeV proton beam accelerated by SIS-18 to produce η′-mesic nuclei via the ^{12}C(*p*,*d*)η′⊗^{11}C reaction. Deuterons emitted at 0° were momentum-analyzed by the FRS used as a high-resolution spectrometer. Details of the experimental method are described in Ref. [3, 4].

Figure 1 (top) presents the obtained excitation spectrum around the η′ production threshold. Data sets with seven scaling factors (f = 0.980–1.020) for the central magnetic rigidity of the FRS have been combined, as indicated in the figure. The spectrum exhibits a continuous increase in the measured region and is fitted well with a polynomial function, as shown by the gray curve and the residual plot (bottom). This continuous component is consistent with estimated cross sections of quasi-free meson production processes, $p + N \rightarrow d + X$ ($X = 2\pi$, 3π, 4π, ω).

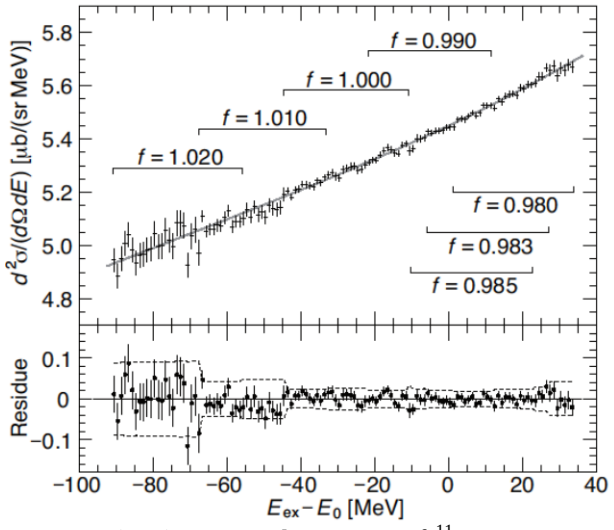

Figure 1: (Top) Measured spectrum of ^{11}C excitation energy (E_{ex}) relative to the η′ production threshold (E_0 = 957.78 MeV). The spectrum was obtained by combining data at seven momentum settings (f = 0.980–1.020) of the FRS. The gray curve displays a third-order polynomial fitted to the spectrum. (Bottom) Residual plot of the polynomial fit. Envelopes of two standard deviations are shown by the dashed lines. This figure is adopted from Ref. [4].

No prominent structures associated with the formation of η′-mesic nuclei are observed, although a very high statistical sensitivity at a level of < 1% has been achieved in the spectrum. We have evaluated upper limits on the formation cross section of η′-mesic nuclei to be ~20 nb/(sr MeV) at the production threshold for assumed Lorentzian width of Γ = 5–15 MeV. Furthermore, a comparison with theoretical calculations [5] has set a constraint on the η′-nucleus interaction, as depicted in Fig. 2 [3, 4].

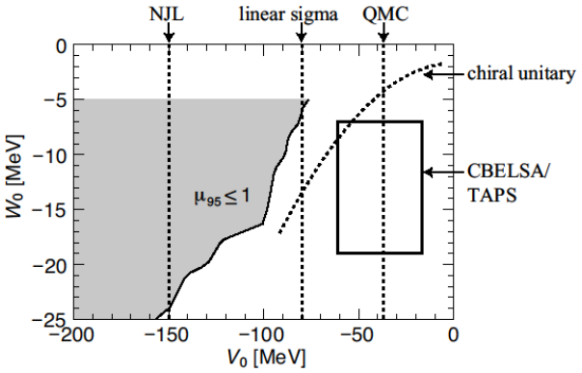

Figure 2: Evaluated constraint on the η′-nucleus potential ($V_0 + iW_0$) at normal nuclear density. The shaded region ($\mu_{95} \leq 1$) is excluded by the analysis of this experiment. Other theoretical and experimental information is displayed as well. See Ref. [4] for further details.

In FAIR Phase-0, we plan a semi-exclusive measurement of the ^{12}C(*p*,*dp*) reaction aiming at achieving higher experimental sensitivity [6]. The continuous background, dominating the inclusive (*p*,*d*) spectrum, can be efficiently reduced by simultaneously measuring the forward emitted deuteron and decay particles from η′-mesic nuclei. In particular, by tagging high-energy protons emitted in the two-nucleon absorption process (η′*NN*→*NN*), the signal-to-background ratio is expected to be enhanced by a factor ~100 compared with the inclusive measurement. The WASA central detector combined with the FRS is an ideal setup for this experiment, and its preparation is in progress.

References

[1] K. Itahashi *et al.*, Prog. Theor. Phys. 128, 601 (2012).
[2] D. Jido *et al.*, Phys. Rev. C 85, 032201(R) (2012).
[3] Y. K. Tanaka *et al.*, Phys. Rev. Lett.117, 202501 (2016).
[4] Y. K. Tanaka *et al.*, Phys. Rev. C 97, 015202 (2018).
[5] H. Nagahiro *et al.*, Phys. Rev. C 87, 045201 (2013).
[6] K. Itahashi, Y. K. Tanaka *et al.*, Experimental Proposal for FAIR Phase-0, S457 (2017).

Experiment beamline: FRS
Experiment collaboration: NUSTAR-SuperFRS-Experiments
Experiment proposal: S437, S457
Accelerator infrastructure: SIS18 / FRS

 DOI:10.15120/GR-2018-1

Observation of nuclear medium effects in the excitation of baryonic resonances

J. L. Rodríguez-Sánchez[1,2], J. Benlliure[2], H. Alvarez-Pol[2], J. Atkinson[1], T. Aumann[1], Y. Ayyad[2], S. Beceiro-Novo[2], K. Boretzky[1], E. Casarejos[2], D. Cortina-Gil[2], P. Dıaz Fernández[2], A. Estrade[1], H. Geissel[1,3], K. Itahashi[4], A. Kelić-Heil[1], Yu. A. Litvinov[1], C. Paradela[2], D. Pérez[2], S. Pietri[1], A. Prochazka[1], T. R. Saito[1], S. Schadmand[5], C. Scheidenberger[1,3], M. Takechi[1], Y. Tanaka[1,3], J. Vargas[2], I. Vidaña[6], H. Weick[1], and J. S. Winfield[1]

[1]GSI, Darmstadt, Germany; [2]USC, Santiago de Compostela, Spain; [3]Giessen Univ, Giessen, Germany; [4]RIKEN, Wako, Japan; [5]IKP, Jülich, Germany; [6]Università di Catania, Catania, Italy

The in-medium properties of baryonic resonances are not well understood. Up to now, the in-medium e ects of Δ-isobars have been studied in heavy-ion collisions at kinetic energies above the production threshold using nuclear reactions at small impact parameters [1], where there is not a good control over the production of residual fragments and thus over the number of interactions during the collision. Further investigations were performed at SATURNE using isobar charge-exchange reactions, in which the Δ resonance is excited at the surface of the nucleus [2]. These experiments provided the missing energy distributions of the (p,n) and (n,p) charge-exchange reactions induced by projectiles of ^{20}Ne at 0.95*A* GeV. The measurements were performed using di erent targets and the analysis showed a clear deviation of 50 - 70 MeV in the average value of the Δ peak between the target of protons and the others. This shift was understood as an in-medium e ect due to the Fermi motion [3] and/or di erences beetwen target and projectile excitations [4].

In this work we report on the results obtained from an experiment carried out at GSI using the fragment separator FRS, which provides unique conditions to perform measurements of isobar charge-exchange reactions with high quality, allowing us to identify the (n,p) and (p,n) charge-exchange reactions from the determination of the atomic and mass numbers of the residual fragments. Here, we measure the Δ excitation in isobar charge-exchange reactions of stable projectiles of ^{112}Sn impinging on carbon and proton targets of around 100 mg/cm^2, placed at the experimental area S0. In Fig. 1 we display the missing-energy spectrum for the isobar charge-exchange reactions C(^{112}Sn, ^{112}In)X and p(^{112}Sn, ^{112}In)X at 1*A* GeV, together with the results obtained at SATURNE for the reaction p(^{20}Ne,^{20}F)X at 0.95*A* GeV [5].

The peak close to zero corresponds to the quasi-elastic channel, while the peak around -300 MeV represents the inelastic contribution due to the excitation of the Δ resonance. Thanks to the thin targets, we obtained these spectra with a bin width of about 12 MeV, improving the resolution by a factor two with respect to experiments performed at SATURNE.

In the gure, one can see that for the reactions in the proton target the Δ peak is around -350 MeV, while for the reaction in the carbon target the peak is around -300 MeV, resulting in a shift of ~50 MeV. Therefore, these new measurements con rm the results obtained in previous experiments at SATURNE [2,5].

New measurements are planned for the phase 0 of the Super-FRS experiments, in which the isobar charge-exchange reactions will be studied in coincidence with the pions emitted from the Δ decay using the WASA@FRS setup, introducing more constraints in the analysis that will help to go further in the understanding of this e ect.

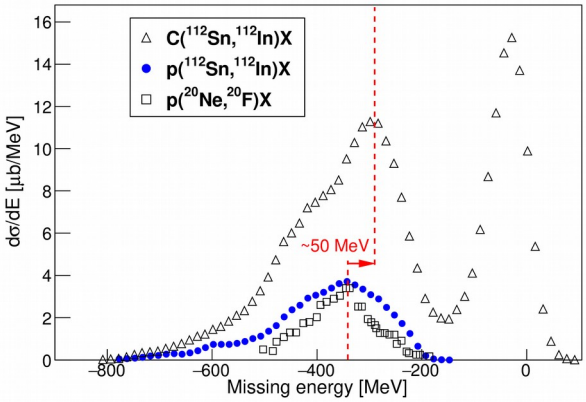

Figure 1: Missing energy distribution for ^{112}Sn and ^{20}Ne induced charge-exchange reactions in a target of protons. For comparison, the distribution of p(^{20}Ne,^{20}F)X was scaled by a factor four (for clarify of the display).

References

[1] S.B. Kaufman et al., Phys. Rev. C 20 (1979) 2293.
[2] D. Bachelier et al., Phys. Lett. B 172 (1986) 23.
[3] T. Hennino et al., Phys. Lett. B 283 (1992) 42.
[4] E. Oset et al., Nuclear Phys. A 468 (1987) 631.
[5] M. Roy-Stephan et al., Nucl. Phys. A 488 (1988) 178.

Experiment collaboration:
NUSTAR-SuperFRS Experiments

Grants: This work has been supported by the Department of Education, Culture and University Organization of the Regional Government of Galicia under the program of postdoctoral fellowships

Design of a double-sided silicon strip tracking system for hypernuclear spectroscopy at FRS & Super FRS

C. Rappold[1,2,3], S. Horta Muñoz[1], M.C. Serna Moreno[1], T. Saito[2], C. Scheidenberger[2,3]

[1]University of Castilla La-Mancha, ETSII, Ciudad Real, Spain; [2]GSI, Darmstadt, Germany; [3]Justus-Liebig-Universität Giessen, Germany

The feasibility of hypernuclear spectroscopy by means of heavy ion beam induced reactions was demonstrated by the results obtained in the first experiment of the HypHI collaboration. A ^{6}Li beam at 2*A*GeV impinged on a stable ^{12}C target. The main results of the experiment showed the measurements of Λ hyperon and $^{3}_{\Lambda}$H, $^{4}_{\Lambda}$H. Results on the invariant masses, lifetime and production cross-sections were published [1, 2, 3]. For the FAIR-Phase 0 beam-time a new hypernuclear spectroscopy experiment was approved by the G-PAC in order to assess the possible existence of the nnΛ bound state. This novel experiment will take place at the FRS fragment separator utilizing the WASA central detector that will be moved and installed in the S2 focal plane of the FRS.

An additional detector system is proposed to improve the measurements of the primary and secondary vertex. The primary vertex corresponds to the initial interaction point between the beam and the target, where the nuclear collision happens. The secondary vertexes correspond to the weak decay of produced hyperons or hypernuclei that will occur behind the target area thanks to their respective Lorentz boost. The purpose of creating such a detection system is to improve the hypernuclear identification by a more precise vertex position measurement. By improving the decay vertex position determination, the lifetime of the hypernucleus of interest will be improved twofold, by increasing the purity of the hypernuclear identification and the position precision. The concept considered for such a device is to use four stations of thin silicon trackers as micro vertex detector. The detector stations will be placed few centimetres behind the target area where particles and fragments from the mid-rapidity and the projectile rapidity are expected to be measured.

The optimization of the design of the detector is based on Monte Carlo simulations that includes the nuclear interactions, the radiation rate and the particle-matter interactions; it has been achieved within the GEANT4 simulation framework. The holding structure of the detector was designed by means of SolidWorks. The design of the mechanical structure of a double-sided silicon strip tracking system was accomplished in collaboration with members of the research group COMES of the university of Castilla-La Mancha.

A light structure with low cross sections was designed to accommodate the silicon tracker planes with a pitch of 1 cm. Light and rigid material for the support was selected for minimizing the possible interaction with the outgoing particles. A schematic view of the final design is shown in Figure 1. Industrial production of the holding structure has been considered and the plan for manufacturing of the different pieces and the procedure for their assembly have been studied and reported.

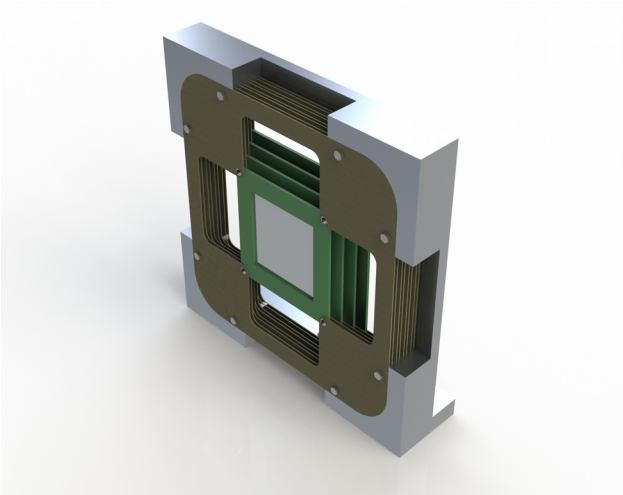

Figure 1: Assembly view of the mechanical holding structure of a double-sided silicon strip detector system. The silicon trackers are silver and green plates. The overall dimensions of the holding structure are 32 cm x 32 cm x 4 cm. The brown plates are made on a fibre-reinforced-polymer based composite. Its low density is optimal for minimizing nuclear interaction. The external frame is made of aluminium for its mechanical properties and light mass.

References

[1] C. Rappold *et al.*, Nucl. Phys. A **913**, 170 (2013).
[2] C. Rappold *et al.*, Phys. Rev. C **88**, 041001 (2013).
[3] C. Rappold *et al.*, Phys. Lett. B **747**, 129 (2015).

Experiment beamline: FRS
Experiment collaboration: NUSTAR-SuperFRS-Experiments / HypHI
Experiment proposal: S447
Accelerator infrastructure: SIS18
Grants: co-funded program of the University of Castilla-La Mancha “Ayudas para estancias de investigadores invitados en la UCLM para el año 2017” and FEDER 2014-2020.
Strategic university co-operation with: JLU - Giessen

 DOI:10.15120/GR-2018-1

Λ hyperon reconstruction using the WASA cylindrical detector system for the FAIR-Phase 0 hypernuclear experiment S447

C. Rappold[1,2], T. Saito[1], C. Scheidenberger[1,2]

[1]GSI, Darmstadt, Germany;[2]Justus-Liebig-Universität Giessen, Germany

For the FAIR-Phase 0, the accepted experiment S447, has proposed to assess the existence of the nnΛ possible bound state. This experiment will be performed at the fragment separator FRS with the WASA central detector. The WASA central detector will be moved from COSY, Juelich, and installed in the S2 area of the FRS.

In addition to the measurement of the nnΛ bound state, $^{3}_{\Lambda}$H and $^{4}_{\Lambda}$H will be measured in order to demonstrate the efficiency of the novel experimental setup, combining a solenoid magnet for the detection of light hadrons from the mid- and forward rapidity and the S2-S4 forward spectrometer of FRS for the precise measurement of the forward decay fragments: d, ^{3}He and ^{4}He from the hypernuclear decay [1, 2].

The performance of the reconstruction and calibration of the magnetic field, tracking detectors and reconstruction algorithms will need an independent physical probe of the FRS setup. For this purpose, the reconstruction of the Λ hyperon within the WASA central detection system will be crucial.

In the heavy ion collisions, the Λ hyperon is produced in the mid-rapidity of the collision. Part of the mid-rapidity phase-space overlaps with the forward rapidity, inducing some Λ hyperons to be forward-Lorentz boosted. With the WASA central detection system placed 1 meter behind the hypernuclear production target, the Λ hyperon can be reconstructed from its decay particules, $\Lambda \rightarrow p + \pi^-$.

A detailed GEANT4 simulation of this specific production and decay has been performed. The analysis of the simulated events involved the analysis framework developed for the future experiment. Track reconstruction, particle identification and vertex reconstruction was realistically performed, including realistic position and time resolution. The differential acceptance efficiencies for the decay proton and π^- is shown in Fig. 1, with an overall acceptance efficiency of 61% and 57% for π^- and proton, respectively. The resulting Λ event reconstruction is shown in Fig 2. The invariant mass resolution is about 3.6 MeV.

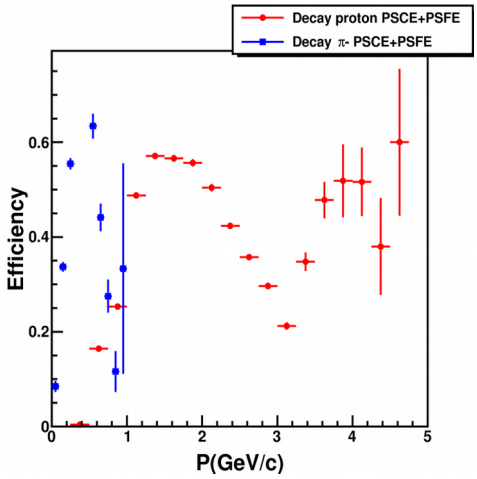

Figure 1: Differential acceptance efficiency for the decay π^- (blue) and proton (red) as a function of its momentum from Λ hyperon within the central plastic barrel, PSCE, and plastic hodoscope wall, PSFE, of the WASA central detector.

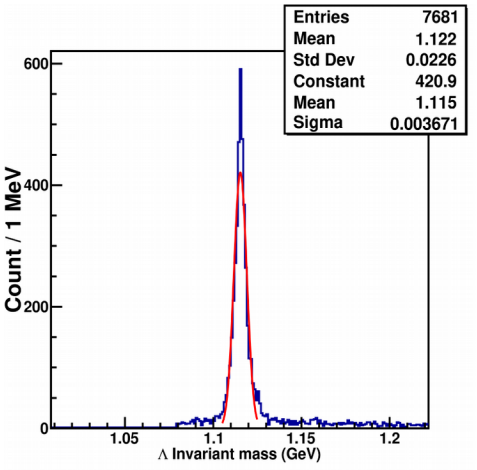

Figure 2: Invariant mass reconstruction of Λ hyperon from the decay $\Lambda \rightarrow p+\pi^-$ within the WASA central detection system. The invariant mass resolution is about 3.6 MeV.

References

[1] C. Rappold *et al.*, GSI Scientific Report 2016 [GSI Report 2017-1] (2017) p. 177.

[2] C. Rappold *et al.*, GSI Scientific Report 2016 [GSI Report 2017-1] (2017) p. 178.

Experiment beamline: FRS

Experiment collaboration: NUSTAR-SuperFRS-Experiments / HypHI

Experiment proposal: S447

Accelerator infrastructure: SIS18

Strategic university co-operation with: JLU - Giessen

Status of the FRS Ion Catcher

W. R. Plaß[1,2], T. Dickel[1,2], D. Amanbayev[1], S. Ayet[1,2], J. Äystö[3], D. Balabanski[4], S. Beck[1,2], J. Bergmann[1], O. Cheriviakova[5], P. Constantin[4], T. Eronen[6], H.Geissel[1,2], T. Grahn[6], F. Greiner[1], E. Haettner[2], C. Hornung[1], J.-P. Hucka[2], A. Jokinen[6], A. Kankainen[6], I. Mardor[7,8], I.Miskun[1,2], I. Moore[6], S. Pietri[2], A. Pikthtelev[9] , I. Pohjalainen[6], S. Purushothaman[2], Z. Patyk[5], M. P. Reiter[1,2,10], A.-K. Rink[1], S. Rinta-Antila[6], C. Scheidenberger[1,2], A. Spataru[4], H. Weick[2], J. Winfield[2], M. Yavor[11] for the Super-FRS experiment collaboration

[1]JLU, Gießen, Germany; [2]GSI, Darmstadt, Germany; [3]Helsinki Institute of Physics, Helsinki, Finland; [4]IFIN-HH/ELI-NP, Magurele, Romania; [5]National Centre for Nucl. Res., Warszawa, Poland; [6]University of Jyväskylä, Jyväskylä, Finland; [7]TAU, Tel-Aviv, Israel; [8]Soreq NRC, Yavne, Israel; [9]BINEP, RAS, Chernogolovka, Russia; [10]TRIUMF, Vancouver, Canada; [11]Institute for Analytical Instrum., RAS, St. Petersburg, Russia

At the FRS Ion Catcher [1] precision experiments with thermalized exotic nuclei can be performed. The fragments are produced by projectile fragmentation or fission at relativistic energies, separated in-flight and energy-bunched in the FRS [2]. With the FRS Ion Catcher (figure 1) these fragments are then slowed down and thermalized in a cryogenic stopping cell (CSC) [3]. A multiple-reflection time-of-flight mass spectrometer (MR-TOF-MS) is used to perform direct mass measurements and to provide an isobarically clean beam for further experiments, such as mass-selected decay spectroscopy [4]. A versatile RF quadrupole transport and diagnostics unit guides the ions from the CSC to the MR-TOF-MS, provides differential pumping, ion identification and includes reference ion sources. The FRS Ion Catcher serves as a test facility for the Low-Energy Branch (LEB) of the Super-FRS and already now enables a variety of new precision experiments in FAIR Phase-0.

The FRS Ion Catcher has been commissioned and its components have been characterized. For the first time, a stopping cell for exotic nuclei was operated on-line at cryogenic temperatures. Using a gas density almost three times higher than ever reached before for a stopping cell with RF ion repelling structures, various ^{238}U projectile and fission fragments were thermalized and extracted with very high efficiency. A combined ion stopping, survival and extraction efficiency of up to 30% and an extraction time of about 25 ms have been measured [5]. The rate capability of the CSC has been investigated [6]. Direct mass measurements of several short-lived fragments (e.g. ^{220}Ra with a half-life of 17.8 ms) have been performed with the MR-TOF-MS. In total for more than 40 short-lived nuclei the ground state masses have been determined and 15 isomeric states have been measured. A data evaluation procedure for MR-TOF-MS data has been developed that allows achieving high accuracies even for low statistics and overlapping peaks. As a part of this work a new mathematical function has been developed to describe the peak shapes in MR-TOF-MS spectra [7]. The error budget of the measurement with the MR-TOF-MS has been made. Mass accuracies down to 10^{-7} have been achieved. Furthermore, the FRS Ion Catcher is the ideal device to search for long lived isomers (> 10 ms), because it is universal, i.e. element and decay mode independent, faster than other mass spectrometry techniques (e.g. SMS, TOF-ICR), very sensitive (non-scanning), has high mass resolving power (>> 10^5), high dynamic range (> 10:1) and is broadband in nature, i.e. can measure all isobars and isomers of several mass units in parallel. Moreover, the isomers can be spatially separated from the ground state and an isomerically clean beam can be provided to experiments, such as decay spectroscopy [8].

In an experiment in 2016 the integration of the Ion Catcher in the FRS DAQ has been started [9]. The aim of this work is to make the data from the FRS Ion Catcher available as a part of the standard FRS particle identification (PID). This enables the use of the system as a mass tagger [10] for the FRS PID or to use high-accuracy mass measurement as the only information for PID, instead of the standard PID [11]. This has been successfully tested even under challenging conditions (with fission and projectile fragments with Z > 70 produced at a primary beam energy of 300 MeV/u). Furthermore the operation of the CSC with argon as stopping gas has been investigated and first tests to use the stopping gas as a reaction target for fusion studies were performed [12].

Recently, the FRS Ion Catcher has been upgraded in several aspects. In particular, (i) in the CSC the electrode structure and the connections have been revised to increase the operational reliability and to allow for higher extraction field strengths and thus shorter extraction times. (ii) A new pre-pump allows operation of the turbo-molecular pumps on the RFQ beamline (first differential pumping stage after the CSC) at higher pressures. (iii) An extension of the RFQ beamline has been developed and commissioned [13]. (ii) and (iii) in combination will allow the operation (for heavy ions) of the CSC at higher areal densities up to 10 mg/cm².

The FRS Ion Catcher is part of four approved experiment proposals for FAIR Phase-0. These experiments cover a wide variety of nuclear physics questions, from detector tests and novel concepts for higher yields (very thick targets) [14] over mass measurements in different regions of the nuclear chart (N=126 [15] and N=Z [14]) to reaction studies on multi-nucleon transfer [16] and measurements of beta-delayed neutron emission probabilities [17]. These experiments will make use of recently developed new ion optical modes of the FRS, that will allow higher transmission and FRS performance tailor-made for these experiments [18].

 DOI:10.15120/GR-2018-1

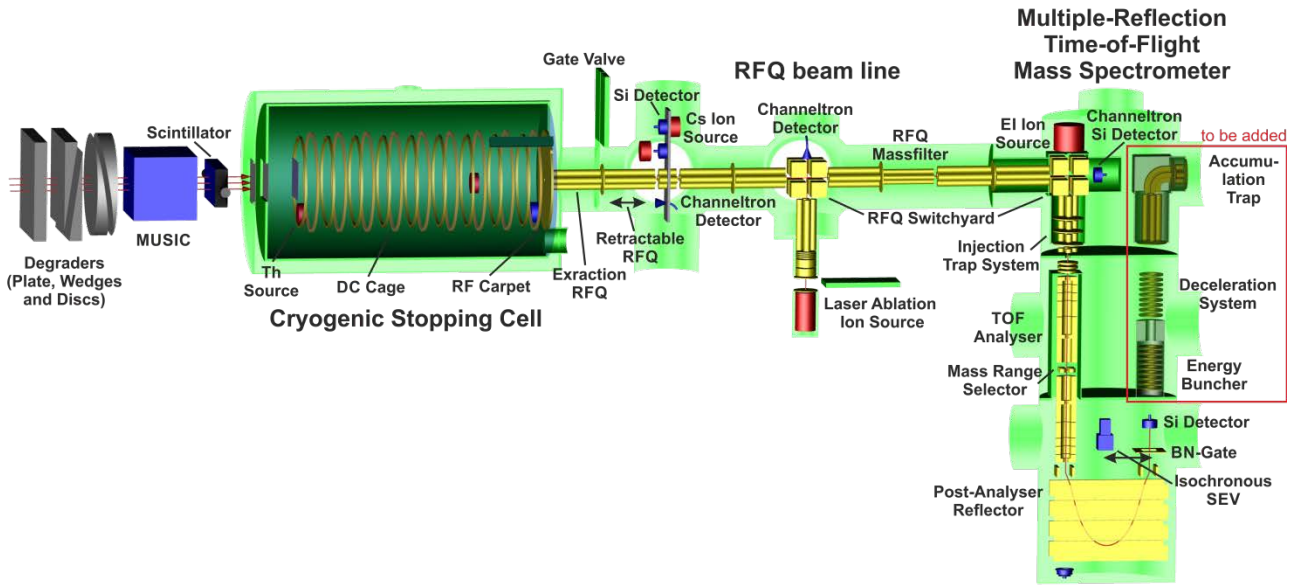

Figure 1: Schematic view of the setup of the FRS Ion Catcher at the final focal plane of the FRS. The beam enters the setup from the FRS from the left and passes the detectors for the PID of the FRS and the variable degrader to adjust the range of the ions. Then the ions are thermalized in the CSC, extracted and transmitted through the RF quadrupole transport and diagnostics unit to the MR-TOF-MS.

For the LEB of the Super-FRS a new **H**igh **A**real **D**ensity **O**rthogonal extraction CSC (HADO-CSC) is under development [19,20]. It will feature significantly improved performance characteristics, including higher rate capability, stopping efficiencies and active area, matching the requirements for beams at the LEB. The LEB stopping cell will be a key device for the research with thermalized projectile and fission fragments that will be performed with the experiments MATS and LaSpec [21]. The development and operation of the stopping cells of the FRS Ion Catcher and of the LEB are performed in the context of the Super-FRS Experiment Collaboration. The HADO-CSC is also the basis for the development of stopping cells at ELI-NP [22] and SARAF [23].

The MR-TOF-MS will be part of MATS and perform mass measurements of very short-lived and rare nuclei complementary to measurements with the Penning trap system of MATS. At the same time it can be operated as isobar and isomer separator for MATS and LaSpec, and it will be an essential tool to perform diagnostics and PID at the LEB. The MR-TOF-MS has been the basis for spin-off developments for analytical mass spectrometry [24] and a system for the TITAN experiment at the ISOL facility ISAC at TRIUMF [25].

References

[1] W.R. Plaß et al., NIM B 317 (2013) 457.
[2] H. Geissel et al., NIM B 70 (1992) 286.
[3] M. Ranjan et al., NIM A 770 (2015) 87.
[4] T. Dickel et al., NIM A 777 (2015) 172.
[5] S. Purushothaman et al., EPL 104 (2013) 42001.
[6] M.P. Reiter et al., NIM B 376 (2016) 240.
[7] S. Purushothaman et al., IJMS 421 (2017) 245.
[8] T. Dickel et al., PLB 744 (2015) 137.
[9] E. Haettner et. al., this issue.
[10] M.P. Reiter, PhD thesis, JLU Gießen (2015).
[11] C. Hornung et al., GSI Sci. Rep. 2016 (2017) 175.
[12] I. Miskun et al., this issue.
[13] C. Hornung et al., this issue.
[14] W.R. Plaß et al., this issue.
[15] S. Pietri et al., this issue.
[16] T. Dickel et al., this issue.
[17] I. Mardor et al., this issue.
[18] E. Haettner et al., this issue.
[19] D. Amanbayev et al., this issue.
[20] T. Dickel et al., NIM B 376 (2016) 216.
[21] D. Rodriguez et al., EPJ Special Topics 183 (2010) 1.
[22] D. L. Balabanski et al., Rom. Rep. Phys. 68 (2016) 621.
[23] I. Mardor et al., arXiv:1801.06493v2.
[24] T. Dickel et al., NIM B 317 (2013) 779.
[25] M.P. Reiter et al., this issue.

Experiment beamline: FRS
Experiment collaboration:
NUSTAR-Super-FRS-Experiments / FRS Ion Catcher
Experiment proposal: S411, S468, S472, S474, S475
Accelerator infrastructure: SIS18
PSP codes: 1.2.1.2; 1.2.3.13; 2.4.11.2.7; 2.4.11.2.8
Grants: BMBF (05P12RGFN8, 05P16RGFN1), HMWK (LOEWE Center HICforFAIR), HGS-HIRe, Helmholtz Association of German Research Centers (NAVI VH-VI-417)
Strategic university co-operation with: Gießen

Reaction studies with the FRS Ion Catcher: A novel approach and universal method for the production, identification of and experiments with unstable isotopes produced in multi-nucleon transfer reactions with stable and unstable beams

T. Dickel[1,2], P. Constantin[3], J. S. Winfield[2], S. Ayet[1,2], S. Bagchi[1,2,4], D. Balabanski[3], S. Beck[1,2], H. Geissel[1,2], F. Greiner[1], E. Haettner[2], S. Heinz[1,2], C. Hornung[1], A. Kankainen[5], A. Karpov[6], D. Kostyleva[1,2], N. Kuzminchuk[2], B. Kindler[2], B. Lommel[2], I. Mardor[7,8], I. Miskun[1], I. Mukha[2], G. Münzenberg[2], S. Pietri[2], Z. Patyk[9], G. Martinez-Pinedo[10], W. Plaß[1,2], A. Prochazka[1], S. Purushothaman[2], C. Rappold[1,2], V. Saiko[6], T. Saito[2,11,12], C. Scheidenberger[1,2], Y. Tanaka[1,2], H. Weick[2] and the Super-FRS experiment collaboration

[1]JLU, Gießen, Germany; [2]GSI, Darmstadt, Germany; [3]IFIN-HH/ELI-NP, Magurele, Romania; [4]Saint Mary's University, Canada; [5]University of Jyväskylä, Jyväskylä, Finland; [6]JINR, Dubna, Russia; [7]TAU, Tel-Aviv, Israel; [8]Soreq NRC, Yavne, Israel; [9]National Centre for Nucl. Res., Warszawa, Poland; [10]TU Darmstadt, Darmstadt, Germany; [11]Helmholtz Institut Mainz, Mainz, Germany; [12]Iwate University Morioka, Japan

Experiments with radioactive ion beams at Coulomb-barrier energies represent a new field for reaction studies which will contribute to a better understanding of multi-nucleon transfer, deep inelastic, fusion-fission and complete fusion reactions. One of the main goals of these experiments is to access new neutron-rich heavy and super heavy isotopes, not reachable in fission or fragmentation reactions [1].

Slowed-down rare ion beams of all chemical elements, including refractory elements, independent of their chemical properties, are available at the FRS and Super-FRS. Their optimum use requires a new philosophy for experiments and instrumentation [2]. For instance multi-nucleon transfer (MNT) reactions inside the cryogenic stopping cell (CSC) of the FRS Ion Catcher is a unique and novel method that is very sensitive, clean, universal and has a high angular acceptance for the reaction products. It is planned to mount targets (e.g., Dy, Pt, U) on a wheel will be installed in the stopping volume of the CSC. The identification and quantification of the reaction products will be performed by a high resolution and broadband mass spectrometer, which allows to identify the reaction products completely by their mass-to-charge ratio. This will pave the way for broad range measurements with primary and secondary beams. The concept is based on the uniqueness of the beams and experimental setups of GSI/FAIR and their combination.

In a first experiment we will perform MNT reaction studies with a 500 MeV/u ^{238}U primary beam slowed-down to Coulomb barrier energies impinging on different targets. We expect to measure in 12 approved shifts more than 150 cross sections (figure 1) and 15 new masses of neutron-rich isotopes. The cross-sections will be used to benchmark reaction models. The proposed nuclei are important for the rare earth abundance peak in the r-process as well as for the understanding the properties of fissioning nuclei involved in the r-process.

This is the first step towards future broad range reaction studies with secondary beams at the (LEB of the Super-)FRS.

References

[1] V. Zagrebaev and W. Greiner, PRL 101, 2–5 (2008).
[2] G. Münzenberg et al., EXON-2014 Proc. (2014).
[3] A.V. Karpov, et al PRC 96 (2017) 024618.

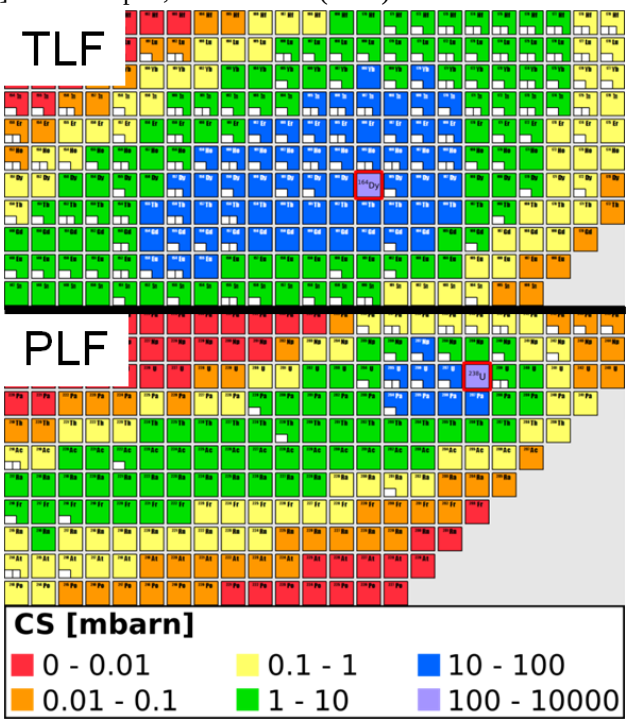

Figure 1: Calculated production cross-sections [3] for ^{238}U on ^{164}Dy. Upper panel: target-like fragments (TLF); lower panel: projectile-like fragments (PLF). The estimated sensitivity limit will be about 0.1 mbarn.

Experiment beamline: FRS
Experiment collaboration:
NUSTAR-SuperFRS-Experiments / FRS Ion Catcher
Experiment proposal: S475
Accelerator infrastructure: SIS18
PSP codes: none
Grants: BMBF (05P12RGFN8 & 05P16RGFN1), HMWK (LOEWE Center HICforFAIR), HGS-HIRe
Strategic university co-operation with: Gießen

 DOI:10.15120/GR-2018-1

Investigation of fusion in inverse kinematics with a target in the cryogenic stopping cell

I.Miskun[1], T. Dickel[1,2], S. Ayet[1,2], S. Bagchi[1,2,3], J. Bergmann[1], J.Ebert[1], A.Finley[4,5], H.Geissel[1,2], F. Greiner[1], E. Haettner[2], C. Hornung[1], S. Kaur[3], W. Lippert[1], J.-H. Otto[1], S. Pietri[2], W. R. Plaß[1,2], S. Purushothaman[2], A.-K. Rink[1], C. Scheidenberger[1,2], Y. Tanaka[1,2], H. Weick[2], J. S. Winfield[2], the FRS Ion Catcher collaboration and for the Super-FRS experiment collaboration

[1]Justus-Liebig-University of Giessen, Giessen, Germany; [2]GSI, Darmstadt, Germany; [3]Saint Mary's University, Canada; [4]TRIUMF, Vancouver, Canada; [5]UBC, Vancouver, Canada

Radioactive ion beams at Coulomb barrier energies will open a wide field for the study of deep-inelastic reactions of heavy nuclei and their application for the synthesis of new exotic heavy and super-heavy nuclei [1]. The slowing-down of heavy-ion fragment beams from relativistic production energies to near Coulomb barrier energies has been done for many years for the stopping cell experiments and tests [2] at the FRS [3].

In experiments with the FRS Ion Catcher secondary beams are stopped inside the cryogenic stopping cell (CSC), extracted and their properties are measured. If a thin reaction target is installed in the CSC and the energy of the secondary beams is adjusted to be close to the Coulomb barrier, fusion products will be generated, which can be stopped, measured and identified with the MR-TOF-MS of the FRS Ion Catcher. Also, the stopping gas itself can be used as reaction target. This is of special interest if heavier noble gases (e.g. argon) are used. This allows the study of fusion reactions in inverse kinematics with low intensity beams (e.g., exotic secondary beams) and high sensitivity. The advantages of inverse kinematics are (i) that the range distribution of the impinging beam is small, so the products will be produced over a narrow depth in the target and (ii) the range of the products is larger, which allows the release over a wider depth of the target. Because of these effects the effective target thickness is much larger, especially for secondary beams, in inverse than in normal kinematics reactions. (iii) For a given areal weight, the target has more reaction centers in inverse kinematics than a target in normal kinematics, since in inverse kinematics the mass number of the target atoms is smaller. If the stopping gas itself is used as a target these advantages are maximized, because one can have very thick targets for fusion reactions (~10 mg/cm²), while having 100% release efficiency from the target. The disadvantages of this concept are the need for very high density stopping cells and the limitation in the available targets/stopping gases, He, Ne, Ar and maybe carbon (methane). For heavier gases the repelling RF electrode structure (RF-carpet), which ensure high efficient ion extraction from the stopping gas, will not work. The CSC was operated with up to 20 mg/cm² neon [2].

Here we report the first tests with more than 10 mg/cm² argon (figure 1). One can see that the extraction efficiency was limited by the available RF carpet electronics. A first test under this non-optimal conditions was done, in an experiment with the FRS in 2016. For this experiment a natural titanium target was installed inside the CSC and the CSC was operated with argon as stopping gas (13 mg/cm²).

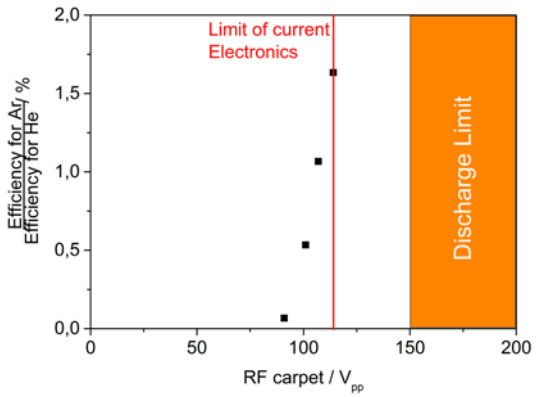

Figure 1: Measured relative extraction efficiency for $^{220}Rn^{+}$ vs. RF voltage on the RF carpet for argon as stopping gas (12 mg/cm²) as compared to operation of the CSC with helium.

A primary beam of $2 \cdot 10^5$ ^{124}Xe/spill with 600 MeV/u was transported to the CSC and slowed down to Coulomb barrier energies in the target and stopping gas. The search for fusion products in the mass spectra was not conclusive. However, it was demonstrated that under the conditions of the experiment the background is very low, such that in the future 10 detected fusion products will be sufficient for an unambiguous identification. An upgraded RF carpet electronics has been developed and is now ready to overcome the limits of past experiments.

In FAIR phase 0 an experiment built on these results has been approved by the G-PAC and will focus on multi-nucleon transfer reactions [4].

References

[1] W. Loveland, Phys. Rev. C 76 (2007) 014612
[2] P. Reiter, PhD JLU Giessen (2015).
[3] H. Geissel et al., NIM B 70 (1992) 286
[4] T. Dickel et al., this issue

Experiment beamline: FRS
Experiment collaboration:
NUSTAR-SuperFRS-Experiments / FRS Ion Catcher
Experiment proposal: S475
Accelerator infrastructure: SIS18
PSP codes: none
Grants: BMBF (05P12RGFN8 & 05P16RGFN1), HMWK (LOEWE Center HICforFAIR), HGS-HIRe
Strategic university co-operation with: Gießen

A novel method for measuring β-delayed neutron emission

I. Mardor[1,2], T. Dickel[3,4], S. Ayet[3], S. Bagchi[5,3,4], S. Beck[3,4], H. Geissel[3,4], F. Greiner[4], E. Haettner[3], C. Hornung[4], D. Kostyleva[3,4], N. Kuzminchuk[3], B. Kindler[3], B. Lommel[3], G. Martínez-Pinedo[6], I. Miskun[4], I. Mukha[3], E. Piasetzky[1], S. Pietri[3], W. R. Plaß[3,4], I. Pomerantz[1], A. Prochazka[3], S. Purushothaman[3], C. Rappold[3,4], T. Saito[3,7,8], C. Scheidenberger[3,4], Y. Tanaka[3,4], H. Weick[3], J. S. Winfield[3], and the Super-FRS Experiment Collaboration

[1]Tel Aviv University, Tel Aviv, Israel, [2]Soreq NRC, Yavne, Israel, [3]GSI, Darmstadt, Germany, [4]Justus-Liebig-Universität, Gießen, Germany, [5]Saint Mary's University, Halifax, NS, Canada, [6]Technische Universität Darmstadt, Darmstadt, Germany, [7]Helmholtz Institute Mainz, Mainz, Germany, [8]Iwate University, Morioka, Japan

β-delayed single- or multi-neutron emission is possible when a mother nucleus β-decay Q-value (Q_b) is larger than the daughter nucleus one- or x-neutron separation energy (S_{1n} or S_{xn}). The probability for β-delayed neutron emission (P_{xn} for x emitted neutrons) increases with neutron number per isotope. Measured P_{xn} values provide important input to the astrophysical r-process, nuclear structure models, and control of nuclear reactors [1].

P_{xn} data is scarce, especially for multi-neutron emission. For present and near-future accessible isotopes, less than 10% of multi-neutron emission candidates have been measured [2]. Moreover, in the fission-product region, the most relevant for the r-process and nuclear reactors, there is published P_{2n} data for only four nuclides.

Therefore, there are several world-wide campaigns to bridge this data gap, mostly by counting β-delayed emission n-β coincidence events [3]. In this method, efficiency decreases with x (higher number of coincident neutrons), β and n detector efficiencies depend on prior energy spectra measurements or models, and the measurement includes neutron background from the beam and cosmic rays. Other proposed methods count the recoil nuclides via gamma spectra [4], time-of-flight [5], or mass measurements, in a series of stopping cells and MR-TOF-MSs (RIKEN) [6], or in the ESR (GSI) [7]. These methods are less efficient and/or prone to systematic errors, especially for multi-neutron emission.

Given the above, we propose a complementary and independent method for measuring P_{xn} at the FRS Ion Catcher, which circumvents the drawbacks of existing methods [8]. Obtain separated isotopes with the FRS, contain them in the Cryogenic Stopping Cell (CSC) for periods long enough for decay, and identify and count the precursor and recoil isotopes with the Multiple-Reflection Time-of-Flight Mass-Spectrometer (MR-TOF-MS).

The required n-rich isotopes will be produced via in-flight fission of ^{238}U primary beam from the SIS18. The areal density of the CSC (10 mg/cm^2) provides another separation stage, ensuring that only the required precursors are stopped in it.

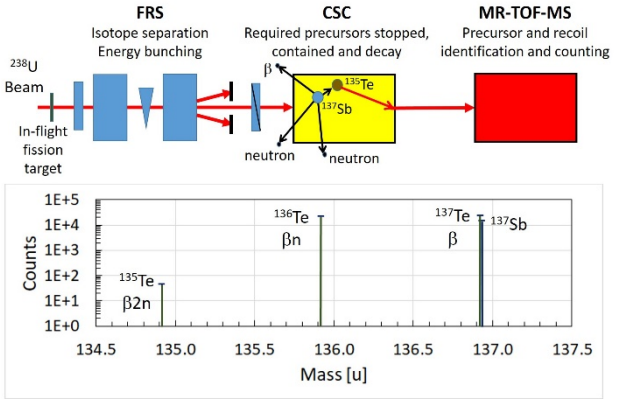

Figure 1: Top - Scheme of the proposed method. A β2n decay of ^{137}Sb in the CSC is depicted. Bottom - expected spectrum in the MR-TOF-MS, when containing the precursors in the CSC for two ^{137}Sb half-lives.

For P_{xn} extraction, the masses of the precursor and all recoils are measured simultaneously at the MR-TOF-MS with accuracy that enables their unambiguous identification. Ratios between the recoil isotopes infer P_{xn} for all x (x=0 is regular β-decay) (Fig. 1). Concurrently, the method will provide measurements of mass, Q-values (precursor-recoil mass difference) and half-lives (precursor to all recoils ratio). The method has the same efficiency for all x, is independent of nuclear models, has practically no background, and is sensitive to isomers.

The proposal has been approved for FAIR Phase-0, pending beam availability. First planned measurements are of P_{xn} of $^{135\text{-}137}$Sb and ^{142}I, the heaviest and highest Z β2n precursor measured yet, setting the stage for a survey of β-delayed neutron emission, including the N~126 region.

References

[1] M.R. Mumpower et al., PRC 94, 064317 (2016)
[2] I. Dillmann et al., AIP Conf. Proc. 332, 1594 (2014)
[3] A. Tarifeño-Saldivia et al., JINST 12 P04006 (2017)
[4] J. A. Winger et al., PRL 102, 142502 (2009)
[5] R. M. Yee et al., PRL 110, 092501 (2013)
[6] P. Schury, Fragment Separator Expert Meeting, Grand Rapids (2016)
[7] A. Evdokimov et al., PoS (NIC XII) 115 (2012)
[8] I. Mardor et al., NUSTAR Week 2017, Ljubljana, (2017)

Experiment beamline: FRS
Experiment collaboration: NUSTAR-SuperFRS-Experiments / FRS Ion Catcher
Experiment proposal: S472
Accelerator infrastructure: SIS18
PSP codes: none
Grants: BMBF (05P12RGFN8 & 05P16RGFN1), HMWK (LOEWE Center HICforFAIR), HGS-HIRe, Israel Ministry of Energy Research Grant
Strategic university co-operation with: Gießen

 DOI:10.15120/GR-2018-1

Detector tests with the prototype CSC for the Super-FRS and direct mass measurements of neutron-deficient nuclides below ^{100}Sn in FAIR Phase-0

W. R. Plaß[1,2], T. Dickel[1,2], S. Ayet San Andrés[1,2], S. Bagchi[1,2,3], S. Beck[1,2], P. Constantin[4], T. Eronen[5], H. Geissel[1,2], F. Greiner[1], E. Haettner[2], C. Hornung[1], A. Jokinen[5], A. Kankainen[5], B. Kindler[2], D. Kostyleva[1,2], N. Kuzminchuk[2], B. Lommel[2], I. Mardor[6,7], I. Miskun[1], I. D. Moore[5], I. Mukha[2], Z. Patyk[8], S. Pietri[2], A. Prochazka[2], S. Purushothaman[2], C. Rappold[1,2], S. Rinta-Antila[4], T. Saito[2,9,10], C. Scheidenberger[1,2], Y. Tanaka[1,2], H. Weick[2], J. S. Winfield[2], J. Äystö[11], and the Super-FRS Experiment Collaboration

[1]Justus-Liebig-Universität Gießen, Germany; [2]GSI, Darmstadt, Germany; [3]St Mary's University, Halifax, Canada; [4]IFIN-HH / ELI-NP, Magurele, Romania; [5]University of Jyväskylä, Jyväskylä, Finland; [6]Tel Aviv University, Israel; [7]Soreq NRC, Yavne, Israel; [8]National Centre for Nucl. Res., Warszawa, Poland; [9]Helmholtz Institute Mainz, Germany; [10]Iwate University Morioka, Japan; [11]Helsinki Institute of Physics, Helsinki, Finland

In the context of the experiment proposal S474, detector tests with the prototype of the cryogenic stopping cell (CSC) for the Low Energy Branch (LEB) of the Super-FRS and direct mass measurements will be performed at the FRS with the FRS Ion Catcher [1] in FAIR Phase-0. The detector tests include (i) the commissioning of the CSC with an areal density of 10 mg/cm^2 and with higher DC fields (doubling the stopping efficiency and reducing the extraction time), (ii) the on-line test of the pumping and He recycling unit and the gas purification techniques to be used with the LEB stopping cell, (iii) the control of charge states of ions thermalized in the CSC for increased stopping and extraction efficiencies of multiply-charged ions, (iv) the on-line commissioning of the upgrade of the RFQ beamline of the FRS Ion Catcher [2], (v) the test of the new large aperture precision degrader system and the scintillator for the Super-FRS Ion Catcher and (vi) the integration of the FRS Ion Catcher in the FRS data acquisition system. In addition the use of a very thick target (>>4 g/cm^2; d/R>0.5 where d is the thickness and R the range) will be investigated, which should increase yields by multi-step fragmentation reactions and enable access to more exotic nuclides at the FRS Ion Catcher and the LEB of the Super-FRS [3].

After many years of R&D and tests, direct mass measurements of rare neutron-deficient nuclides under challenging realistic conditions can be performed and shall demonstrate the overall performance of the system. Projectile fragments in the range from Zr to Rh produced by projectile fragmentation of ^{124}Xe and ^{107}Ag are ideal to perform these measurements. They are refractive and can therefore be ideally produced and separated in-flight. Furthermore, depending on the ionization potentials of the various elements, the ions are expected to be thermalized in different charge states (+1 and +2). The controlled manipulation of charge states can thus be tested with these fragments. The mass measurements aim at N=Z and N=Z+1 nuclides in the element range from Y to Ag and will provide experimental mass values for many of these nuclides for the first time (Fig. 1). These nuclides are of high interest because of their impact on the rp process, isospin symmetry as well as pairing and the Wigner energy, the region of nuclear deformation in the vicinity of ^{80}Zr [4], and the high-spin isomer in ^{94}Ag [5,6].

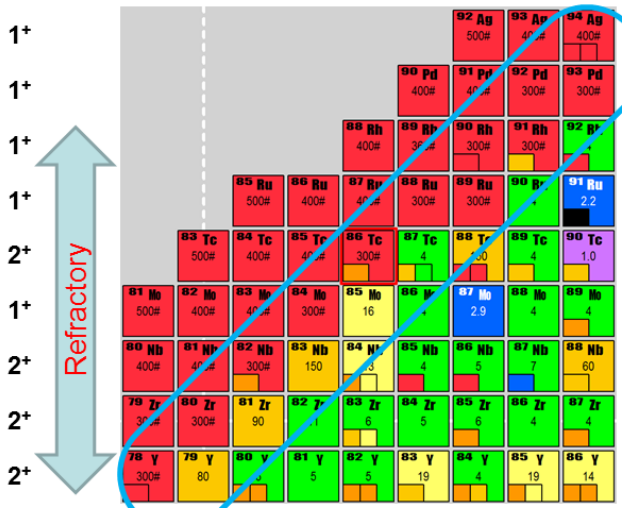

Figure 1: Section of the chart of the nuclides showing the region of interest for the experiment proposal and the uncertainty of mass values in the elemental range from Y to Ag (in keV). For nuclides shown in red the mass has not been measured yet [7]. Left: Expected charge states of the ions extracted from the CSC and range of refractory elements in this region.

References

[1] W.R. Plaß et al., Nucl. Instrum. Methods B 317 (2013) 457.
[2] C. Hornung et al., this issue.
[3] E. Haettner et al., this issue.
[4] C. J. Lister et al., Phys. Rev. Lett. 59 (1987) 1270.
[5] I. Mukha et al., Nature 439 (2006) 298.
[6] A. Kankainen et al., PRL 101, (2008) 142503.
[7] M. Wang et al., Chin. Phys. C 41 (2017) 030003.

Experiment beamline: FRS
Experiment collaboration: NUSTAR-Super-FRS-Experiments / FRS Ion Catcher
Experiment proposal: S474
Accelerator infrastructure: SIS18
PSP codes: 1.2.1.2; 1.2.3.13; 2.4.11.2.7; 2.4.11.2.8
Grants: BMBF (contract No. 05P16RGFN1), HMWK (LOEWE Center HICforFAIR), HGS-HIRe
Strategic university co-operation with: Gießen

An upgrade to the RFQ beam line of the FRS Ion Catcher

C. Hornung[1], D. Amanbayev[1], S. Ayet[1,2], J. Bergmann[1], T. Dickel[2], H. Geissel[1,2], F. Greiner[1], L. Gröf [1], W. R. Plaß[1,2], A.-K. Rink[1], and C. Scheidenberger[1,2]

[1]JLU, Gießen, Germany; [2]GSI, Darmstadt, Germany

At the FRS Ion Catcher the cryogenic stopping cell (CSC) and the MR-TOF-MS are connected via an RFQ beam line. To achieve highest mass accuracies with the MR-TOF-MS it is necessary to have calibrant ions over a broad mass range at a high repetition rate (≈ 100 Hz) in order to match the repetition rate of the MR-TOF-MS. These requirements can be fulfilled by the laser ablation carbon cluster ion source (LACCI) [1], which is a part of the upgrade of the RFQ beam line [2] of the FRS Ion Catcher. An overview of the FRS Ion Catcher setup including main features of the RFQ beam line is shown in fig. 1.

LACCI is equipped with a x-y-movable target table, which enables a fast (≈ s) change of targets and a permanent 2D movement of the targets during ion production. In the 2D movement the targets are scanned by a horizontal and vertical meander, in which the step size and the velocity can be adjusted. This allows long-term stable operation (>10 hours), even at high repetition rates (≈ 100 Hz, two orders of magnitude higher than with systems used at other facilities world-wide). A first proof-of-principle demonstrating the long-term stability of LACCI is shown in fig. 2 for erbium ions.

In order to couple LACCI to the existing RFQ beam line an RFQ based switchyard [3] is used. An RFQ switchyard is a novel device which acts like six gas-filled RFQs leading away from a central point along three perpendicular axes. Modes with input or output along multiple axes at once are possible, allowing for beam splitting or merging, and switching between input/output configurations during operation.

The upgrade of the RFQ beam line improves differential pumping between the CSC and the MR-TOF-MS. This will enable a higher helium gas pressure in the CSC, while keeping the pressure in the MR-TOF-MS low, to avoid collisional losses during the TOF measurement. A decoupling of the pressure in the CSC and the MR-TOF-MS enables to operate the MR-TOF-MS with optimum performance even with the highest pressure in the CSC.

A dedicated RFQ mass filter will be added to the existing beam line. The expected mass resolution (<1 u) will be high enough to perform a pre-separation of ions accordingly to their mass numbers in the beam line in front of the MR-TOF-MS. The extension of the RFQ beam line also enables an improved operation of the collision induced dissociation inside the RFQ beam line [4], by including several activation stages. This provides a higher suppression of molecular background.

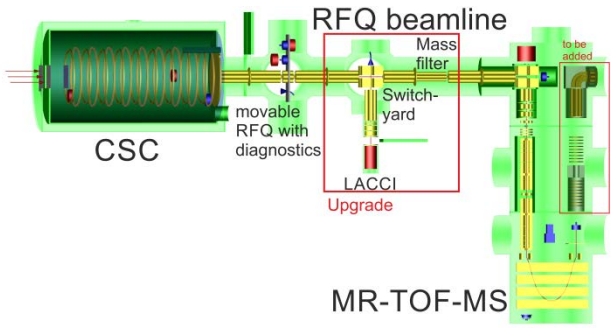

Figure 1: Schematic view of the FRS Ion Catcher with the CSC, the upgraded RFQ based beam line, including diagnostics tools, LACCI, a dedicated RFQ mass filter, and the MR-TOF-MS (from the left to the right).

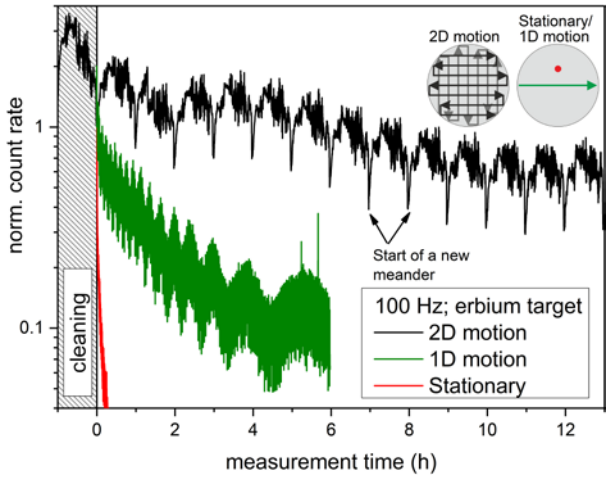

Figure 2: Measurement of the long-term stability of the count rate for erbium ions produced in laser ablation in LACCI with a repetition rate of 100 Hz. The count rate vs. time with a 2D motion of the movable target is compared to a stationary target and 1D motion. The latter is the established state-of-the-art technique for similar laser ion sources. The data are normalized to the count rate after cleaning of the target surface, since it was seen that the first target layer has different properties than the following layers.

References

[1] C. Hornung et al., GSI Sci. Rep. 2013 (2014) 105.
[2] L. Gröf, Bachelor thesis, JLU Gießen, 2017.
[3] W. Plaß et al., Phys. Scr. T166 (2015) 014069.
[4] F. Greiner, Master thesis, JLU Gießen, 2017.

Experiment beamline: FRS
Experiment collaboration:
NUSTAR-SuperFRS-Experiments / FRS Ion catcher
Experiment proposal: S474
Accelerator infrastructure: SIS18
PSP codes: none
Grants: BMBF (05P12RGFN8 & 05P16RGFN1), HMWK (LOEWE Center HICforFAIR), HGS-HIRe
Strategic university co-operation with: Gießen

 DOI:10.15120/GR-2018-1

Development of the stopping cell for the Low-Energy Branch of the Super-FRS

D. Amanbayev[1], S. Ayet San Andrés[1,2], T. Dickel[1,2], H. Geissel[1,2], F. Greiner[1], I. Miskun[1], S. Purushothaman[2], W. R. Plaß[1,2], A.-K. Rink[1], C. Scheidenberger[1,2] for the FRS Ion Catcher Collaboration and for the Super-FRS Experiment Collaboration

[1]Justus-Liebig-Universität Gießen, Germany; [2]GSI, Darmstadt, Germany

The technical design of the cryogenic stopping cell (CSC) for the Low-Energy Branch (LEB) of the Super-FRS [1] has been developed. The CSC will thermalize exotic nuclei, which have been produced in the Super-FRS at relativistic energies, and make them available to the experiments MATS and LaSpec. A prototype of the stopping cell has been successfully commissioned as a part of the FRS Ion Catcher at GSI and enabled an access to short-lived exotic nuclei, providing high areal densities of up to 6.3 mg/cm^2, short extraction times of 25 ms, a rate capability of more than 10^4 ions/s and total efficiencies of up to 30% [2].

The CSC for the LEB will be a high areal density orthogonal extraction CSC (HADO-CSC). It will use the techniques of cryogenic operation to ensure a high purity of the stopping gas and high-density operation enabled by using an RF carpet with a small electrode structure size, which have been successfully applied in the prototype CSC. In addition it will implement several novel concepts, which will result in important performance advantages compared to conventional stopping cells, such as very high stopping efficiencies, short extraction times and high rate capability [1]. The CSC consists of two chambers (Fig 1.). The outer chamber provides the insulation vacuum for the inner chamber, which is operated at a temperature of 70 K. The inner chamber contains a stopping volume with high buffer gas pressure and an extraction volume with low pressure and is pumped differentially. The beam is injected horizontally into the CSC and stopped in the buffer gas. Using electric fields the termalized ions are transported in vertical direction onto an array of RF carpets, which focusses the ions to several nozzles. The ions are swept out by the gas flow from the stopping volume to the extraction volume and there they are transported on a low-pressure RF carpet to the extraction nozzle and into an extraction RFQ.

Detailed simulations of the CSC have been performed. The RF carpet in the stopping volume will have a density of 6 electrodes/mm and be operated at frequencies up to 15 MHz. The stopping volume has a length of 2 m, and the maximum areal density will amount to 30 mg/cm^2. In parallel to the simulation studies, experiments with the prototype of the CSC have been performed at the FRS Ion Catcher to investigate the operation of the CSC at the high field strengths (>> 10 V/cm) planned for the CSC of the LEB [3]. From these, extraction times of 10 ms can be projected. The rate capability of the CSC will exceed 10^7 ions/s. The cryogenic system of the CSC will use electrically driven cryo-coolers. The pumping system of the CSC will include a helium recovery unit (HRU) [4] that allows the helium stopping gas to be re-circulated and continuously purified.

The HADO-CSC is also the basis for the development of stopping cells at ELI-NP [5] and SARAF [6].

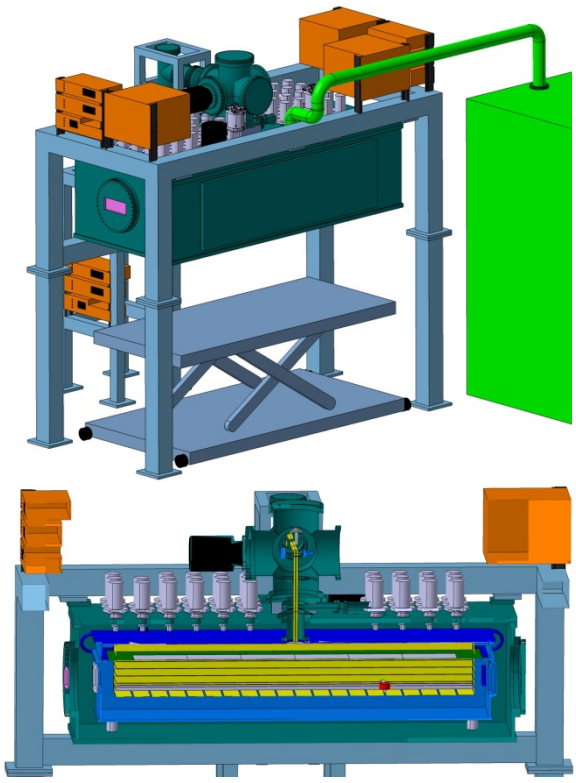

Figure 1: Digital mock-up of the stopping cell system for the LEB. Upper panel: Overview showing the stopping cell (dark green), HRU (light green), frames (grey) and electronics (brown). Lower panel: Cut along the longitudinal direction, showing the inner cryogenic chamber (blue) with the stopping volume (lower) and extraction volume (upper), the electrode system (yellow), the outer vacuum chamber (dark green), the extraction RF quadrupole, and the cryo-coolers (grey).

References

[1] T. Dickel et al., NIM B 376 (2016) 216.
[2] S. Purushothaman et al., EPL 104 (2013) 42001.
[3] A.-K. Rink, PhD thesis, JLU Gießen (2017).
[4] T. Sonoda et al., Rev. Sci. Instr. 87 (2016) 065104.
[5] D. L. Balabanski et al., Rom. Rep. Phys. 68 (2016) 621.
[6] I. Mardor et al., arXiv:1801.06493v2.

Experiment beamline: FRS / Super-FRS
Experiment collaboration: NUSTAR-Super-FRS-Experiments / FRS Ion Catcher
Experiment proposal: none
Accelerator infrastructure: none
PSP codes: 1.2.1.2; 1.2.3.13; 2.4.11.2.7; 2.4.11.2.8
Grants: BMBF (contract No. 05P16RGFN1), HMWK (LOEWE Center HICforFAIR), HGS-HIRe
Strategic university co-operation with: Gießen

Combining the in-flight particle identification with high resolution mass spectrometry at the FRS

E. Haettner[1], A. Spataru[1,2], S. Ayet[1,3], S. Bagchi[1], J. Bergmann[3], T. Dickel[1,3], J. Ebert[3], A. Finlay[4], H.Geissel[1,3], C. Hornung[3], S. Kaur[5], W. Lippert[3], I.Miskun[3], J.-H. Otto[3], S. Pietri[1], W. R. Plaß[1,3], A. Prochazka[1], S. Purushothaman[1], C. Rappold[1,3], A.-K. Rink[3], C. Scheidenberger[1,3], Y. Tanaka[1], H. Toernqvist[1], H. Weick[1], J. S. Winfield[1], the FRS Ion Catcher collaboration, and the Super-FRS Experiment collaboration

[1]GSI, Darmstadt, Germany; [2]University of Bucharest, Romania; [3]Justus Liebig University Giessen, Germany; [4]TRIUMF, Vancouver, Canada; [5]Saint Mary's University, Halifax, Canada.

The mass resolving power of the multiple-reflection time-of-flight mass spectrometer (MR-TOF-MS) [1], which is a part of the FRS Ion Catcher [2], can be as high as 600000 [1]. Thus it can provide an unambiguous identification by mass [3] of the various exotic ions produced and separated at the FRS [4]. This method of identification is independent on the standard identification scheme at the FRS which relies on measurement of magnetic rigidity, velocity, and nuclear charge at high velocity. In particular, identification by mass becomes valuable if the energies are not high enough to keep the ions of interest fully ionized, then a mixture of charge states appears which obscures the standard identification scheme of FRS. Moreover, the method allows the identification and counts long-lived isomers which are not possible with the standard PID of the FRS.

In an experiment, the time-of-flight signals from the MR-TOF-MS were fed into the FRS data acquisition system. A common clock gives the time for each ion passing the scintillation detector in front of the CSC and each ion detected by the MR-TOF-MS. This makes a correlation between particles passing the FRS and particles identified in the MR-TOF-MS possible for the first time. It was shown [5], that the particles of interest could be identified unambiguously by their mass-to-charge ratio also in the time-of-flight spectrum measured with the FRS DAQ.

In an experiment with ^{124}Xe fragments, the measured distributions in time of all particles passing in front of and ^{109}In ions behind the CSC were evaluated [5]; an example showing the time distribution during the spills is shown in Fig. 1. This comparison has applicability in several ways: (i) As a monitor of the efficiency of the setup as a function of the time. Thus it enables a more efficient optimization of the experiment and also serves as a monitor of the CSC performance during the experiment, e.g. detect losses during beam on time due to build-up of space charge. (ii) It is a measurement of the average extraction time of the ions from injection into the CSC to detection in the MR-TOF-MS. This information is crucial in experiments were correction for decay losses are needed, e.g. production cross section mesaurements or measurement of probability for β-delayed neutron emission [6]. Finally, the time of each event recorded in the MR-TOF-MS were compared to the time signal for beam on and beam off. This was successfully used to suppress background from the mass spectrum.

In future, the method will be developed as standard techniques to allow a more efficient setup of experiments with the FRS Ion Catcher, e.g. range adjustment. In purposive experiments even mass tagging by event-by-event correlation of the ions in front of and behind the CSC at an incoming rate of approximately 100Hz will be possible. This will for example allow measuring the ground-to-isomer ratio in dependence of the momentum transfer in the production, and thus, will give important insights to the production and population of exotic isotopes and their isomers [7].

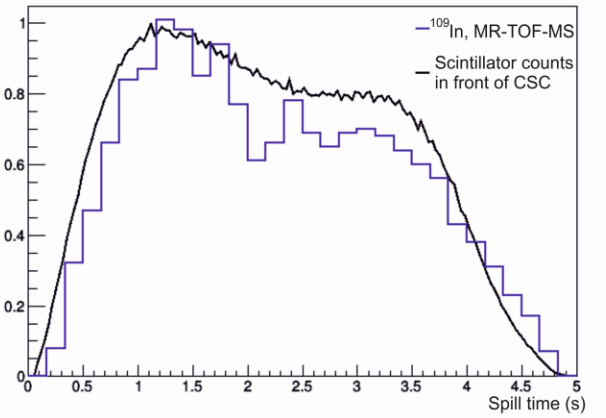

Figure 1: Measured time distribution of fragments passing the scintillation detector in front of the CSC (black) and ^{109}In ions detected by the MR-TOF-MS (blue).

References

[1] T. Dickel et al., Nucl. Inst. Meth. A 777 (2015) 172.
[2] W. R. Plaß et al., Nucl. Inst. Meth. B 317 (2013) 457.
[3] C. Hornung et al., GSI Sci. Rep. (2016) (GSI Report 2017-1) p. 175.
[4] H. Geissel et al., Nucl. Inst. Meth. B 70 (1992) 286.
[5] A. Spataru, Master thesis (2017), University of Bucharest, Romania.
[6] I. Mardor et al., this issue.
[7] U. Sauerwein, GSI Summer student report 2015.

Experiment beamline: FRS
Experiment collaboration:
NUSTAR-SuperFRS-Experiments / FRS Ion Catcher
Experiment proposal: S474
Accelerator infrastructure: UNILAC / SIS18
PSP codes: none
Grants: BMBF (05P12RGFN8 & 05P16RGFN1), HMWK (LOEWE Center HICforFAIR), HGS-HIRe
Strategic university co-operation with: Gießen

 DOI:10.15120/GR-2018-1

Mass measurements of neutron-rich Ti isotopes with the newly commissioned multiple-reflection time-of-flight mass spectrometer at TITAN, TRIUMF

M. P. Reiter[1,2], S. Ayet San Andres[1,3], C. Hornung[1], J. Bergmann[1], T. Dickel[1,3], J. Dilling[2,4], A. Finlay[2,4], H. Geissel[1,3], C. Jesch[1], A. A. Kwiatkowski[2], E. Leistenschneider[2,4], W. R. Plaß[1,3], D. Short[2], C. Scheidenberger[1,3], C. Will[1] and the TITAN collaboration

[1]JLU-Giessen, Giessen, Germany; [2]TRIUMF, Vancouver, Canada; [3]GSI, Darmstadt, Germany; [4]UBC, Vancouver, Canada;

TRIUMF's Ion Trap for Atomic and Nuclear science (TITAN) [1] is a multiple ion trap system capable of performing high-precision mass measurements and in-trap decay spectroscopy. In particular TITAN has specialised in fast Penning trap mass spectrometry of short-lived exotic nuclei using its Measurement Penning Trap (MPET). In order to reach the highest possible precision, ions can be charge bred into higher charge states by an Electron Beam Ion Trap (EBIT), reducing the required measurement time for a needed precision. Using highly charged ions, TITAN is capable of performing mass measurements of short-lived heavy species with very high precision. Although the Isotope Separator and Accelerator (ISAC) facility at TRIUMF, Vancouver, Canada can deliver high yields even for some of the most exotic species, some measurements suffer from a strong isobaric background. This background often prevents the high precision measurement of the exotic species of interest. To overcome this limitation an isobar separator based on the Multiple-Reflection Time-Of-Flight Mass Spectrometry (MR-TOF-MS) technique has been developed at the JLU-Giessen [2] and installed recently at TITAN (Fig. 1). The MR-TOF-MS is based on the design of the MR-TOF-MS developed for MATS [3,4] which is currently in use at the FRS Ion Catcher [5]. In contrast to this system, mass selection is achieved using dynamic re-trapping of the ions of interest after a time-of-flight analysis in an electrostatic isochronous reflector system [6]. Use of this novel technique allowed installation of the MR-TOF-MS with minimal impact on the existing TITAN beam line and also provides cooled and clean isobaric beams for downstream ion traps. Additionally the MR-TOF-MS enables mass measurements of very short-lived nuclides that are weakly produced, complementing TITAN's existing mass measurement program of short-lived exotic nuclei.

After a first online commissioning with stable beam from ISAC in early 2017 the MR-TOF-MS was employed in a measurement campaign trying to investigate the evolution of the N = 32 neutron shell closure around Ca-52. This shell closure forms several neutrons away from stability and has been established in neutron-rich K, Ca and Sc isotopes, where as in the higher Z elements, V and Cr, no shell effects had been found, leaving the intermediate Ti isotopes as the ideal test case for state-of-the-art ab-initio shell model calculations.

High-precision mass measurements with TITAN's MPET and the new MR-TOF-MS were able to prove the existence of a weak shell closure in Ti and were able to challenge four of the most successful modern ab-initio theories, which all over predict the strength of the weak N=32 shell closure [7]. The unexpected reduction in shell strength will be used to refine the aforementioned and forthcoming nuclear models.

Being able to detect all isobars at the same time, the new MR-TOF-MS has become a routine device during TITAN beam times, being used for real-time determination of the radioactive beam composition and optimization of the ISAC mass separator, for precision mass measurements and in the near future for isobar separation. The experiences gained at TITAN go hand in hand with further developments of the MR-TOF-MS system used at GSI as part of the FRS Ion Catcher and for future experiments with MATS and LaSpec at the Low-Energy Branch of the Super-FRS at FAIR.

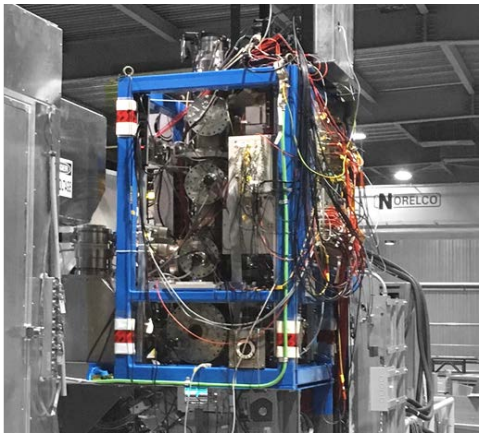

Figure 1: The new TITAN MR-TOF-MS system coupled to the existing TITAN beam line at TRIUMF.

References

[1] J. Dilling et al., IJMS 251, 198 (2006)
[2] C. Jesch et al., Hyperfine Interact. 235, 97 (2015)
[3] W. R. Plaß et al., NIM B 266, 4560 (2008)
[4] Dickel et al., NIM A 777, 172 (2015)
[5] W. R. Plaß et al., IJMS 349-350, 134 (2013)
[6] T. Dickel et al., JASMS 28, 1079 (2017)
[7] E. Leistenschneider et al., PRL. 120, 062503 (2018)

Experiment beamline: not applicable
Experiment collaboration: FRS Ion Catcher
Experiment proposal: not applicable
Accelerator infrastructure: not applicable
PSP codes: 1.2.3.13
Grants: NSERC, NRC, CNPq (249121/2013-1), Helmholz (VH-VI-417), HMWK (LOEWE), US-NSF (PHY-1419765), DFG (FR 601/3-1), BMBF (05P15RDFN1, 05P12RGFN8), NRC
Strategic university co-operation with: Gießen

Status of the EXPERT experiment

V. Chudoba[1,2], O. Kiselev[3], I. Mukha[3], L.V. Grigorenko[1,4,5], C. Scheidenberger[3,6], H. Geissel[3,6], S.G. Belogurov[1], A.A. Bezbakh[1,2], W. Dominik[7], V.B. Dunin[8], V. Eremin[9], I. Eremin[9], S.N. Ershov[10], N. Fadeeva[9], A.S. Fomichev[1,11], M.S. Golovkov[1,11], A.V. Gorshkov[1], Z. Janas[7], G. Kaminksi[1,12], A.G. Knyazev[1,13], Y.N. Kopach[14], A.A. Korsheninnikov[5], D. Kostyleva[6], E. Kozlova[3], S.A. Krupko[1], E.A. Kuzmin[5], Ch. Mazzocchi[7], I.A. Muzalevsky[1,2], E.Yu. Nikolskii[1,5], Y.L. Parfenova[1], M. Pfützner[7], S. Pietri[3], S.A. Rymzhanova[1], V. Schetinin[15], P.G. Sharov[1], S.I. Sidorchuk[1], H. Simon[3], R.S. Slepnev[1], G.M. Ter-Akopian[1,11], E. Terukov[9], Yu. Tuboltsev[9], E. Verbitskaya[9], H. Weick[3], X. Xu[16], and the Super-FRS Experiment collaboration

[1] Flerov Laboratory of Nuclear Reactions, JINR, Dubna, Russia; [2] Institute of Physics, Silesian University, Opava, Czech Republic; [3] GSI, Darmstadt, Germany; [4] University MEPhI, Moscow, Russia; [5] Kurchatov Institute, Moscow, Russia; [6] II. Physikalisches Institut, Justus-Liebig-Universität, Gießen, Germany; [7] Faculty of Physics, University of Warsaw, Poland; [8] Veksler and Baldin Laboratory of High Energy Physics, JINR, Dubna, Russia; [9] Ioffe Physical-Technical Institute, St.-Petersburg, Russia; [10] Bogolyubov Laboratory of Theoretical Physics, JINR, Dubna, Russia; [11] State University DUBNA, Dubna, Russia; [12] Heavy Ion Laboratory, Warsaw University, Warszawa, Poland; [13] Physics Department, Lund University, Lund, Sweden; [14] Frank Laboratory of Neutron Physics, JINR, Dubna, Russia; [15] Laboratory of Information Technologies, JINR, Dubna, Russia; [16] School of Physics and Nuclear Energy Engineering, Beihang University, Beijing, China.

The EXPERT (EXotic Particle Emission and Radioactivity by Tracking) setup is a part of the Super-FRS Experiment Collaboration [1]. Prototype detectors of EXPERT are being used in pilot experiments at the FRS in the FAIR Phase-0 (S443, S459).

Physics program and methods

The EXPERT experiments aim at studies of exotic nuclear systems in the most-remote part of the nuclear landscape close to the proton and neutron drip lines [2]. Nuclear decays with very small decay energies emitting proton(s) or neutron(s) in-flight, i.e., proton radioactivity and neutron radioactivity, can be studied by tracking the trajectories of the decay fragments and reconstructing their decay vertices. This technique allows for investigations of nuclei with short half-lives down to 10^{-12} s. Also proton–proton and neutron–neutron correlations, even in case of multiple proton or neutron decays, can be studied by tracking charged particles and neutrons. Complementarily, two-proton radioactivity will be studied by using an Optical Time-
Projection Chamber (OTPC) placed at the final focus of the (Super-)FRS, where exotic nuclei are first implanted into the OTPC and then decay. These two detection schemes of EXPERT may utilize the same radioactive beam simultaneously and therefore efficiently. Together they cover half-life ranges from 10^{-12} to 10^{-7} s (with the in-flight decay technique) and from 10^{-7} to 1 s (with the implantation-decay method). Such a combination has successfully been demonstrated at the FRS [3].

The EXPERT modular detector assembly consists of 5 subsystems sketched in Fig.1, whose locations at the future Super-FRS are shown in Fig.2. The silicon (Si) beam-detector subsystem consists of the Si-strip timing detectors SSD, the tracking module (double-sided Si microstrip detectors), the γ-ray detector GADAST (128 CsI(Tl) and 32 LaBr3(Ce) crystals), the neutron detector NeuRad (~10000 scintillator fibers), and the implantation detector on the basis of OTPC.

The SSD detectors should provide timing information of the heavy ions up to U with the precision of 50 ps and for lighter ions of 100 ps. In addition, hit coordinates of the ions need to be measured with a precision of 0.3 mm and the deposited ionisation energy with a precision of 5%.
The microstrip Si tracking detectors should deliver proton-hit coordinates with an accuracy of 30 μm. The energy-deposition measurement should identify ions with Z < 28 at counting rates up to 10^4 s^{-1}.

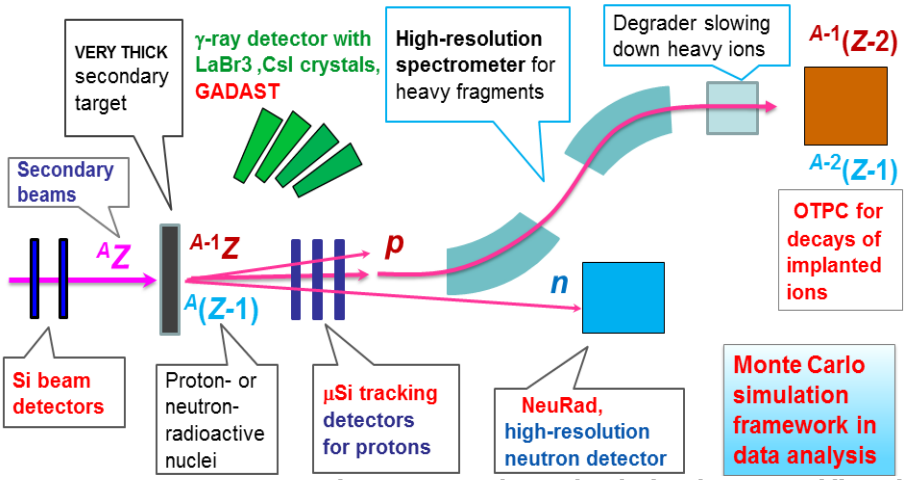

Figure 1. The EXPERT main components and experiment scheme sketched at the FRS middle and final focal planes.

 DOI:10.15120/GR-2018-1

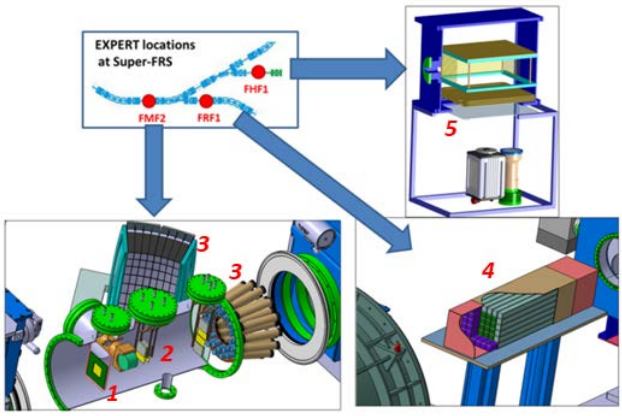

Figure 2: Locations of the EXPERT detectors at the Super-FRS middle and final focal planes (upper-left panel). Itemized instrumentation: 1 – Si beam detectors, SSD; 2 – microstrip Si tracking detectors; 3 – γ-ray detectors GADAST; 4 – neutron detector NeuRad; 5 – optical time-projection chamber OTPC.

The energy resolution of the γ-ray detector GADAST should be ~5% at 3 MeV. GADAST should work at a flux up to 1000 cm^{-2} s^{-1} of γ-rays and charged particles.

The OTPC should provide 3D reconstruction of implanted multi-particle decays of fragments and measure the charge, energy and emission angle of the decay products. With respect to the existing device the size needs to be increased by 20-30%, and the angular and energy resolution to be improved by a more advanced digital photo camera.

The angular resolution of the neutron detector NeuRad must be below of 0.2 mrad. The detection threshold for the energy deposited after one interaction of a neutron should not exceed 1 MeV and the time resolution of 0.5 ns. The total angular range covered by the detector is supposed to be 12 mrad. The planned size and location of the detector as well as its high granularity shall allow for distinguishing multiple neutron interactions as well.

EXPERT technical status

The technical feasibility of EXPERT has been proven by two successful experiments with the exotic ion beams performed at GSI and several test experiments at GSI and JINR, which resulted in a dozen publications (see e.g., Refs. [3,4]). The most recent result is the observation of previously-unknown isotopes ^{29}Ar, ^{28}Cl, ^{30}Cl and the first spectroscopy of ^{31}Ar. The data have been obtained as a by-product of the main objective ^{30}Ar (see the recent article [4]) during the pilot EXPERT experiment S388 in 2012. The corresponding contribution by D. Kostyleva et. al. follows this report.

The parameters of the different subsystems are proven by testing the prototypes or using final detectors during the pilot experiments at GSI. Prototypes of all components have shown good functionality in high-precision tracking and time measurements of light and heavy ions simultaneously; in neutron detection with the highest spatial resolution; in tagging of the radioactive decays with fine structure by using a segmented γ-ray detector GADAST with efficiency of 10% of 4π; and in implantation-decay measurements with OTPC. The EXPERT Technical Design Report has been approved by the ECE/FAIR in 2017 [5].

Tests in 2017

The NeuRad timing properties have been tested with a 20 cm long, 16x16 bundle of scintillation fibers BCF-12, two multi-anode PMTs H9500 and a 128-channel readout system based on TOFPET ASICs [6]. A new updated version of this system is under investigation. The first results on performance of such a NeuRad prototype have been obtained by detecting tracks produced by cosmic radiation, which is presented in the contribution by D. Kostyleva et. al.

Several Si microstrip detectors have been refurbished in order to use new front-end ASICs IDE1140 from IDEAS. The detectors have been tested in the laboratory and are ready for GSI-beam tests in 2018. Lower noise level, better linearity and higher dynamic range allow for a better resolution in tracking and identification of ions and protons.

A new readout system for the TOF Si detectors has been assembled and tested. It uses the last version of the front-end amplifier/discriminator ASIC PADI-X and FPGA TDC providing the highest time resolution down to 11 ps per channel. This system is prepared for beam tests of the new Si TOF detectors at GSI in 2018.

For GADAST, newly purchased LaBr3(Ce) crystals have been tested at the INP Krakow, Poland. GADAST has been prepared for commissioning as a detector for heavy charged particles in experiments at JINR in 2018.

The day-0 experiments with EXPERT in 2018/2019

The EXPERT components (new Si timing and Si tracking detectors) are planned to be tested during the beamtime assigned to the experiments S443 (Search for four-proton decay of Mg-18) and S459 (Two-proton radioactivity of unobserved S-26). In total, 4+4 shifts of beamtime in parasitic and main-user modes have been granted. The allocated beamtime is sufficient for testing the developed EXPERT instrumentation. For this purpose, in-flight detection of two-proton (^{12}O) or four-proton (^{8}C) decay precursors has been proposed, which is possible with primary beams ^{16}O or ^{12}C, respectively. The scheme of such test experiment is shown in Figure 3.

The proposed experiment allows for testing all components of EXPERT (except the neutron detector NeuRad) by using the known decay schemes and levels of 2p/4p emitters ^{12}O/^{8}C [7,8] whose decay energies will be re-measured by registering ^{9}C+p+p or ^{4}He+p+p+p+p coincidences, respectively. Such a calibration is feasible within the granted beam-time because of sufficiently high production rates of the nuclei of interest at FRS.

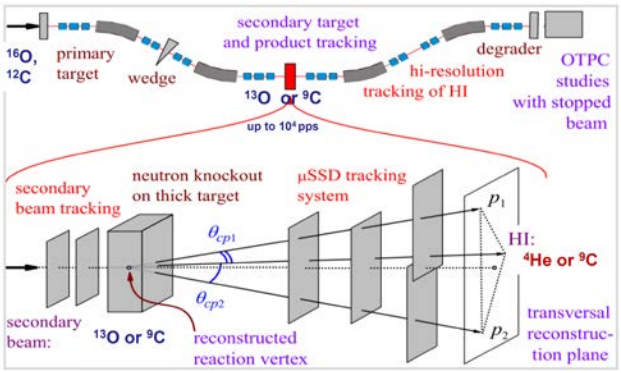

Figure 3. Sketch of the EXPERT test experiment at FRS. Beams of $^{16}O/^{12}C$ are fragmented in a primary target, and a secondary $^{13}O/\ ^{9}C$ beam is selected and focused on the middle focal plane in achromatic ion-optics mode. Nuclei of interest $^{12}O/^{8}C$ are produced in the secondary target in one-neutron knock-out reaction. Heavy-ion decay products $^{9}C/^{4}He$ are identified by their energy-loss and time-of-flight as well as the magnetic rigidity by using the standard FRS beam detectors. At the final focal plane of FRS, the studies of beta-delayed proton radioactivity of the stopped $^{13}O/\ ^{9}C$ ions will be performed by using the implantation-decay method with OTPC. The lower inset shows the EXPERT decay-in-flight detectors located downstream the secondary target, where the trajectories of incoming ions as well as the trajectories of the decay products $^{9}C/^{4}He$ and protons p1, p2 are measured.

References

[1] J. Aysto et al., Nuclear Instruments and Methods in Physics Research B **376**, 111 (2016).
[2] H. Geissel et al., Proc. Int. Symposium on Exotic Nuclei (EXON2014), World Scientific, 2015, ISBN 978-981-4699-45-7, p. 579.
[3] I. Mukha et al., Phys. Rev. Lett. **115**, 202501 (2015).
[4] X. Xu et. al., Phys. Rev. C **97**, 015202 (2018).
[5] Technical Design Report of the EXPERT setup for FAIR, 2017, https://edms.cern.ch/document/1865700.
[6] D. Kostyleva et al., GSI Scientific Report 2016, DOI:10.15120/GR-2017-1, p.171.
[7] M.F. Jager et al., Phys. Rev. C **86** (2012).
[8] R.J. Charity et al., Phys. Rev. C **84** (2011).

Experiment beamline: FRS

Experiment collaboration: NUSTAR-SuperFRS-Experiments

Experiment proposal: S443, S459

Accelerator infrastructure: UNILAC / SIS18 / FRS /

PSP codes: 1.2.10.7

Grants: HRS-HIREe / BMBF GSI-JINR grant /

Strategic university co-operation with: Darmstadt / Gießen /

New isotopes ^{29}Ar and ^{28,30}Cl observed during the EXPERT pilot experiment

D. Kostyleva[1], I. Mukha[2], L.V. Grigorenko[3,4,5], L. Acosta[6], E. Casarejos[7], A.A. Ciemny[8], W.Dominik[8],J. Duénas-Díaz[9], V. Dunin[10], J.M. Espino[11], A. Estradé[12], F. Farinon[2], A. Fomichev[3], H. Geissel[1,2],A. Gorshkov[3], Z. Janas[8], G. Kaminski[3,15], O. Kiselev[2], R. Knöbel[2], S. Krupko[3], M. Kuich[8],Yu.A. Litvinov[2], G. Marquinez-Durán[9], I. Martel[9], C. Mazzocchi[8], C. Nociforo[2], A. K. Ordúz[9],M. Pfützner[8], S. Pietri[2], M. Pomorski[8], A. Prochazka[2], S. Rymzhanova[3], A.M. Sánchez-Benítez[9],C. Scheidenberger[1,2], P. Sharov[3], H. Simon[2], B. Sitar[13], R. Slepnev[3], M. Stanoiu[14], P. Strmen[13], I. Szarka[13],M. Takechi[2], Y.K. Tanaka[15], H. Weick[2], M. Winkler[2], J.S. Winfield[2], X. Xu[1,16], and M.V. Zhukov[17]

[1]II. PhysikalischesInstitut, Justus-Liebig-Universität, Gieβen, Germany; [2]GSI, Darmstadt, Germany; [3]Flerov Lab of Nuclear Reactions, JINR, Dubna, Russia; [4]University MEPhI, Moscow, Russia; [5]Kurchatov Institute, Moscow, Russia; [6]Instituto de Física, Universidad Nacional Autónoma de México, Mexico; [7]University of Vigo, Spain; [8]Faculty of Physics, University of Warsaw, Poland; [9]Department of Applied Physics, University of Huelva, Spain; [10]Veksler and Baldin Lab of High Energy Physics, JINR, Dubna, Russia; [11] Department of Atomic, Molecular and Nuclear Physics, University of Seville, Spain; [12]University of Edinburgh, UK; [13]Faculty of Mathematics and Physics, Comenius University, Bratislava, Slovakia; [14]IFIN-HH, Bucharest, Romania;[15]Heavy Ion Laboratory, University of Warsaw, 02-093 Warszawa, Poland; [16]School of Physics and Nuclear Energy Engineering, Beihang University, Beijing, China; [17]Department of Physics, Chalmers University of Technology, Göteborg, Sweden

The EXPERT pilot experiment S388 has been performed at FRS in 2012. Here we report the preliminary results of the data analysis indicating an observation of previously-unknown isotopes ^{29}Ar, ^{28}Cl, ^{30}Cl and the first spectroscopy of ^{31}Ar [1]. The data have been obtained as a by-product of the main objective, ^{30}Ar [2,3].

EXPERT pilot experiment at FRS. The proton-unbound argon and chlorine isotopes were detected by measuring trajectories of their decay-in-flight products by using a tracking technique with micro-strip detectors.

The primary ^{36}Ar beam hit a thick target, and a secondary beam of ^{31}Ar was selected and focused on the middle focal plane, where nuclei of interest ^{31}Ar*,^{29}Ar were produced in the secondary target in reactions of in-elastic scattering and two-neutron knock-out. Decay products ^{27,30}S were identified by their energy-loss and time-of-flight as well as the magnetic rigidity by using the standard beam detectors of FRS. The proton (1p) and two-proton (2p) emission processes have been identified in the measured angular correlations of decay products, heavy ions (HI) with protons, HI+p and HI+p+p, respectively.

Monte-Carlo simulations. The ground states of the previously unknown isotopes ^{30}Cl and ^{28}Cl have been discovered, providing the 1p-separation energies of about 0.48(2) and 1.60(8) MeV, respectively, see [1] for details. In order to interpret the angular spectra quantitatively and precisely identify the 1p and 2p decay energies, one has to perform detailed Monte-Carlo simulations of the setup response. Such simulations were performed by using the GEANT-based program which was calibrated on the known 2p-decay pattern of ^{19}Mg [2]. The states of interest were fit by varying the assumed values of their 1p-decay energies. Each simulated spectrum was then compared with the corresponding experimental angular correlation. The simulated distribution and experimental data were tested for compatibility by applying the Kolmogorov-Smirnov algorithm, see details in [3]. This test provides a probability that the data and simulation distributions have the same shape. The probability plotted as a function of decay energy provides the best-fit decay energy and its uncertainty. For example, on Fig.1, one can see the distribution of probability obtained for different 1p-decay energy of the ^{30}Cl first excited state. The derived 1p-decay

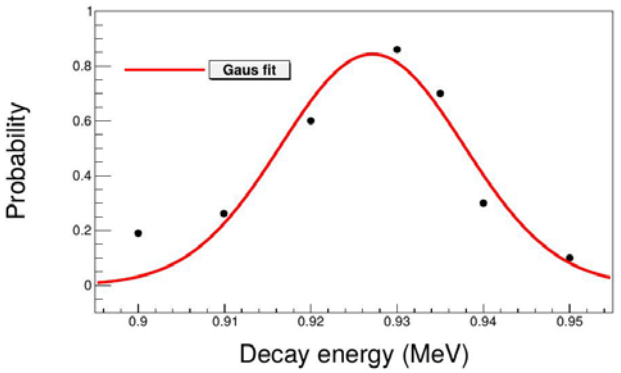

Figure 1:Probability that the ^{30}Cl data are reproduced by the respective simulations as a function of 1p-decay energy.

energy of the first excited state of ^{30}Cl is about 0.93(3) MeV. In a similar way, the observed excited states of ^{31}Ar allow to infer 2p-separation energy of 6(34) keV for its ground state. Moreover, one level was observed in ^{29}Ar. The observed state in ^{29}Ar with the derived 2p-decay energy of 5.50(18) MeV may be identified either as a ground or an excited state depending on the systematics applied in analysis. The relevant systematics of 1p and 2p separations energies have been studied theoretically in the HI+p and HI+p+p cluster models.

References

[1] I. Mukha, L.V. Grigorenko, D. Kostyleva et al., arXiv:1803.10951 [nucl-ex] (2018).
[2] I. Mukha et al., Phys. Rev. Lett. **115**, 202501 (2015).
[3] X. Xu et. al., Phys. Rev. C **97**, 015202 (2018).

Experiment beamline: FRS
Experiment collaboration: SuperFRS Experiments
Experiment proposal: [S338]
Accelerator infrastructure: SIS18 / FRS / Super-FRS /
PSP codes: 1.2.10.7
Grants: HRS-HIREe/BMBF GSI-JINR grant /
Strategic university co-operation: Darmstadt/Gießen/

 DOI:10.15120/GR-2018-1

Tracking cosmic radiation by the NeuRad neutron detector prototype with multi-channel readout electronics

D. Kostyleva[1], A.A. Bezbakh[2,3], V. Chudoba[2,3], A.S. Fomichev[2], A.V. Gorshkov[2], O. Kiselev[4], S.A. Krupko[2], I. Mukha[4], I.A. Muzalevskii[2,3], C. Scheidenberger[1,4] for the Super-FRS Experiment collaboration

[1] II.PhysikalischesInstitut, Justus-Liebig-Universität, Gießen, Germany; [2]Flerov Laboratory of Nuclear Reactions, JINR, Dubna, Russia; [3] Institute of Physics, Silesian University, Opava, Czech Republic; [4]GSI, Darmstadt, Germany.

The NeuRad (Neutron Radioactivity) detector for high-energy neutrons belongs to the EXPERT (EXotic Particle Emission and Radioactivity by Tracking) setup which is a part of the Super-FRS Experiment Collaboration [1]. NeuRad is constructed out of ~10^4 scintillation fibers, and it is aimed at high-precision measurements of the angular correlations between the neutrons and heavy fragments stemming from exotic neutron decays. Due to a high granularity, an important feature of the NeuRad is the ability to track trajectories of the recoil protons produced by incident neutrons. The results of the tests of NeuRad tracking properties measured with cosmic radiation are presented in this report.

The first tests of NeuRad prototype. The first test of the timing properties of the NeuRad detector prototype has been performed at FLNR JINR and later on at GSI [2]. The demonstrator, consisting of a 16x16 bundles of BCF-12 scintillation fibers (each fiber is 25 cm long and has 3x3 mm^2 cross section) coupled with two PMT's H9500, has been irradiated by a ^{60}Co gamma-ray source. The time uncertainty between two opposite PMT channels was determined to be ~ 1 ns (sigma). The reference measurement with a BC-420 0.4 cm thick scintillator and two H9500 PMTs showed the time resolution of 0.5-0.7 ns.

PETsys TOFPET2 ASIC readout chip. The next test of the NeuRad prototype has been done with the multi-channel electronics. For this purpose, the readout system provided by the PETsys Electronics has been chosen. This system is based on the high performance TOFPET2 ASIC, which is a new 64-channel chip combining a current amplifier, discriminator, TDC and QDC. It is developed for the readout and digitization of signals from fast photon detectors in applications where high data rates and fine time resolution are required [3]. In order to test the TOFPET2 performance, the PETsyscompany provided an Evaluation Kit which includes two LYSO crystals of 3x3x5 mm^3 viewed by two KETEK SiPM PA3325-WB-0808 arrays mounted on a board that plugs into the TOFPET2 ASIC test board. The kit has been tested with a standard ^{22}Na source. The time resolution, obtained with the kit, is ~95 ps, see Fig. 1(a), or ~67 ps per channel.

The NeuRad prototype test with TOFPET2 ASIC. The NeuRad prototype module (see above for the details) has been tested with the PETsys e-kit using cosmic radiation. H9500 MAPMTs were coupled to the electronics via special connectors, so the signals from only 64 fibers on each side were measured. The data acquisition was set in a coincidence mode, i.e. only the events creating signals on both PMTs with a time difference less than 20 ns were recorded. Precise timing of the signals in each channel (fiber) allowed for restoration of the track of the cosmic particle crossing the NeuRad prototype. In Fig.1(b) one can see a typical track from a cosmic-ray particlepresented in the transverse cross-section of the prototype. The presented event has the time resolution 0.5(3) ns.

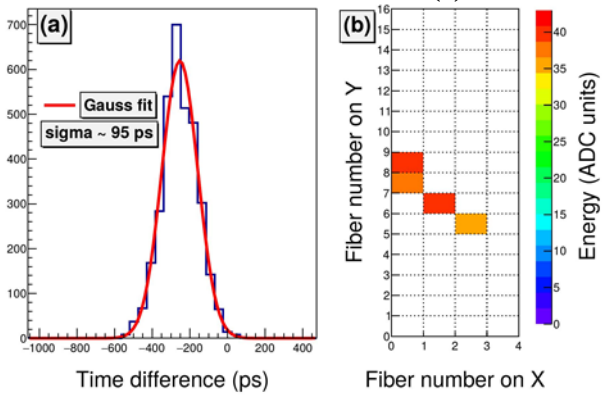

Figure 1: (a) Time resolution with LYSO crystals, SiP-Mphotosensors and TOFPET2 ASIC. (b) The track of a cosmic-ray particle in a transverse cross-section of the NeuRad prototype. Both sides of 4 x 16 fibers are readout by the PMTs and TOFPET2 system. The measured light intensity (due to ionization energy loss in a fiber) is shown in colours.

The measurement has shown that the tracks of minimum-ionizing cosmic-ray particles can be determined within each fiber of the NeuRad detector prototype by using the TOFPET2 ASIC electronics.

The day-0 experiments with NeuRad/EXPERT in 2018/2019. The NeuRad prototype will be tested at FRS during the beam-time assigned to the experiments S443 and S459.

References

[1] Technical Design Report of the EXPERT setup for FAIR, 2017, https://edms.cern.ch/document/1865700.

[2] D. Kostyleva et al., GSI Scientific Report 2016, DOI:10.15120/GR-2017-1, p.171.

[3] http://www.petsyselectronics.com

Experiment beamline: FRS
Experiment collaboration: NUSTAR-SuperFRS-Experiments
Experiment proposal: [S443, S459]
Accelerator infrastructure: SIS18 / FRS / Super-FRS /
PSP codes: 1.2.10.7
Grants: HRS-HIREe / BMBF GSI-JINR grant /partial support by RSF (project No.17-12-01367) / FAIR-Russia Research Center/
Strategic university co-operation: Darmstadt / Gießen

Measurements of proton and matter radii of neutron-rich isotopes

S. Bagchi[1,2,3], Y. Tanaka[1,2,3], R. Kanungo[1,4], H. Geissel[2,3], C. Scheidenberger[2,3], K. -H. Behr[2], A. Prochazka[2] and the S395 and the NP1412-RIBF132 Collaborations

[1]Saint Mary's University, Halifax, Canada; [2]GSI, Darmstadt, Germany; [3]JLU, Giessen, Germany; [4]TRIUMF, Canada.

Recent trends in nuclear physics research are moving towards studies with radioactive ions or rare isotopes where the neutron-to-proton ratio is quite exotic. Since the discovery of exotic nuclei, characterized by halos and skins, interaction cross section measurements and high-resolution momentum measurements have played a key role to identify nuclei with new properties due to extended spatial distributions of the valence nucleons [1]. The proton distribution radius is crucial for determining the neutron-skin thickness if the matter radius is known. The proton radius is also necessary to understand the spatial correlation between the halo and the core. The experiments based on high-energy electron scattering, atomic hyperfine structure or isotope shift have limitations for very short-lived nuclei available with low beam intensity. On the other hand, charge changing cross section measurements are a versatile tool which can be applied very well for stable nuclei as well as for exotic nuclei far from the β-stability line.

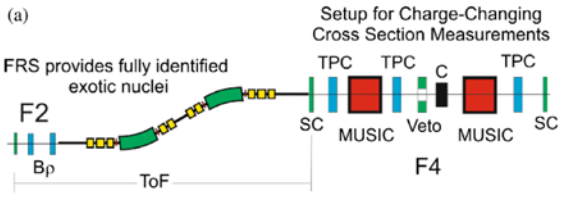

Figure 1: Schematic view of the second half of the FRS spectrometer at GSI with the detector setup to measure the charge changing cross section.

The exotic nuclei facility at GSI is unique in having energies up to 1*A* GeV. Experiments for precise radii measurements are best suitable at this energy as a wide variety of isotopes of interest is fully ionized. It is also possible to perform such studies for light nuclei at beam energies around 200-300 MeV/u that are available at RIKEN. In Fig. 1, second half of the fragment separator at GSI [2] is shown along with the detector configuration at the final focus of the FRS. Details of the experimental setup and methodology is mentioned in Refs.[3-5].

To obtain the proton radii from the measured σ_{cc}, finite-range Glauber model framework is used. For stable isotopes (e.g. ^{10}B, $^{12-14}$C, ^{14}N), the obtained proton radii are in good agreement with the electron scattering data [3-5]. Together with information on the matter distribution radii from interaction cross section measurements, a very thick neutron-skin has been obtained for ^{22}N [5].

Extending these investigations of halo and shell evolution to the neutron-rich fluorine isotopes, in this context we also mention our recent experiment at the BigRIPS [6] and ZeroDegree Spectrometer (ZDS) facilities at the RIKEN RI Beam Factory. The interaction cross section, charge changing cross section and longitudinal momentum distribution measurements were performed. The details on the experiment and the detector setup can be found in Ref.[7].

A carbon reaction target placed at the F8 focus was surrounded by the DALI2 gamma detector array [8] to detect excited states of the nucleus and/or the fragment. The analysis of the work is in progress.

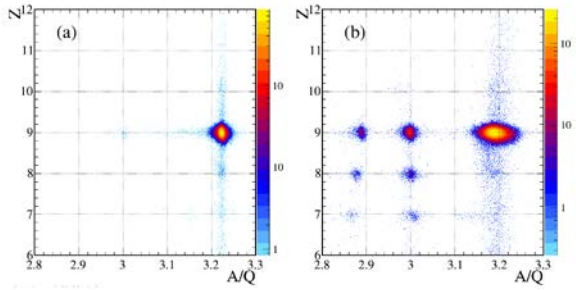

Figure 2: Particle identification spectrum using the ZDS spectrometer set for (a) ^{29}F and (b) ^{27}F

References:

[1] I. Tanihata et al., PRL 55, 2676 (1985).
[2] H. Geissel et al.,Nucl. Instrm. Meth. B 70, 286 (1992).
[3] A. Estrade et al., PRL 113, 132501 (2014).
[4] R. Kanungo et al., PRL 117, 102501 (2016).
[5] S. Bagchi et al., submitted for publication.
[6] T. Kubo et al., Nucl. Instrm. Meth. B 204, 97 (2003).
[7] R. Kanungo et al.,RIKEN Accel. Prog. Rep. 50 (2017).
[8] S. Takeuchi et al.,Nucl. Instrm. Meth. A 763, 596 (2014).

Experiment beamline: FRS
Experiment collaboration: NUSTAR-SuperFRS-Experiments
Experiment proposal: S395
Accelerator infrastructure: SIS18 / FRS
PSP codes:
Grants: (experiment) NSERC, Canada; PR China government and Beihang University under the Thousand Talent program

Strategic university co-operation with: Saint Mary's University, JLU Gießen, Hokkaido University, University of Tennessee, Nihon University, Santiago de Compostela University, Comenius University, Dalhousie University, Osaka University, Beihang University, University of Tokyo.

 DOI:10.15120/GR-2018-1

Charge changing cross section measurement of cobalt isotopes

S. Kaur[1,2], R. Kanungo[1,4], S. Bagchi[1,3], S. Ayet[3,5], J. Bergmann[5], T. Dickel[3,5], J. Ebert[5], A. Finley[4,6], H. Geissel[3,5], E. Haettner[3], C. Hornung[5], W. Lippert[5], I. Miskun[5], J.-H. Otto[5], S. Pietri[3], W. R. Plaß[3,5], S. Purushothaman[3], A.-K. Rink[5], C. Scheidenberger[3,5], Y. Tanaka[3,5], H. Weick[5], J. Winfield[3] and the Super FRS experiment Collaboration

[1]Saint Mary's University, Halifax, Canada; [2]Dalhousie University, Halifax, Canada; [3]GSI, Darmstadt, Germany; [4]TRIUMF, Vancouver, Canada; [5]JLU, Giessen, Germany; [6]UBC, Vancouver, Canada

The charge radius is an important bulk property of a nucleus for investigating nuclear structure. The knowledge of proton radii is crucial for understanding halo and skin formation and also the shell evolution in unstable nuclei. The proton radii also serve as a test of newly developed structure models including those based on ab-initio theory. Electron scattering measurements are ideal for probing the distribution but so far not applicable to short-lived unstable nuclei. Isotope shift measurements allow us to precisely deduce the charge (proton) radius for some unstable nuclei. The measurement of the charge-changing cross sections (σ_{CC}) is a potential method that can be used to extract the proton radius for stable nuclei and as well as for exotic nuclei far from the β-stability line. The proton radii of light unstable nuclei have been successfully determined from the σ_{CC} measurements using the Glauber Model framework in ref. [1-3].

We report here the charge-changing cross section measurements of $^{57-59}$Co that were performed to investigate the application of this new tool to extract proton radii of medium mass projectiles at intermediate energy. The test measurement was performed at the fragment separator (FRS) [4] at GSI, Germany. Beams of $^{57-59}$Co were produced by fragmentation of a ^{124}Xe beam at 600 MeV/u, on a 1612 mg/cm^2 thick Be target. The isotopes of interest were separated in flight and identified through the magnetic rigidity (Bρ) - time of flight (TOF) - energy loss (ΔE) method. In Fig. 1(a), the second half of the FRS is shown along with the detector configuration at the final focus of the FRS. The TOF of the incoming beam was measured from the intermediate focal plane F2 to F4 using plastic scintillators. The event-by-event Bρ of the incoming particles was determined from the horizontal position of particles, measured with a scintillator detector at F2 and time-projection chambers (TPC) at F4. Multisampling ionization chambers provided the energy loss (ΔE) measurements (Fig.1b). A 2.5 g/cm2 thick carbon reaction target was placed at F4. A veto scintillator with a central aperture placed in front of the target rejected beam events incident on the edges of the target scattered by matter upstream and the multi-hit events. The σ_{CC} is measured using the transmission technique, where the σ_{CC} is obtained from the relation:

$$\sigma_{CC} = \frac{1}{t} ln\left(\frac{R_{out}}{R_{in}}\right)$$

Here $R_{in(out)}$ = N_{sameZ}/N_{in} is the transmission ratio with (without) the target and t denotes the target nuclei per cm^2. In this method, the number (N_{in}) of incident nuclei ^{A}Z before the reaction target are identified and counted. After the target, we only require to identify and count the nuclei with the same charge Z (Fig.1c). The losses due to interactions with non-target materials are accounted by taking the measurements without the target in the setup.

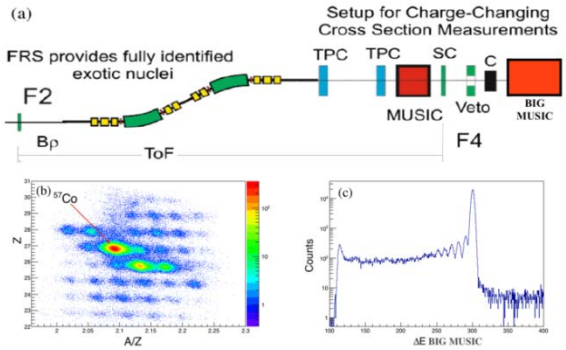

Figure 1: (a) Schematic view of the second half of the FRS spectrometer. (b) Particle identification spectrum before the C reaction target. (c) The energy loss spectrum in MUSIC after the reaction target with ^{57}Co incident beam.

The point proton radii (protons considered as point particles) will be determined from the measured σ_{CC} using the Finite-range Glauber model. This technique has been successfully applied to determine the proton radii of B, C and N isotopes where proton radii of stable isotopes (^{10}B, $^{12-14}$C, ^{14}N) agree very well with the electron-scattering experiments [1-3]. The measured σ_{CC} of ^{59}Co will be used to compare to known proton radii from electron scattering.

References:

[1] A. Estrade et al., Phys. Rev. Lett. 113, 132501 (2014).
[2] R. Kanungo et al., Phys. Rev. Lett. 117, 102501 (2016).
[3] S. Bagchi et al., submitted to journal.
[4] H. Geissel et al., Nucl. Instrum. Methods Phys. Res., Sect. B 70, 286 (1992).

Experiment beam line: FRS
Experiment collaboration: NUSTAR-SuperFRS-Experiments
Experiment proposal:
Accelerator infrastructure: SIS18 / FRS
PSP codes:
Grants: NSERC, Canada.
Strategic university co-operation with: Saint Mary's University / University of Giessen / Dalhousie University

Energy-dependent total charge changing cross-sections of ^{12}C

A. Prochazka[1], S. Bagchi[1,2], H. Geissel[1,2], E. Haettner[1], C. Hornung[2], S. Pietri[1], S. Purushothaman[1], C. Scheidenberger[1,2], Y. Tanaka[1,2], H. Weick[1] , J. Winfield[1], X. Xu[1] and the Super-FRS Experiment Collaboration

[1]GSI, Darmstadt, Germany; [2]Justus-LiebigUniversität, Gießen, Germany

Charge changing reactions are used to determine the root mean square radius of the nucleus proton distribution. In this work we measured total charge changing cross-sections of ^{12}C ions in carbon, polyethylene and lead targets at 350, 450 and 600 MeV/u. The measurements were done at the FRS using the transmission method as described in [1]. The experimental setup shown in Figure 1 was located at the final focal plane of the FRS. The incoming beam was identified in mass and charge using the FRS spectrometer, TPC tracking detectors, time-of-flight detectors and the multiple sampling ionization chamber MUSIC [2] in front of the target on event-by-event basis. The reaction rate was measured using the second MUSIC detector placed behind the reaction target.

The goal of the measurement was to measure total charge changing cross sections at intermediate energies where previous partly contradicting experimental values exist. Multiple data sets are compared in Figure 2, where it can be seen that the data measured in [3] and [6] are not in agreement with the data published in [1],[4],[5] and [7]. The preliminary cross sections measured at the FRS from this work (shown by red points in Figure 2) support the group of measurements with higher cross-section values.

Glauber model type calculations are used to describe the charge changing cross sections and relate them to effective proton radii. Two Glauber Model calculations reproducing the same experimental effective charge radius of ^{12}C (2.47 fm) are show in Figure 2. The blue line corresponds to the optical limit zero range calculation corrected by the empirical energy dependent scaling as described and used in [8] which reproduces the ^{28}Si charge changing cross sections. The orange line corresponds to optical limit finite range calculations as used in [3].

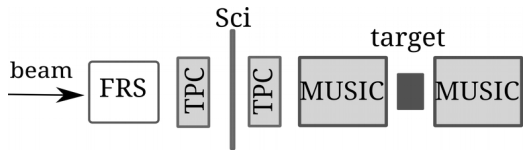

Figure 1: Experimental setup at S4 focal plane of the FRS.

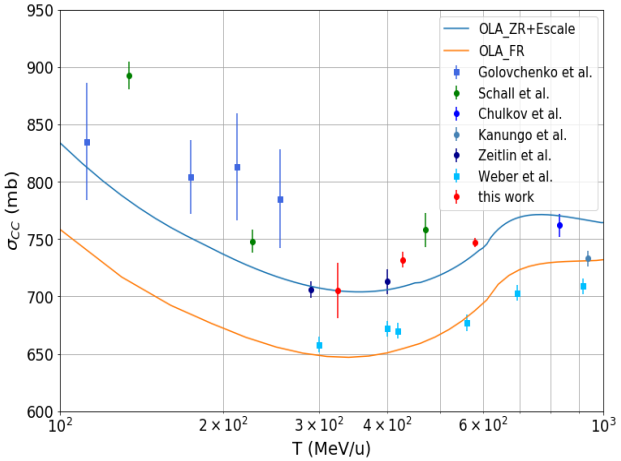

Figure 2: Experimental total charge changing cross-sections of ^{12}C ions on C targets as a function of energy. The data from this work (red points) are compared to the other experimental data shown by green and blue squares. Glauber Model calculations are shown by solid lines.

Using the two different models the same radius leads to cross sections which differ by ~5%. Therefore we aim to develope a model which reproduces the measured total charge changing and also total reaction cross-section data with the same time and without empirical corrections. As a first attempt we extended the models used in [3] and [8] by correction to the residual nucleus evaporation after one- and multi-neutron removals. The development is ongoing and the code will be published as an open source.

References

[1] L.V. Chulkov et al., Nuclear Physics A 674 (2000) 330-342
[2] MUSIC manual: https://www-win.gsi.de/frs/technical/FRSsetup/detectors/music80/music80_manual.pdf
[3] R. Kanungo et al., Phys.Rev.Lett.117(2016) 102501
[4] A.N. Golovchenko et al., Phys. Rev. C66, 014609
[5] I. Schall et al., NIM B117 (1996) 221-234
[6] W.R. Weber et al., Phys. Rev. C41 (1990)
[7] C. Zeitlin et al., Phys. Rev. C76 (2007) 014911
[8] T. Yamaguchi et al., Phys. Rev. C82 (2010) 014609

Experiment beamline: FRS
Experiment collaboration: NUSTAR-SuperFRS-experiments
Experiment proposal:
Accelerator infrastructure: SIS18
PSP codes:

 DOI:10.15120/GR-2018-1

Concept of a MUSIC detector for high Z-resolution measurements

S. Bagchi[1,2,3], B. Voss[2], C. Scheidenberger[2,3], R. Kanungo[1,4], K-H. Behr[2] and the Super-FRS Experiment Collaboration

[1]Saint Mary's University, Halifax, Canada; [2]GSI, Darmstadt, Germany; [3]JLU, Giessen, Germany, [4]TRIUMF, Canada

Research in nuclear physics is now moving towards studies with radioactive ions or exotic isotopes far from the line of stability. Facilities like FRS at GSI, Darmstadt, Germany, BigRIPS at RIKEN, Tokyo, Japan and NSCL, USA produce the extensive part of the exotic nuclei in the nuclear landscape. In order to identify the exotic nuclei after production Bρ-ΔE-TOF technique is used. Energy loss measurements give the Z identification of the products since $\Delta E \propto Z^2$. The nuclear charge Z of the secondary ion is obtained by measuring the energy loss in MUltiple-Sampling Ionization Chamber (MUSIC) [1, 2].

Here we report on the concept of compact portable detector for high-resolution Z measurements for experiments at GSI and possibly other RI beam facilities worldwide. The main goal of this MUSIC detector is to measure the Z for light to medium heavy nuclei, i.e., having a larger dynamic range. A sketch of the experimental set-up is shown in Fig. 1 after a fragment separator. The MUSIC detector before the secondary target is to allow Z identification and the one after the secondary target is for nuclear reaction studies.

The MUSIC detector should be able to stand with the 10^5-10^6 particle counts per second. Working pressure inside the active volume of the detector is 1 atm. The outer dimension of the detector is 440 (X) x 240 (Y) x 400 (Z) mm^3 while the volume of the active area is 220 (X) x 100 (Y) x 300 (Z) mm^3. There will be 8 segmented anodes for charge collection.

The main idea is to fabricate a MUSIC detector whose Z resolution is as good as the SOFIA Twin-MUSIC. The design will be similar as the prototypes that are developed in GSI since 2010 [3-5]. The energy-loss resolution for SOFIA Twin-MUSIC is measured to be σ(ΔE)/E = 0.34% with P25 gas[3]. In Fig. 2, the charge distribution for electromagnetically exited fission using SOFIA Twin-MUSIC is shown. Fine adjustment of drift time inside the active volume with the help of position sensitive detector must lead to the position resolution of single anode of the order of μm.

Newly developed preamplifiers (MUSAMP/CEA made) that are with low noise, high rate capability and very short rise time will be used. In addition, a new VME read-out module from MESYTEC (MDPP-16) will be adopted. It has low noise analogue input stage coupled to a high sensitivity digitizer; multi hit ADC, TDC; pileup tagging; adjustable shaper and online processing. These detectors are the central part of a compact, movable setup for the complementary measurements of charge-changing cross section at various facilities mentioned above in the coming years. See also the contribution by A. Prochazka et al. to this report.

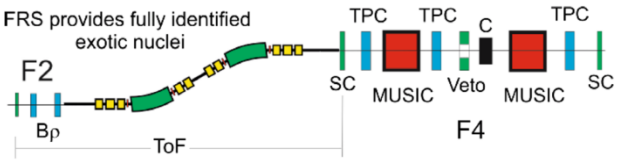

Figure 1: Experimental setup to identify the exotic nuclei and for nuclear reaction study. The MUSIC detectors provide the full Z identification of exotic nuclei.

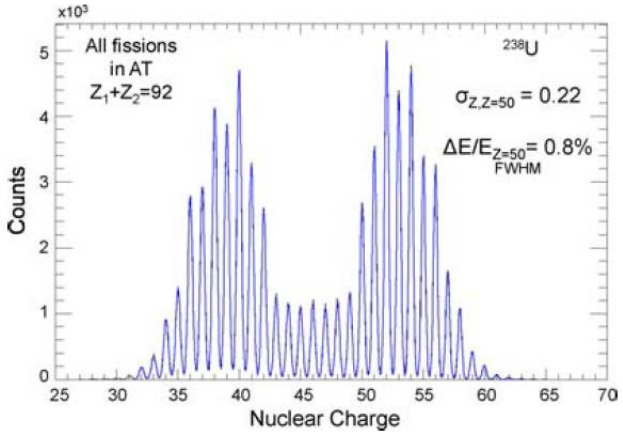

Figure 2: Nuclear charge distribution for electromagnetic exited fission using SOFIA Twin-MUSIC [3].

References:

[1] A. Stolz et al., Phys. Rev. C 65, 064603 (2002).
[2] R. Schneider and A. Stolz, Technical manual Ionization Chamber MUSIC80.
[3] I. Kaufeld, M. Takechi, and B. Voss, GSI Scientific Report 2013,GSI Report 2014-1 (2014) p.345.
[4] B.Voss et.al., GSI Scientific Report 2012,GSI Report 2013-1 (2013) p.204.
[5] B. Voss et al., GSI Scientific Report 2010, GSI Report 2011-1 (2011) p.223.

Experiment beamline:
Experiment collaboration: NUSTAR (R&D)
Experiment proposal: none
Accelerator infrastructure:
PSP codes:
Grants:
Strategic university co-operation with: Giessen, Saint Mary's University

Improved accuracy of the code ATIMA for energy loss of heavy ions in matter

H. Weick[1], H. Geissel[1,2], N. Iwasa[3], C. Scheidenberger[1,2], J. L. Rodriguez Sanchez[1], A. Prochazka[1], S. Purushotaman[1], for the Super-FRS experiment collaboration

[1]GSI, Darmstadt, Germany; [2]Justus-Liebig Universität Gießen, Germany, [3]Tohoku University, Sendai, Japan

The precise knowledge of the energy loss of heavy ions penetrating through layers of matter is essential for experiments, heavy ion therapy, separation of projectile fragments and many more accelerator applications. The program ATIMA (ATomic Interaction with MAtter) predicts the energy loss, energy-loss straggling and angular scattering of ions penetrating matter. Its predictions compared to data measured at the fragment separator FRS have demonstrated that an accuracy of ~1% in the stopping force (dE/dx) can be achieved. This has been accomplished for bare ions by using the LS-theory [1], whereas the pure Bethe theory deviates up to 10% [2] and by up to a factor of two in energy-loss straggling for high projectile atomic number (Z_1) ions at 1 GeV/u [3]. However, for ions with a few or many electrons the simple charge formula of Pierce and Blann [4] used in the ATIMA up to version 1.3 is not accurate [5], because it is not dependent on the target material. The experimental data also show that with an improved projectile mean charge description a good agreement can be achieved for high Z_1 ions (Au-U) down to 100 MeV/u where the K and L shells are partially filled.

Compared to the many mean charge formulas, theory-based analytical cross sections work best at sufficiently high velocity, as theory distinguishes correctly between the various electron capture and ionization processes. Yet for lower velocities the involved perturbation theory shows significant deviations. Based on the large amount of measured data with the FRS, a simple correction to the results from the GLOBAL program [6] with only three parameters was derived. The calculated mean charge depends on the velocity, the projectile (Z_1) and the target material (Z_2). This new description implemented in ATIMA, works for the entire range of projectile and target combinations down to 40 MeV/u.

Figure 1 shows the mean charge state prediction of uranium projectiles compared to our experimental data. The predicted mean charge varies considerably with Z_2, from <q>=86.2 in Be down to <q>=79.6 in Pb at 30 MeV/u. For even lower energies down to 10 MeV/u a pure fit formula [7] is used. For smoothening in the transition region a weighted average is used.

Unlike most other programs, in ATIMA we use the mean charge as it can be observed directly in experiments, whereas often an effective charge is used in stopping-power predictions to adjust for many effects. All other contributions to dE/dx are described by separate formulas such as the Barkas effect, shell corrections, and the Fermi-density effect [8]. With this approach we can gain a deeper understanding and improve the theoretical descriptions.

The accuracy of our new description has been tested with experimental data of projectiles with many electrons and different materials. The experimental data have been collected with the FRS in the last decades. This is an independent test as none of these measured data was used as a parameter in ATIMA 1.4 except for the mentioned mean charge. The data include U, Bi, Pb, Au, Xe, Kr, Ni projectiles on mainly solid targets ranging from Z_2=4 to 82 with energies from 1000 MeV/u down to 45 MeV/u.

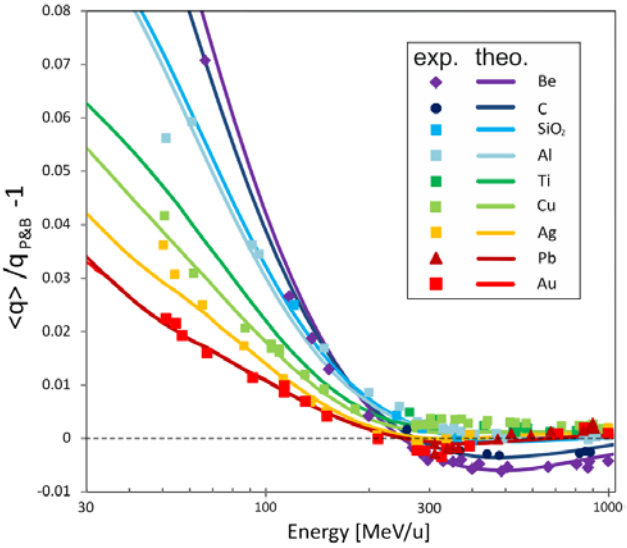

Figure 1: New predictions for the mean charge states of uranium ions after penetration of different target materials as function of energy are compared with experimental data. The comparison is normalized to the simple mean charge formula [4] used in the previous ATIMA versions.

Figure 2 shows a comparison of measured and predicted stopping forces in the energy range with the biggest differences to the previous ATIMA. The improvement is clearly demonstrated. In a limited energy range other programs, based on fits to measured data [9, 10], are better than the previous ATIMA version, but they fail for higher energies due to the simple effective charge approach and missing fully relativistic theory. At high energies for bare ions the results of ATIMA are accurate and remain unchanged.

The comparison of ATIMA 1.4 with experimental data includes all the available measured dE/dx values above 30 MeV/u. Table 1 shows the average standard deviations to theory from five experiments with the FRS. For the listed average relative standard deviations, the differences were weighted with the experimental errors. Of course the accuracy of the comparison is limited by the experimental errors.

For the data of ref. [11] up to 1 GeV/u with mainly bare ions ATIMA 1.4 naturally yields only a small improvement, but theories based only on perturbation theory show large deviations. The data of ref. [12] for Au-Bi ions in the range of 110 to 880 MeV/u with projectiles carrying a few electrons can be described better with ATIMA1.4. The same holds for the data of ref. [13] for Xe ions in the

 DOI:10.15120/GR-2018-1

energy range of 60 to 290 MeV/u. The new yet unpublished Uranium data down to 80 MeV/u with many electrons require ATIMA1.4. In this case the remaining deviations are only as small as the experiment errors themselves, while ATIMA1.3 - and other formulas even more - deviate significantly. At even lower energies (ref. [14]) the charge prediction and also the Barkas and shell corrections become less accurate, which explains the larger remaining deviation to ATIMA 1.4. Here the simple charge formula of ATIMA1.3 is not useful anymore as could already be seen in the comparison of Figure 1. Still ATIMA 1.4 is slightly better or is as good as the fit formulas.

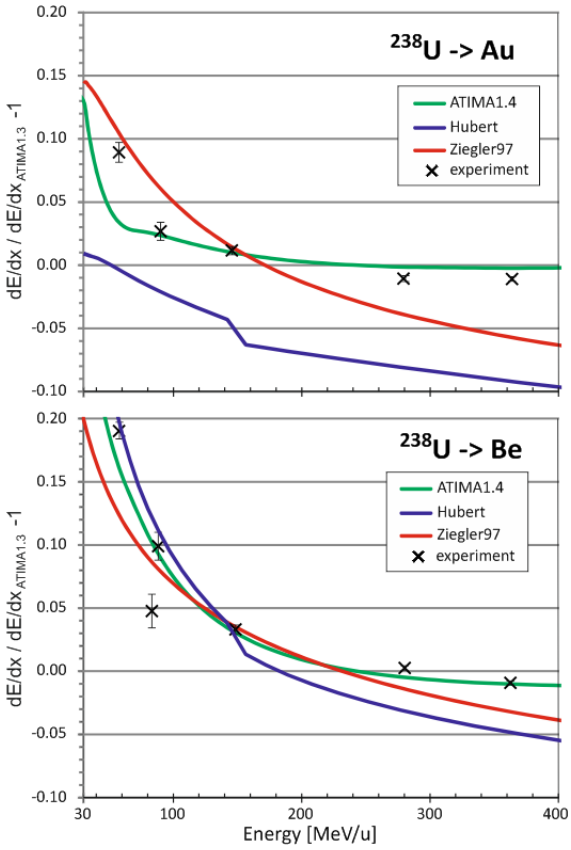

Figure 2: Comparison of new experimental dE/dx values of uranium ions in Au and Be targets to different formulas.

References

[1] J. Lindhard, A.H. Sørensen, Phys. Rev. A53 (1996) 2443.
[2] C. Scheidenberger et al., Phys. Rev. Lett. 73 (1994) 50.
[3] C. Scheidenberger et al., Phys. Rev. Lett. 77 (1996) 3987.
[4] T.E. Pierce, M. Blann, Phys. Rev. 173, 390 (1968).
[5] H. Weick et al., Nucl. Instr. Meth. B164 (2000) 168.
[6] C. Scheidenberger, et al., Nucl. Instr. Meth. B 142 (1998) 441.
[7] J. Winger et al., Nucl. Instr. Meth. B70 (1992) 380.
[8] C. Scheidenberger, H. Geissel, Nucl. Instr. Meth. B 135 (1998) 25.
[9] F. Hubert, R. Bimbot, H. Gauvin, Atomic and Nuclear Data Tables 46 (1990) 1.

Table 1: Comparison of experimental data for different projectiles (Z_1) and number of data points (N) with different theories: ATIMA1.3 ATIMA 1.4, Hubert [9], and Ziegler97 [10]. Listed are the average relative experimental errors and the average deviations of the theory from experimental data.

			[%]	[%]	[%]	[%]	[%]
Ref.	Z_1	N	exp.	A1.3	A1.4	Hub.	Z97
[10]	8-92	31	1.9	0.88	0.84	8.6	6.7
[11]	79-83	41	1.1	1.8	1.3	8.1	6.1
[12]	54	21	0.84	2.6	1.5	3.4	2.7
[13]	92	21	2.2	10.0	3.6	4.6	3.3
new	92	23	0.78	1.5	0.78	5.0	1.8

In the energy region much below 100 MeV/u the gas-solid difference in stopping powers of heavy ions makes the description more difficult. The gas-solid difference has been discovered at GSI about 40 years ago and has been confirmed in many experiments [15]. New experiments (approved proposal S469) are planned in different gaseous or solid targets.

Presently, below 10 - 30 MeV/u the region where direct theory becomes unreliable fit formulas with an effective charge as a variant of Ziegler's code [10] are applied in ATIMA and in addition a calculation for the contribution by elastic atomic collisions.

Since ATIMA version 1.3 the calculation includes projectiles up to Z_1=120 and targets up to Z_2=99 based on extrapolations. On the higher energy side ATIMA 1.4 calculates up to 450 GeV/u and also includes the then important nuclear size effect of the projectile [1, 8].
Integration of ATIMA into other programs such as MOCADI [16], PHITS [17], GEANT4, or ion optical codes has been done or is in progress. For an easy application, we provide a program as an interface to pre-calculated tables, as well as an online calculator [18].

[10] J.F. Ziegler, J.B. Biersack, U. Littmark, "The Stopping and Range of Ions in Solids", Vol.1, Pergamon Press (1985).
[11] C. Scheidenberger, PhD thesis, University of Giessen, 1994.
[12] H. Weick, PhD thesis, University of Giessen, 2000.
[13] M. Maier, PhD thesis, University of Giessen, 2004.
[14] A. Fettouhi, PhD thesis, University of Giessen, 2006.
[15] H. Geissel et al., Nucl. Instr. Meth. B195 (2002) 3.
[16] N. Iwasa et al., Nucl. Instr. Meth. B126 (1997) 284.
[17] T. Sato et al., J. Nucl. Sci. and Tech. (2018).
[18] ATIMA web page, http://web-docs.gsi.de/~weick/atima

Experiment beamline: FRS
Experiment collaboration: NUSTAR-SuperFRS-Experiments
Experiment proposal: S469
Accelerator infrastructure: SIS18 / FRS / Super-FRS
PSP codes:
Grants: SATNURSE EU project number 654002
Strategic university co-operation with: JLU Gießen

Implementation of ATIMA code in the Geant4 transport model

J. L. Rodríguez Sánchez[1,2], H. Weick[1], C. Scheidenberger[1], H. Geissel[1], N. Iwasa[3], A. Prochazka[1], S. Purushotaman[1]

[1]GSI, Darmstadt, Germany; [2]USC, Santiago de Compostela, Spain; [3]Tohoku University, Sendai, Japan

Geant4 [1] is a toolkit for Monte Carlo particle transport simulation in a wide range of applications, based on the object oriented technology. *Geant4* contains different models to compute the scattering and energy loss of the propagated particles and ions in matter. A great effort was carried out to improve and to validate the transport of γ-rays, leptons, mesons, and hadrons [2] as well as ions at low kinetic energies [3]. However, in *Geant4* there are few improvements concerning the transport of heavy ions at high energies (>400 MeV/u) [3]. Fortunately, in this energy range it was demonstrated that ATIMA code provides a precise description of the stopping power and angular scattering of ions when passing through matter [4]. For this reason, we will implement this code in *Geant4*. The first step was already performed translating the ATIMA code, written in Fortran language, to C++.

In this report, we present the benchmark of ATIMA [5] and *Geant4* for the stopping power of medium and heavy projectiles impinging on different targets. The experimental data were obtained with an accuracy around 1% at FRS-GSI during the last 30 years [5].

The stopping power of fast ions moving through matter is mainly due to the process of ionisation and excitation in target atoms. In *Geant4*, stopping power (dE/dx), range and inverse-range tables are constructed only for proton, antiproton, muons, pions, and kaons. The energy loss of other particles like ions is computed from these tables. The mean value of the energy loss is given by the Bethe-Bloch formula, in which the energy loss is calculated as a function of the ion velocity. For light particles like protons, the Bethe-Bloch formula provides an accuracy better than 1% [2], while deviations up to 9% are observed for heavy ions. According to this formula the energy loss of any fast ion can be expressed via the energy loss of another ion by using scaling factors. Therefore, the stopping power of an ion (ΔE_i) is proportional to the energy loss of a proton with a scaled velocity, such as: $\Delta E_i(T) = Z^2_i \Delta E_p(T_{scaled})$, where Z_i is the charge of the ion and ΔE_p is the stopping power of a proton with the scaled velocity, which corresponds to the so-called scaled kinetic energy: $T_{scaled} = T\ M_{proton}/M_i$, where T and M_i are the kinetic energy and the mass of the ion, respectively, and M_{proton} is the proton mass. As shown in Fig. 1, this model underestimates the stopping power around 7% at high kinetic energies (E_{kin}>400 MeV/u), while for lower energies the standard deviation is of about 3%. In the same figure, we can also see that ATIMA model predicts better results, for instance, ATIMA-1.2 provides a standard deviation around 1.8% while ATIMA-1.4 leads to deviations of about 1.3%.

Therefore, in order to improve the stopping power predictions in *Geant4*, we are implementing the ATIMA code according to the common structure based on the interfaces *G4VEmModel* and *G4VEnergyLossProcess* [6]. The first steps will be submitted to the *Geant4* repository at the end of May 2018.

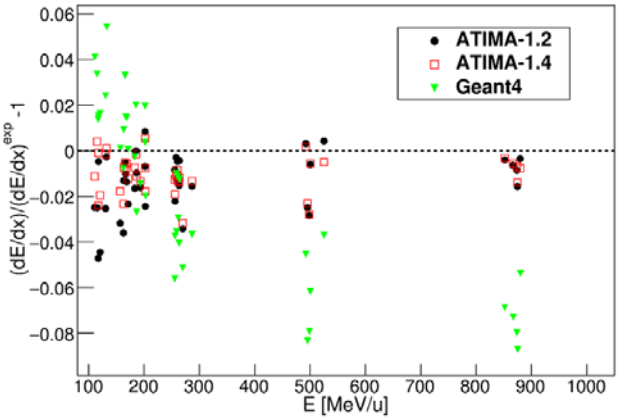

Figure 1: Comparison of the stopping power predicted by *Geant4* and different versions of ATIMA with experimental data taken from Ref. [5].

References

[1]S. Agostinelli et al., Nucl. Inst. Meth. A 506 (2003) 250.
[2]V. N. Ivanchenko et. al., J. Phys: Conf. Ser. 219 (2010) 032045.
[3]A. Lechner et al., Nucl. Inst. Meth. B 268 (2010) 2343.
[4]C. Scheidenberger et al., Phys. Rev. Lett. 73 (1994) 50.
[5]H. Weick et al., "Improved accuracy of the code ATIMA for energy-loss of heavy ions in matter", GSI Scientific Report 2017.
[6]J. Apostolakis et al., Rad. Phys. Chem. 78 (2009) 859.

Experiment collaboration: NUSTAR-SuperFRS-Experiments
Grants: SATNURSE EU project number 654002. This work has been also supported by the Department of Education, Culture and University Organization of the Regional Government of Galicia under the program of postdoctoral fellowships
Strategic university co-operation with: JLU Gießen

 DOI:10.15120/GR-2018-1

Accurate slowing-down measurements of heavy ions in gases and solids

S. Purushothaman[1], H. Geissel[1,2], H. Weick[1], S. Bagchi[1], T. Dickel[1,2], P. Egelhof[1], T. Grahn[3], E. Haettner[1,], A. Jokinen[3], B. Kindler[1], S. Kraft-Bermuth[2], N. Kuzminchuk-Feuerstein[1], B. Lommel[1], C. Montanari[4], Z. Patyk[5], S. Pietri[1], Y. Pivovarov[6], W.R. Plaß[1,2], A. Prochazka[1], C. Scheidenberger[1,2], V.P. Shevelko[7], D. Severin[1], P. Sigmund[8], A. Sørensen[9], T. Stöhlker[1], Y. K. Tanaka[1], M. Tomut[1], B. Voss[1], J.S. Winfield[1], M. Winkler[1]
and the Super-FRS Experiment Collaboration

[1]GSI Helmholtzzentrum für Schwerionenforschung GmbH, Darmstadt, Germany; [2]Justus-Liebig-Universität Gießen, Germany; [3]University of Jyväskylä, Finland; [4] Institute of Astronomy and Space Physics, Buenos Aires, Argentina; [5]National Centre for Nuclear Research, Warszawa, Poland; [6]Tomsk Polytechnic University, Tomsk, Russia; [7]P.N.Lebedev Physical Institute, Moscow, Russia; [8]University of Southern Denmark, Odense M, Denmark; [9]University of Aarhus, Aarhus C, Denmark

Accurate knowledge of heavy-ion slowing down in matter is crucial for a variety of scientific disciplines [1, 2]. Material science, heavy-ion therapy, astronautics, and accelerator physics are some of the examples. In the context of FRS experiments [3] at GSI and Super-FRS [4] at the future FAIR facility, the atomic interaction of heavy ions has to be known with high accuracy over the full energy range down to thermalization for efficient spatial isotope separation, energy-bunching and implantation experiments for spectroscopy or with gas-filled chambers. For kinetic energies close to the stopping power maximum the theoretical descriptions and widely used computer programs still fail to reproduce the experimentally observed gas-solid difference of stopping-powers and energy loss straggling [1, 5]. In the upcoming beam time at GSI in 2018-19 the stopping powers and charge-state distribution of xenon, lead and uranium ions penetrating amorphous monoatomic solids and gases of neighbouring proton numbers in the range of specific kinetic energies from 30 to 300 MeV/u will be measured. The main goal of this experiment is to obtain precision data and develop a valid description of this density effect, especially to observe where it vanishes at the higher velocities. This will also depend on the atomic number of the slowing down medium.

The absolute mean energy of the SIS beam is known with a relative accuracy of better than 10^{-3}. The FRS will be operated as a high-resolution magnetic spectrometer. A thin foil will be mounted at the entrance of FRS to prepare the desired charge-state population which will impinge on the atomic collision targets placed at the dispersive central focal plane.

The overall ion-optical mode of the FRS in these measurements will be achromatic to be independent of beam energy fluctuations from the accelerators which is a basis for high-resolution energy straggling measurements. We plan to use a microcalorimeter to enhance the precision for low ion energies. A schematic setup is shown in Figure 1

References

[1] P. Sigmund, Particle Penetration and Radiation Effects, Vol. 179. Springer Berlin, 2014.
[2] H. Geissel, et al., Nucl. Instr. Meth. B 195 (2002) 3.
[3] H. Geissel, et al., Nucl. Instr. Meth. B 70 (1992) 286.
[4] H. Geissel, et al., Nucl. Instr. Meth. B 204 (2003) 71.
[5] J. F. Ziegler, et al., Nucl. Instr. Meth. B 268 (2010) 1818.
[6] N. Iwasa, H. Weick, H. Geissel, Nucl. Instr. Meth. B269 (2012) 752

Experiment beamline: FRS
Experiment collaboration: NUSTAR-SuperFRS-Experiments
Experiment proposal: S469
Accelerator infrastructure: UNILAC / SIS18 / FRS
Strategic university co-operation with: Justus-Liebig-Universität Gießen

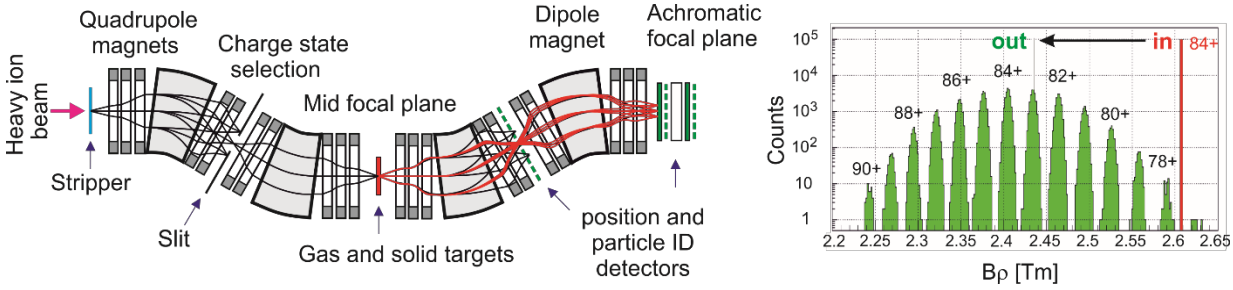

Figure 1: Experimental scenario for atomic collision experiments at the magnetic spectrometer FRS. The 4 dipole magnet stages are displayed with the focusing multipole magnets. The experimental detector setup at the focal planes will be used to measure the charge-state and energy-loss distributions. Simulated (MOCADI) charge state distribution and energy loss of an example case of 238U ions with (green) and without (red) a titanium target are shown in the inset [6].

Cherenkov radiation and half-wave crystal channeling as possible new mass/charge/velocity detectors of relativistic heavy ions

Yu. L. Pivovarov [1], O. Bogdanov[1], A. Bräuning-Demian[2], N. Kuzminchuk-Feuerstein[2], H. Geissel[2], S. Purushothaman[2], E. I. Rozhkova[1], C. Scheidenberger[2], T. A. Tukhfatullin[1], and the Super-FRS Experiment collaboration

[1]National Research Tomsk Polytechnic University, Russia; [2]GSI, Darmstadt, Germany.

Several basic atomic physics experiments are integral part of the scientific program of the Super-FRS Experiment Collaboration [1], including the study of Cherenkov radiation in liquid [2] and solid radiators [3] and channeling in thin half-wave crystals (HWC) [3] and the application of these effects as charge/mass/velocity detectors of relativistic heavy ions (RHI).

According to recent models [2, 3, 4] the slowing-down of the ions in the radiator at Super-FRS energies leads to broadening and complicated diffraction structures of the spectral and angular distributions (see in Fig.1).

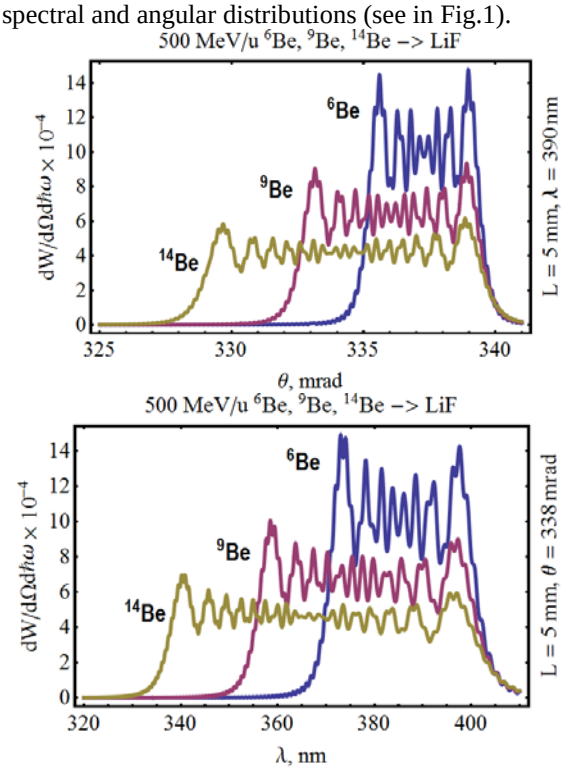

Figure 1. Angular (upper panel) and spectral (lower panel) distributions of Cherenkov Radiation from 500-MeV/u ^{6}Be, ^{9}Be, ^{14}Be isotopes in a LiF radiator of thickness L = 5 mm.

These distributions are very sensitive to the charge and velocity of RHI, and to the radiator thickness [2, 3, 4], thus the experiments with the Super-FRS will contribute to a detailed understanding of ChR from RHI ions and will lay the ground for improved and novel detector developments, like charge/mass/velocity detectors [3]. This topic is also discussed in Refs. [5, 6].

The FRS research collaboration has already performed channeling experiments at the FRS [7], the necessary equipment exists and can be used to continue these experiments at the FRS and later Super-FRS. We suggest to include studies of RHI channeling in a half-wave crystal into experimental program, which is a very recent trend in high-energy physics [8]. According to simulations, the achievable deflection angle through the mirror effect is of the order of critical channeling angle θc (see, in Fig. 2). Important is that the critical channeling angle depends both on the charge and mass of RHI.

The effect of HWC channeling can be used as effective beam deflector and even as charge/velocity selector.

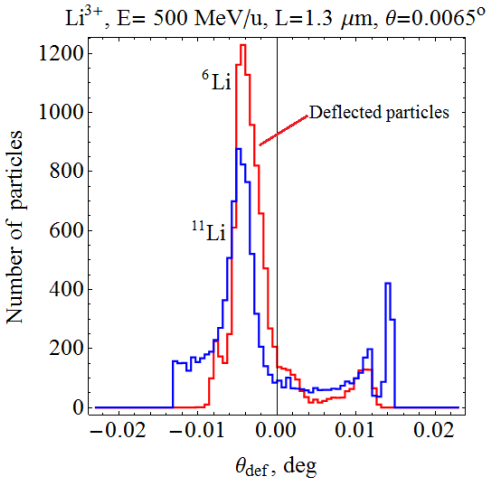

Figure 2. Deflection of 500 MeV/u Li isotopes by a (100) tungsten half-wave crystal. The critical channeling angle is θc = 0.0178° for ^{6}Li and θc = 0.0132° for ^{11}Li.

References

[1] CDR for the Scientific Program of the Super-FRS Experiment Collaboration (2016) DOI: 10.15120/GSI-2016-03763.
[2] H. Geissel et. al., GSI Scientific Report 2016, 179.
[3] E. I. Fiks et. al., Phys. Lett. A 380 (2016), 2386.
[4] O.V. Bogdanov et. al., Journ. Instr. Vol. 13 C02015 (2018) 7.
[5] T. Yamaguchi et. al., Nucl. Instrum. Methods A 766 (2014) 123.
[6] M. Machida et. al., POS (INPC2016) 084.
[7] D. Dauvergne et. al., Phys. Rev. A 59 (1999) 2813.
[8] W. Scandale et. al., Phys. Lett. B 734 (2014) 1.

Experiment beamline: FRS
Experiment collaboration: APPA / NUSTAR-SuperFRS-Experiments
Experiment proposal:
Accelerator infrastructure: UNILAC / SIS18 / FRS / SIS100 / Super-FRS
PSP codes:
Grants
Strategic university co-operation with: Tomsk Polytechnic University, Russia

 DOI:10.15120/GR-2018-1

A new modular detector design as a possible TOF detector for the Super-FRS

N. Kuzminchuk-Feuerstein[1], A. Neeb[2], E. Rozhkova[3], C. Scheidenberger[1], R. Siegert[4], B. Voss[1], and the Super-FRS collaboration

[1]GSI, Darmstadt, Germany; [2]Frankfurt University of Applied Science; [3]National Research Tomsk Polytechnic University, Russia; [4]RheinMain University of Applied Sciences, Rüsselsheim.

A high performance Time-of-Flight (TOF) detector is one of the key detectors in sub-atomic physics experiment to measure the velocity and mass of particles. Aiming to develop a TOF detector with a precision down to about 50 ps in time and resistant to a high radiation rate of relativistic ions of up to 10^7per spill a liquid medium, e.g. an Iodine Naphthalene ($C_{10}H_7I$) liquid radiator, was proposed for investigation of using Cherenkov radiation as a diagnostic tool for relativistic heavy ions [1], [2], [3].

The first-proof-of principle experiment with a TOF prototype detector using a $C_{10}H_7I$ radiator was performed at the SIS facility at GSI in April 2014 with nickel beam at 300-1500 MeV/u and ion beam intensities of up to 4×10^6 ions/spill [1]. Recently (2016), TOF measurements were performed with xenon ions at 600 MeV/u and a timing resolution of 63 ps (σ) was achieved [4].

To achieve the required time resolution and not to limit the application to a certain material we have initiated a development of a new design based on modular TOF detector employing Cherenkov or fast-plastic scintillator light emitted media (see Fig. 1).

The active media is a disk of 1 to 50 mm in thickness and a diameter of 18 cm. The system is designed with the possibility of quick exchange of the active media. The light is read out by 16 PMTs (ø 15 mm) of type Photonis XP1918, which are placed around the circumference of the disk. The time difference detected by two opposite PMTs (e. g. t_1 and t_9) are constant at a given ion position on a disk. As all PMTs are of the same type and show similar time characteristics the full detector time resolution is assumed to be equal to the average time accuracy of each PMT pair. In particular, in the TOF measurements between two detectors with 16 PMTs each time difference is expected to average out.

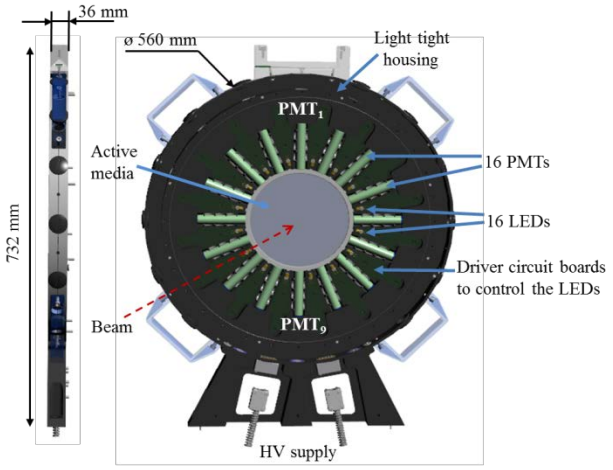

Figure 1: Conceptual design of the modular TOF detector with exchangeable active media. Arrangement of 16 PMTs and LEDs are shown.

The calibration system is based on short-pulsed LEDs placed around the active media between PMTs. The photons created in the media by the emitted light from LEDs can be detected by opposite placed PMTs. For the operation of LEDs, an avalanche generator was developed, based on the avalanche effect in a transistor [5]. With an avalanche transistor it is possible to generate needle pulses of less than 1 ns duration. The view of the setup used for test of LEDs is shown in Fig. 2. To trigger the LED's the driver circuit board has to be developed.

In-beam test of the detector design as well as of the data acquisition including VFTX-TDC are necessary and will be performed at GSI in 2018.

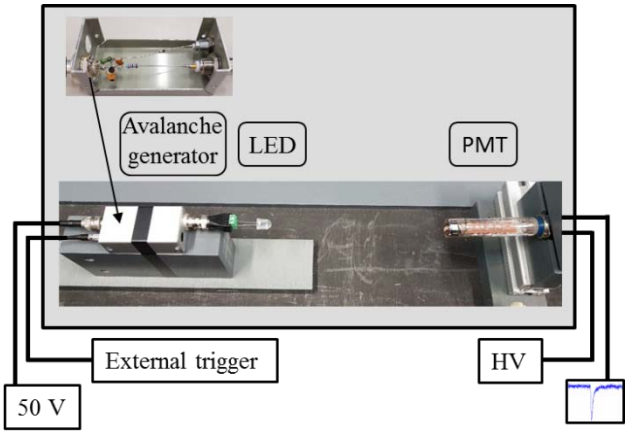

Figure 2: View of the setup used for measurements of the LEDs pulse duration with an avalanche generator [5].

References

[1] CDR for the Scientific Program of the Super-FRS Experimental Collaboration (2016). DOI: 10.15120/GSI-2016-03763

[2] N. Kuzminchuk-Feuerstein et. al., Nucl. Instrum. Methods A 821 (2016) 160-168.

[3] N. Kuzminchuk-Feuerstein et. al., GSI Scientific Report 2013, 141.

[4] N. Kuzminchuk-Feuerstein et. al., GSI Scientific Report 2016, 173.

[5] R. Siegert, "Entwicklung einer Treiberschaltung für Kurzpuls-LEDs", Bachelor Thesis, Hochschule RheinMain (2018).

Experiment beamline: FRS
Experiment collaboration: NUSTAR-R&D / FRS / SuperFRS /
Experiment proposal:
Accelerator infrastructure: SIS18 / SIS100 / Super-FRS

Development of the dual time-of-flight detector system for ILIMA

N. Kuzminchuk-Feuerstein[1], S. Ayet San Andreas[1], T. Dickel[1,2], M. Diwisch[2], O. Dolinskyy[1], H. Geissel[1,2], O. Gumenyuk[1], R. Knöbel[1], S. Litvinov[1], Y. A. Litvinov[1], W. R. Plaß[1,2], C. Scheidenberger[1,2], M. Steck[1], B. Sun[1,2], H. Weick[1], and the ILIMA collaboration

[1]GSI, Darmstadt, Germany; [2]Justus-Liebig-Universität, Gießen, Germany.

The Isomeric Beams LIfetimes and MAsses (ILIMA) collaboration will exploit heavy-ion storage rings at FAIR for the study of exotic nuclei. The CR is designed to allow for the operation in the isochronous ion-optical mode, a prerequisite for Isochronous Mass Spectrometry (IMS) with nuclei with lifetimes as short as several tens of µs, and for an acceptance many orders of magnitude larger than previous isochronous storage ring ESR. The masses of exotic nuclei can be deduced from a precise revolution time measurements by a TOF detector [1]. When the ions penetrate the thin detector foil, secondary electrons (SEs) are emitted from both surfaces and transported by perpendicular superimposed electric and magnetic fields to two microchannel plate (MCP) detectors (see Fig.1).

In the CR, we are aiming at in-ring measurement of the velocity of each particle in addition to its revolution time to correct for a wide mass-to-charge range in the mass measurement. Two TOF detectors with a distance of 16.9 m on a straight section are planned in the CR layout [2]. In this case the timing accuracy measured between the two detectors can be estimated from the resolution for a single passage of $\sigma_t = 35$ ps and averaging over many turns. Over a distance of 16.9 m at $\gamma_t = 1.67$ the TOF is 70 ns. Then the accuracy of measurement of one turn by two detectors is equal to $dt/t = (0.035 \cdot \sqrt{2})/70\ \text{ns} = 7 \cdot 10^{-4}$. Already after 10 turns this can be improved to $dt/t < 1 \cdot 10^{-4}$, which allows for correcting Bρ through dedicated velocity measurement. The design of new TOF detectors is based on the proven concept implemented in the present ESR-TOF detector [3].

The new CR will accept more intense stored beams with an acceptance of ΔBρ/Bρ=±0.5% and a transverse emittance of ε = 100 mm mrad, which results in larger beam diameters on the detector. Furthermore, the ring will run at a higher magnetic rigidity of up to Bρ = 13 Tm and a higher ion optical transition point (up to γ_t=1.84). The choice of the detector foil size (ø=80 mm) increases the area by a factor of four and the phase space acceptance by a factor of 16. It is motivated by the large emittance of the CR. The main challenge was to incorporate a larger diameter foil into the design and thus, to develop a larger construction with optimized fields.

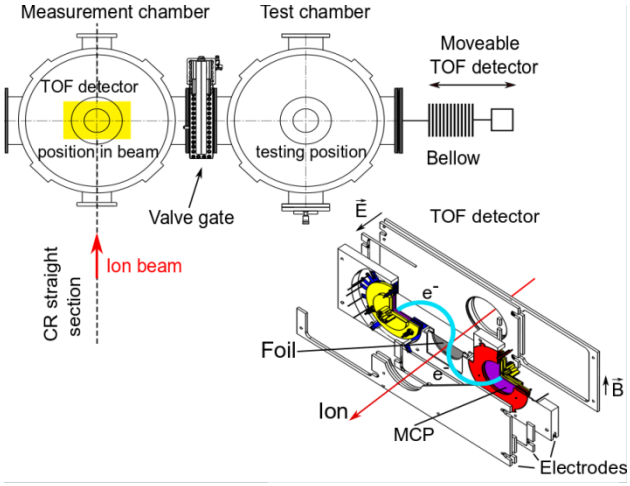

Figure 1: The overall setup of new TOF detector with vacuum chambers at measurement and test position as it will be installed twice on the straight section in the CR.

The dual time-of-flight detector system consists of two separated TOF detectors. Two vacuum chambers will be installed in the CR for each TOF detector. The movement of the detector into the beam line and back will be done using a long bellow, rails and stepper motors. The mounting and the offline tests of the detector will be done inside the test chamber, separated from the measurement chamber with a valve gate, which will be opened only after having reached sufficient UHV condition not to deteriorate the vacuum in the CR.

An optimized electrode system with only three electrode plates has been developed based on the results of simulations [4]. The pole-shoe and outer diameter of the dipole magnet are equal to 900 mm and 1000 mm. The preliminary design, checked with a manufacturer, foresees about 320 windings and applied current of 5.2 A.

Recently, a method of data analysis, using a correlation-matrix (first developed for Schottky) for the combined data set from different experiments, was adapted and used to determine new mass values [5] [6].

The TDR was submitted to FAIR through the NUSTAR collaboration board in December 2017 and currently is under review.

References

[1] N. Kuzminchuk-Feuerstein et. al., Nucl. Instrum. Methods A 821 (2016) 160-168.
[2] N. Kuzminchuk-Feuerstein et. al., TDR of the dual TOF - detector system for ILIMA (2017). https://edms.cern.ch/document/1896955
[3] J. Trötscher PhD Thesis, JLU Gießen (1993).
[4] M. Diwisch, PhD Thesis, JLU Gießen (2015).
[5] R. Knöbel et. al., Eur. Phys. J. A (2016) 52:138.
[6] R. Knöbel et. al., Phys. Lett. B 754, 288 (2016).

Experiment beamline: CR
Experiment collaboration: NUSTAR-ILIMA
Experiment proposal:
Accelerator infrastructure: SIS18 / SIS100 / CR / Super-FRS /
PSP codes: 1.2.6.4, 1.2.6.6
Grants: BMBF (Contract no.05P09RGFN9, 05P16RGFN1)
Strategic university co-operation with: Gießen

 DOI:10.15120/GR-2018-1

Fast timing with FATIMA - From νBall at ALTO to DESPEC at GSI

P.-A. Söderström[1,2], M. Rudigier[3], T. Arici[2], S. Bottoni[4], M. Brunet[3], R. Canavan[3], N. Cieplicka-Oryńczak[5], S. Courtin[6], D. Doherty[3], J. Gerl[2], M. Gorska[2], K. Hadyńska-Klęk[3], M. Heine[6], Ł. W. Iskra[5], N. Jovančević[7], V. Karayonchev[8], A. Kennington[3], I. Kojouharov[2], P. Koseoglou[1,2], M. Lebois[7], N. Kurz[2], C. Lizarazo[1,2], G. Lorusso[3,9], G. Lotay[3], M. Nakhostin[3], C.R. Niță[10], S. Oberstedt[11], N. Pietralla[1], S. Pietri[2], Zs. Podolyák[3], L. Qi[7], P.H. Reagan[3,9], J.-M. Régis[8], S. Saha[1,2], H. Schaffner[2], R. Shearman[3], J. Vesić[2], J. Wilson[7], W. Witt[1,2]

[1]TU-Darmstadt, Darmstadt, Germany; [2]GSI, Darmstadt, Germany; [3]University of Surrey, Guildford, U.K.; [4]University of Milano, Milano, Italy; [5]Institute of Nuclear Physics, PAN, Kraków, Poland; [6]IPHC, Strasbourg, France; [7]IPN, Orsay, France; [8]Universität zu Köln, Köln, Germany; [9]NPL, Teddington, UK; [10]IFIN-HH, Magurele, Romania; [11]European Commission, Geel, Belgium

Lifetime measurements of excited states using fast $LaBr_3$ scintillators is a strongly emerging field within nuclear physics that has gained significant popularity in recent years. Most of the experiments performed to date have taken place using γγ-coincidences at stable beam facilities [1]. With the upcoming generation of high-intensity radioactive ion beam facilities, this technique is becoming increasingly used to study the structure of more exotic nuclei [2]. For example, in one of the recent experiments at RIKEN, βγ-coincident fast-timing with $LaBr_3$ and plastic scintillators have been very successful [3,4]. This type of experiment will be one of the foci of the upcoming DESPEC beam times.

Implementing FATIMA with νBall

In November 2017 the first experiment with the new mixed EUROBALL HPGe and FATIMA $LaBr_3$ spectrometer, νBall, was performed in Orsay. It's aim was to measure the lifetime of the low-lying states in ^{166}Dy as well as to search for a predicted 4^- isomer. The experiment was performed using a pulsed ^{18}O beam from the ALTO tandem to induce two-neutron transfer reactions on a ^{164}Dy target as well as fusion-evaporation reactions to reach high-spin states in ^{178}W. One of the key features in this experimental setup is the possibility to use the high resolution pulsed beam to extract lifetimes from beam radiofrequency-γ coincidences. A typical example of the spectra obtained is shown in Figure 1. Within the data from this experiment the transitions of interest in ^{166}Dy were clearly observed in singles and in γγ-coincidences, the lifetime of the first excited state in the Coulex of ^{164}Dy was well reproduced, and γ rays originating from the decay of the high-spin isomers of ^{178}W could also be identified. The full data from this experiment is currently under analysis. However, the data already shows stable operation and a high quality of the output data from FATIMA.

Experiments within DESPEC in 2018

For the DESPEC campaign the FATIMA detectors will be moved to GSI in spring 2018. One of the proposed experiments at GSI is the study of neutron-rich Hf, W, and Os isotopes. The advanced implantation detector AIDA will be used as an active stopper consisting of three layers of silicon detectors. AIDA will be complemented by thin plastic scintillators for electron tagging and these will be read out via regular or silicon photomultipliers. FATIMA will be configured into three rings upstream, and for high-resolution spectroscopy an array of HPGe detectors will be installed; currently proposed as seven DEGAS triple-clusters. The proposed readout of FATIMA will consist of 10-bit resolution and 1 GS/s V1751 8-channel digitizers, and V1290 16-channel multihit TDCs. These electronic units will be integrated into the GSI readout system MBS via a RIO4 CPU, TRIVA trigger module, and a VULOM4b VME universal logic module. The results and experience from these experiments will be crucial for future implementation of NUSTAR at FAIR.

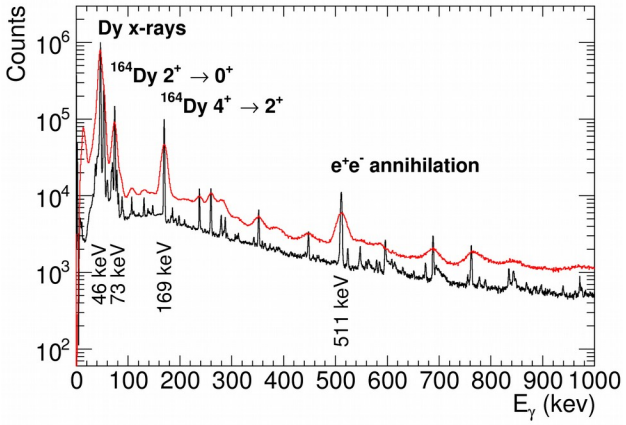

Figure 1: Example spectra of γ rays detected in the HPGe (black) and $LaBr_3$ (red) detectors. The most intense features are labelled.

References

[1] N. Mărginean, et al., Eur. Phys. J. A 46 (2010) 329
[2] P. H. Regan, et al., EPJ Web Conf. 63 (2013) 01008
[3] F. Browne, et al., Phys. Lett. B 750 (2015) 448
[4] F. Browne, et al., Phys. Rev. C 96 (2017) 024309

Characterization of a Sunpower CryoTel CT cooling engine for DEGAS

W. Witt[1,2], P. Koseoglou[1,2], P.-A. Söderström[1,2], E. Adamska[3], J. Gerl[2], I. Kojouharov[2], N. Pietralla[1]

[1]TU Darmstadt, Darmstadt, Germany; [2]GSI, Darmstadt, Germany; [3]University of Warsaw, Warsaw, Poland

As one of the four experimental pillars of the FAIR project the NUSTAR collaboration aims at investigating exotic beams provided by the accelerator through the Super-FRS. This includes the decay spectroscopy setup DESPEC, which is to be located at the low-energy branch of the facility. To obtain maximum output from DESPEC, new detector systems for high-efficiency measurements are being developed and adapted to the facility's requirements. One of the key instruments is the DEGAS germanium-array, which, due to its compact design, makes the standard liquid nitrogen cooling impossible. Therefore, new technology based on compact electrical coolers of the type Cryotel CT by Sunpower is under development [1].

One of the main obstacles in the application of electrical cooling are the vibrations originating from the Stirling engine, which transfer directly to the Ge-crystal to be cooled and affect its energy resolution. To characterize the thermal properties of the cooler and, in particular, to quantify the vibrations and explore possible countermeasures, several measurements were performed at the Helmholtz-Institut Mainz during summer 2017. The purpose of this measurements was to observe time-dependent temperature and acceleration developments at the cooling point during the cooling-down process and the effect of different mechanical holding structures on the oscillations.

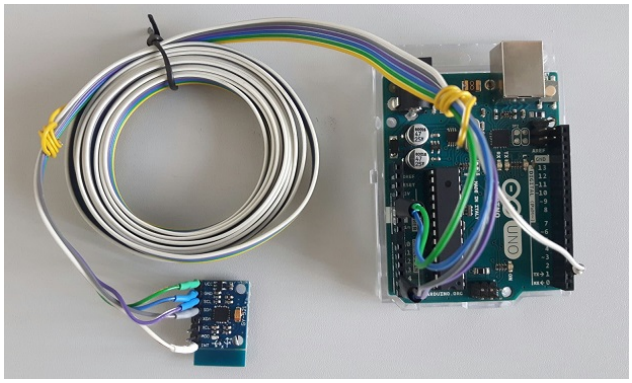

Figure 1: The MPU6050 sensor connected to an Arduino Uno Board for readout.

The thermal measurement performed with a PT-100 sensor showed a gradual cooling-down process towards the operating temperature of 77K, which was achieved within 150 minutes. The power consumption did not exceed 170 W and remained at 60 W at 77K. These properties met the expectations and requirements for the DEGAS cooling.

The accelerometry was performed using an Arduino Uno Board and a MPU6050 sensor [2], as shown in Fig. 1. The MPU6050 sensor is equipped with an accelerometer and a gyroscope and the Arduino Uno board was programmed to read the values from the sensor and stream them to a computer at 500 kbps. The effective sampling frequency was determined globally for the full setup by the sampling frequency of the sensor, and the internal clocks of the sensor and the Arduino board. The maximum sampling frequency of the MPU6050 sensor's accelerometer is 1 kHz and the highest sampling frequency reached during these measurements was around 600 Hz. The acceleration measuring range was set to ±16 G.

The obtained data were analysed using a three-dimensional Fast Fourier Transform (FFT), including a low-pass filter. One main product of these measurements can be seen in Fig. 2. showing the vibration frequency as a function of time during 30 minutes of the cooling-down phase. Besides lower-intensity vibrational features four strong bands are dominant, which coincide with the frequency of the cooler's gear (60 Hz) [3] and it's harmonic modes (120 Hz, 180 Hz, 240 Hz).

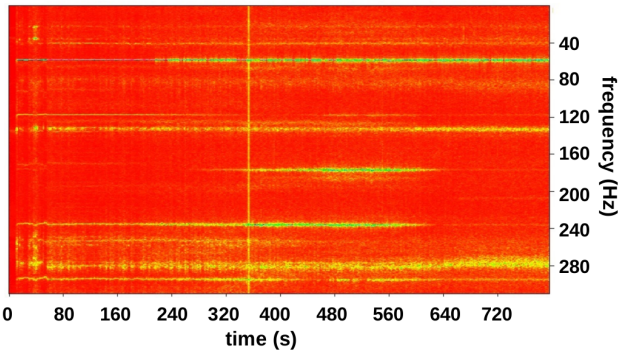

Figure 2: Typical frequency-time spectrum of oscillations at the cooling point of the Cryotel CT during the cool-down process.

In previous tests of the cooler [1], the malfunction or wrong setting of the AVC (active vibration cancellation, a mechanical attachment to the cooler to perform anti-phase oscillations for a net-zero vibration of the cooler) remained unclear. This was ruled out in this work. The AVC was shown to work correctly and dampen the oscillations slightly.

Furthermore, accelerometry was performed after changing the properties of the cooler's holding structure (damping legs, Styrofoam, additional weight on top), cp. Fig. 3. The structure variation proved to have a potentially damping effect on the measured oscillations and, hence, the adaption of the holding structure in terms of mechanical decoupling of the cooler from the cooling point, e.g. employed in [4], was persued.

 DOI:10.15120/GR-2018-1

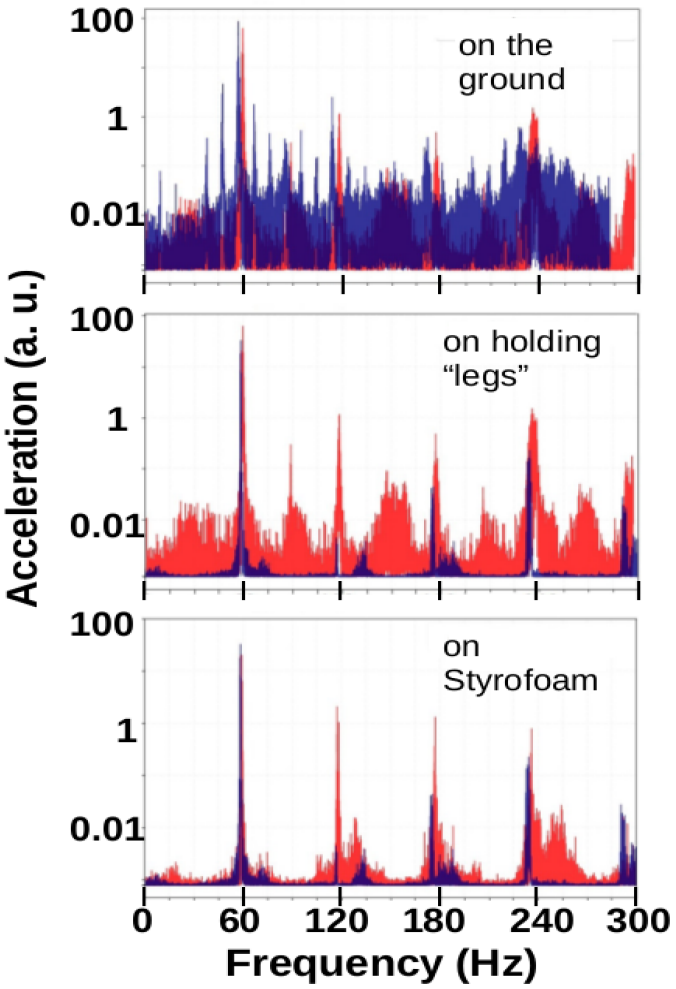

Figure 3: Variation of the cooler oscillations with changing holding structure and with (blue) /without (red) lead on top.

The design and manufacture company Ortec could be convinced to design and produce such adapted holding structure. A first draft of the design based on vacuum bellows and flexible copper rods for the decoupling is shown in Fig. 4. The production is planned to be finished in April 2018.

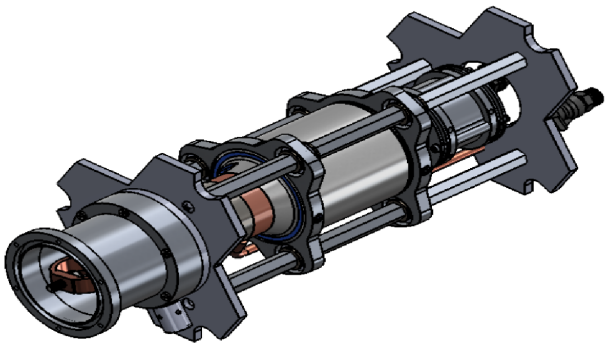

Figure 4: New Cryotel CT holding structure as designed by Ortec employing oscillation-decoupling mechanics.

Further tests will show the efficiency of the modifications. Should the oscillations prove to be sufficiently reduced, the electrical Cryotel CT coolers will be used in the DEGAS array as foreseen starting Fall 2018 with the FAIR-0 DESPEC experiments.

This work was supported by HGS-HIRe and the German ministry for education and research (BMBF) within the project NUSTAR R&D under grant no. 05P15RDFN1.

References

[1] W. Witt et al., GSI Scientific Report 2016, 186 (2017)
[2] http://www.arduino.cc/ accessed in September, 2017
[3] Sun Power CryoTel User Manual V.7 (2012)
[4] G. Raskin et al., Compact Stirling cooling of astronomical detectors, Instr. and Meth. for Astrophys. (2013)

First spectroscopy of neutron-rich Sc isotopes using FAIR instrumentation in the third SEASTAR campaign

P. Koseoglou[1,2], V. Werner[1], P.-A. Söderström[1,2], M. Lettmann[1], N. Pietralla[1], P. Doornenbal[3], A. Obertelli[1,4,3], N. Achouri[4], H. Baba[3], F. Browne[3], D. Calvet[4], F. Château[4], S. Chen[5,6,3], N. Chiga[3], A. Corsi[4], M. L. Cortés[3], A. Delbart[4], J-M. Gheller[4], A. Giganon[4], A. Gillibert[4], C. Hilaire[4], T. Isobe[3], T. Kobayashi[7], Y. Kubota[3,8], V. Lapoux[4], H. Liu[4,9], T. Motobayashi[3], I. Murray[3,10], H. Otsu[3], V. Panin[3], N. Paul[4], W. Rodriguez[11,3], H. Sakurai[3,12], M. Sasano[3], D. Steppenbeck[3], L. Stuhl[8], Y. L. Sun[4], Y. Togano[13,3], T. Uesaka[3], K. Wimmer[12,3], K. Yoneda[3], O. Aktas[9], T. Aumann[1], L. X. Chung[14], F. Flavigny[10], S. Franchoo[10], I. Gasparic[3,15], R.-B. Gerst[16], J. Gibelin[17], K. I. Hahn[18], D. Kim[18], T. Koiwai[12], Y. Kondo[19], J. Lee[6], C. Lehr[1], B. D. Linh[14], T. Lokotko[6], M. MacCormick[10], K. Moschner[16], T. Nakamura[19], S. Y. Park[18], D. Rossi[1], E. Sahin[20], D. Sohler[21], S. Takeuchi[19], H. Törnqvist[1], V. Vaquero[22], V. Wagner[1], S. Wang[23], X. Xu[6], H. Yamada[19], D. Yan[23], Z. Yang[3], M. Yasuda[19] and L. Zanetti[1].

[1]Institut für Kernphysik, Technische Universität Darmstadt; [2]GSI Helmoltzzentrum für Schwerionenforschung GmbH; [3]RIKEN Nishina Center; [4]IRFU, CEA, Université Paris-Saclay; [5]School of Physics, Peking University; [6]Department of Physics, The University of Hong Kong; [7]Department of Physics, Tohoku University; [8]Center for Nuclear Study, the University of Tokyo; [9]Department of Physics, Royal Institute of Technology; [10]Institut de Physique Nucléaire Orsay, IN2P3-CNRS; [11]Universidad Nacional de Colombia; [12]Department of Physics, University of Tokyo; [13]Department of Physics, Rikkyo University; [14]Institute for Nuclear Science & Technology, VINATOM; [15]Rudjer Boskovic Institute, Zagreb; [16]Institut für Kernphysik, Universität zu Köln; [17]LPC Caen, ENSICAEN, Université de Caen; [18]Ewha Womans University; [19]Department of Physics, Tokyo Institute of Technology; [20]Department of Physics, University of Oslo; [21]MTA Atomki; [22]Instituto de Estructura de la Materia, CSIC; [23]Institute of Modern Physics, Chinese Academy of Sciences.

Recent results for the level structure of ^{54}Ca have shown evidence for the existence of a new magic neutron number N=34 [1]. At the same time there might not be a corresponding shell gap in Ti isotopes [2, 3]. Scandium isotopes lie between calsium and titanium. In scandium isotopic chain the valence proton occupies the $\pi f_{7/2}$ orbital, interacting with the $\nu f_{5/2}$ orbital in $^{55-61}$Sc. The evolution of the proton orbitals of these isotopes can reveal the nature of both the magic number N=34, recently proved to vanish in ^{55}Sc [4], and the N=40 *pf*-shell closure.

Gamma-ray spectroscopy of the neutron-rich $^{55-61}$Sc isotopes was performed at the Radioactive Isotope Beam Factory (RIBF) in Wako-shi, Japan, as part of the third SEASTAR campaign [5]. A ^{70}Zn beam at 345 MeV/u, delivered from the RIBF accelerator complex, produced a cocktail of secondary radioactive beams by impinging on a 10-mm-thick ^{9}Be target. The secondary beams, that were identi ed and separated by the BigRIPS fragment separator [6], produced the isotopes of interest by knock-out reactions in the MINOS target system [7], consisting of a 150-mm-thick LH_2 target surrounded by an active TPC. The emitted gamma-quanta of the isotopes produced were measured by the DALI2+ array [8], consisting of 226 NaI(Tl) detectors, surrounding MINOS. The reaction products were reconstructed event-by-event in SAMURAI [9] using two drift chambers and a hodoscope plastic-scintillator array. Additionally, NeuLAND [10] and NEBULA [11] were used for neutron detection. The experimental set-up is shown in Figure 1.

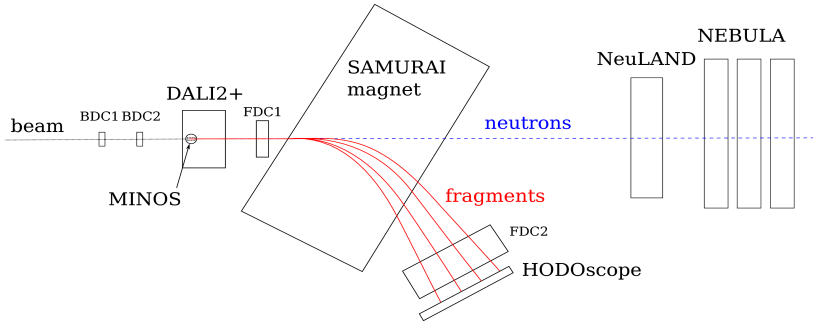

Figure 1: Experimental set-up of the 3rd SEASTAR campaign at RIBF.

 DOI:10.15120/GR-2018-1

The γ transitions reported previously for ^{55}Sc in Ref. 4 have been already identified in the current early state of our data analysis from the neutron knock-out reaction, ^{56}Sc(p,pn)^{55}Sc. The analysis for $^{55\text{-}61}$Sc is on-going. Figure 2 shows the particle identification in BigRIPS after gating on $^{55\text{-}61}$Sc nuclei in SAMURAI.

The large number of detectors together with the BigRIPS fragment separator and the SAMURAI magnet formed a complex experimental set-up similar to the planned NUSTAR HISPEC/DESPEC experiments at FAIR.

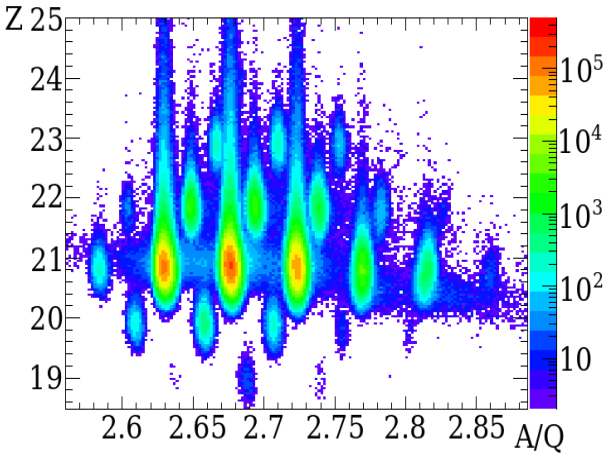

Figure 2: The particle identification in BigRIPS after gating on $^{55\text{-}61}$Sc in SAMURAI.

The first author would like to thank the Helmholtz Graduate School for Hadron and Ion Research (HGS-HIRe) for FAIR for its support though the HGS-HIRe abroad program.

References

[1] D. Steppenbeck, et al., Nature **502**, 207-210 (2013).
[2] D.-C. Dinca, et al., Phys. Rev. C **71**, 041302(R) (2005).
[3] S. N. Liddick, et al., Phys. Rev. Lett. **92**, 072502 (2004).
[4] D. Steppenbeck, et al., Phys. Rev. C **96**, 064310 (2017).
[5] P. Doornenbal and A. Obertelli, RIKEN Proposal for Scientific Program (2013).
[6] T. Kubo, et al., Prog. Theor. Exp. Phys. 2012, 03C003 (2012).
[7] A. Obertelli, et al., Eur. Phys. J. A **50**, 8 (2014).
[8] S.Takeuchi, et. al., Nucl. Instr. and Meth., A **763** (2014) 596-603.
[9] T. Kobayashi, et. al., Nucl. Instr. and Meth., B **317** (2013) 294-304
[10] NeuLAND-TDR, https://edms.cern.ch/document/1865739.
[11] T. Nakamura, Y. Kondo, Nucl. Instr. Meth. B **376**, 1 (2015).

Fuzzy Bayes Tracking – Experimental results

P. Napiralla[1,2], H. Egger[3], P. R. John[1], N. Pietralla[1], M. Reese[1], and C. Stahl[1]

[1]Institut für Kernphysik, Technische Universität Darmstadt, Darmstadt, Germany; [2]GSI, Darmstadt, Germany;
[3]AG Numerik und wissenschaftliches Rechnen, Technische Universität Darmstadt, Darmstadt, Germany

The Advanced GAmma Tracking Array AGATA [1] will be the key instrument for nuclear structure investigations in the upcoming HISPEC and DESPEC experimental campaigns at the Facility for Antiproton and Ion Research FAIR. Due to its germanium shell without any Compton-shielding, γ-ray tracking algorithms are essential for experiments with high reaction rates.
Based on the mathematical framework of the *Bayes-Tracking* (see [2]), the Fuzzy Bayes Tracking (FBT) adds a geometrical clustering algorithm into the framework. This clustering algorithm is based on a *Fuzzy c-means* algorithm (see [4]), which forms simple geometrical clusters via a minimization process. These clusters are then either physically confirmed or torn further by the Bayesian analysis of the tracking algorithm, if a higher amount of clusters is more likely. This is achieved by comparing all possible sub-combinations of observed clusters via *marginalization* [3]

$$P(cluster) = \sum_{n=1}^{N} P(cluster|n)\,P(n)$$

where n is the number of possible sub-clusters and N is the number of observed interaction points. For each sub-cluster, the probability $P(cluster|n)$ is calculated using known cross sections of Compton scattering and photo-electric absorption. In addition, the plausibility of the resulting photon paths are considered by comparing geometrical scattering angles with energetic Compton scattering angles under the metrological restraints of the AGATA detectors. Comparing all possible probabilities $P(cluster|n)$, the most probable sub-clusters are chosen and their respective total deposited energies are set as the tracked energies.

Using ^{60}Co source data from the AGATA-Demonstrator experiment 09.08 conducted at LNL in 2011, a first benchmark test of the Fuzzy Bayes Tracking can be made. The achieved performance of the Fuzzy Bayes Tracking can be seen in Figure 1. By suppressing cluster formation with very low probabilities (mostly belonging to escaped photons), the tracked spectrum can be cleaned significantly (see Fig. 1).

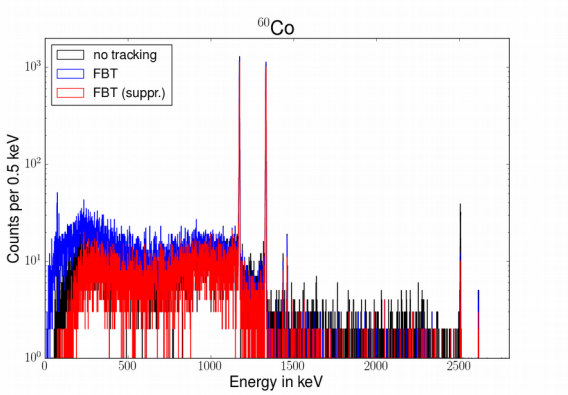

Figure 1: Performance of the Fuzzy Bayes Tracking on a ^{60}Co spectrum. Black is without any tracking, blue the tracked spectrum without suppression and red with suppression.

Comparing the Peak-to-Total ratios with and without the Fuzzy Bayes Tracking yields:

- no tracking: 38 %
- FBT: 31 %
- FBT with suppression: 43 %

To improve the Fuzzy Bayes Tracking further, future work will focus on merging FBT's methods with the reconstruction methods mentioned in [2]. In addition, further improvements of the geometrical clustering process will be made.

References

[1] A. Akkoyun *et. al.*, AGATA – Advanced Gamma Tracking Array, Nuclear Instruments and Methods in Physics Research A, 668:26-58, 2012.
[2] P. Napiralla *et. al.*, Bayes-Tracking – A novel approach to γ-ray tracking, GSI Scientific Report 2016, 2016.
[3] D. Sivia and J. Skilling, Data Analysis – A Bayesian Tutorial, volume 2, Oxford University Press, Oxford, 2006.
[4] M.S. Yang and Y. Nataliani, Robust-learning fuzzy c-means clustering algorithm with unknown number of clusters, Pattern Recognition, 71:45-49, 2017.

Experiment beamline: none
Experiment collaboration: NUSTAR-DESPEC-HISPEC
Experiment proposal: none
Accelerator infrastructure: none
PSP codes: 1.2.2.8
Grants: BMBF 05P15RDFN1, BMBF 05P15RDFN9
Strategic university co-operation with: Technische Universität Darmstadt

 DOI:10.15120/GR-2018-1

Position sensitive Ge detector

T. Arici[1], I. Kojouharov[1], J. Gerl[1]

[1]GSI, Darmstadt, Germany

Position sensitivity of gamma-ray detection is required for a wide range of applications. In order to achieve good position sensitivity, segmentation of the contacts of the crystal must be applied. Recently, segmentation of HPGe has been applied to coaxial crystals, such as the AGATA detectors, results in a position resolution of 3-5 mm with a high energy resolution [1]. Despite the impressive results obtained by these detectors, the demand for increased position resolution of 1 mm requires focusing on segmented planar detectors. Nevertheless, having a superior position resolution, the physics of the operation and the feasible technical solutions resulted in a large dead volume in the crystal and large insensitive space around it, which affects negatively the performance of a planar detectors array. To solve the problem, a new geometry, namely the semi-planar detector geometry, which severely minimizes this layer, has been proposed.

Detector Test

The project proposed is aimed at development of semi-planar detector with point contacts as a segmentation tool. This includes a detailed study by numerically simulating the electric field and the charge transport inside the detection crystal and a search for the optimal geometry.
The crystal processing is supposed to be carried out by an industrial partner and the detector to be scanned by the GSI Detector Scanner. The main idea is to make several point read-outs on a planar crystal which are sensitive to certain area. The distribution and number of these points can be estimated by performing simulations taking the electric field and charge transportation into account. In this framework, semi-planar HPGe detector with a single point contact read-out was studied in order to characterize the behaviour of such a novel contact technology replacing the segmentation of the crystal. A non-segmented p-type HPGe crystal with a dimension of 33.2x33.2x15.5 mm^3 and Carrier concentration of 3.3x109 atom/cm^3 was used for the test purposes. The charge signal was extracted from the p+ electrode. The detector was operated at 100 V and 1.2 pA leakage current was observed. Sudden increase of the leakage current when increasing the bias voltage caused the saturation of the pre-amplifier which is related to the type of the coupling used for the signal read-out. Detector was tested using ^{57}Co and ^{60}Co sources in order to cover the low and high energy regions. For each source different shaping times were tested. Experimental data was fitted using an exponentially modified Gaussian function and the results for two different shaping times are given in Figure 1 for ^{60}Co source. Using the ^{57}Co source, 2.1 keV and 2.3 keV energy resolutions at 122 keV line was obtained respectively for 3 µs and 6 µs shaping times. While with ^{60}Co source, 4.5 keV and 4.3 keV energy resolution was obtained for the 1332 keV transition respectively for 3 µs and 6 µs shaping times.

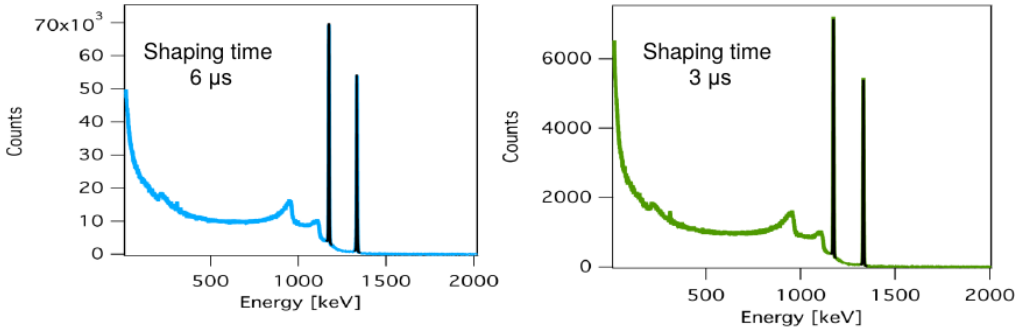

Figure 1: The observed energy spectrum with ^{60}Co source. The spectrum on the left side was recorded using 6 µs shaping time while the one on the right side obtained with 3 µs shaping time.

References

[1] S. Akkoyun and A. Algora, "AGATA – Advanced Gamma Tracking Array", NIM volume 668, 26-58 2012

Experiment beamline: Gamma-Spectroscopy
Experiment collaboration: NUSTAR-DESPEC-HISPEC
Grants: ENSAR2

Fast-timing lifetime measurement of ^{152}Gd with FATIMA-type $LaBr_3$ detectors

J. Wiederhold[1], R. Kern[1], C. Lizarazo[1,2], W. Witt[1,2], V. Werner[1], N. Pietralla[1], D. Bucurescu[3], N. Florea[3], D. Ghita[3], T. Glodariu[3], R. Lica[3], N. Marginean[3], R. Marginean[3], C. Mihai[3], R. Mihai[3], I.O. Mitu[3],A. Negret[3], C. Nita[3], A. Olacel[3], S. Pascu[3], L. Stroe[3], S. Toma[3], A. Turturica[3]

[1]Institut für Kernphysik,TU Darmstadt, Germany; [2]GSI, Darmstadt, Germany, [3]IFIN-HH, Bucharest, Romania

In preparation of the upcoming DESPEC campaign at FAIR with the Fast TIMing Array (FATIMA), experiments were performed at the 9-MV FN Tandem of the National Institute for Physics and Nuclear Engeneering Horia Hulubei in Bucharest. The experimental setup at IFIN-HH for γ-ray spectroscopy uses the RoSphere Array [1] consisting of 11 FATIMA-type $LaBr_3$ detectors and 14 HPGe detectors, which is similar to the planned setup for the upcoming DESPEC campaign in 2018/19 with the DEGAS and FATIMA detectors.

Fast electronic scintillation timing (FEST)

The lifetime of an excited nuclear state is determined using FEST by measuring the time di erence between a start and a stop signal. The respective time signals originate from the detection of γ quanta from nuclear transitions feeding and depopulating the state of interest. The resulting time-di erence distribution is a convolution of the prompt response of the experimental setup and the exponential decay of the excited nuclear state. Lifetimes in the range of dozens of ps can be determined by measuring the centroid shift of the time-di erence distribution after a correction for the energy dependent time-walk of the experimental setup is applied. A more detailed overview of the experimental technique and the setup can be found in [1-3].

Lifetimes of ^{152}Gd

The region around neutron number N=90 is a well-known example for a rather rapid change in structure as a function of the nucleon number, i.e., a rst order quantum phase transition (QPT) [4]. Excited states of ^{152}Gd (N=88 neutrons) were populated via the ^{149}Sm(α,n)^{152}Gd reaction and lifetimes were measured using FEST. In particular, the lifetime of the second 0^+ was investigated, searching for a possible new signature of a QPT [5]. Figure 1 shows the obtained energy spectrum of the HPGe detectors. Many transitions of ^{152}Gd can be identi ed.

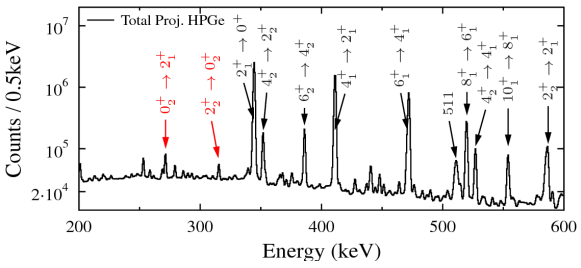

Figure 1: Partial energy spectrum of the HPGe detectors.

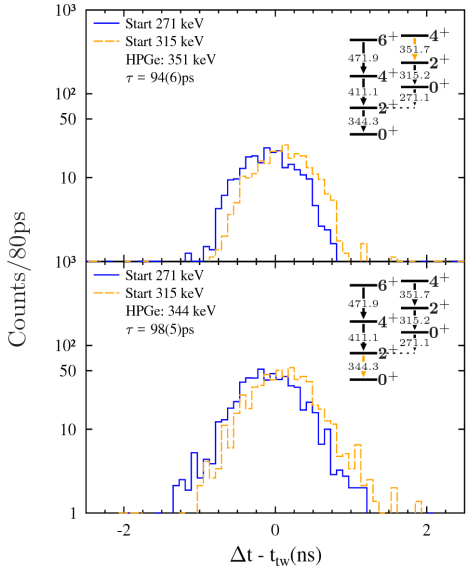

Figure 2: Time-di erence spectra for the combination of gates on the 2^+_2 0^+_2 and 0^+_2 2^+_1 transitions of ^{152}Gd.

Figure 2 shows the nal time-di erence spectrum for the combination of gates on the populating (315 keV) and decaying (271 keV) transitions of the second 0^+ state of ^{152}Gd. Additional gates were set in the pulse-height spectra from the HPGe detectors, selecting the cascade of interest and eliminating background contributions.

The newly determined mean lifetime of the second 0^+ state of ^{152}Gd of τ=96(6) ps [5] turned out to be nearly two times larger than the literature value of 53(12) ps [6] with direct implications for the charaterization of the QPT in the Gd isotopic chain [5].

Supported by the BMBF under the grants 05P15RDFN1 and 05P15RDFN9 and by HIC for FAIR.

References

[1] D. Bucurescu *et al.*, Nucl. Instrum. Methods Phys. Res. A **837**, 1 (2016).
[2] N. Marginean *et al.*, Eur. Phys. J. A **46**, 329 (2010).
[3] J.-M. Régis *et al.*, Nucl. Instrum. Methods. Phys. Res. A **726**, 191 (2013).
[4] R. Casten, Nature Physics **2**, 811 (2006).
[5] J. Wiederhold *et al.*, Phys. Rev. C **94**, 044302 (2016).
[6] N. R. Johnson *et al.*, Phys. Rev. **C** 26, 1004 (1982).

 DOI:10.15120/GR-2018-1

Activities in superheavy element research at SHIP and TASCA

H. David[1], Ch.E. Düllmann[1,2,3], M. Götz[1,2,3], S. Götz[1,2,3], E. Jäger[1], J. Khuyagbaatar[1,3], J. Krier[1], L. Lens[1,2], A. Di Nitto[1,2], V. Pershina[1] , J. Runke[1,2], B. Schausten[1], A. Yakushev[1,3,] for the SHE Chemistry department and the TASCA Collaboration,

M. Block[1,2,3], P. Chhetri[4,1], M. Eibach[5,1], F. Giacoppo[1,3], F. P. Hessberger[1,3], O. Kaleja[2,6], M. Laatiaoui[2,3], J. Maurer[1], A. K. Mistry[1,3], T. Murböck[1], S. Raeder[1,3] for the SHE Physics department and the SHIP/SHIPTRAP Collaborations.

[1]GSI, 64291 Darmstadt, Germany; [2]Universität Mainz, 55099 Mainz, Germany [3]Helmholtz Institut Mainz, 55099 Mainz, Germany; [4]Technische Universität Darmstadt, 64289 Darmstadt, Germany; [5] Universität Greifswald, 17489 Greifswald, Germany; [6]MPIK Heidelberg, 69117 Heidelberg, Germany

In the year 2017, efforts of the Superheavy Element Chemistry department focused on analysis of data obtained in the past UNILAC beamtime period. Major modifications to the experimental setups were performed: i) an upgrade of the cave X8 (TASCA) to install improved shielding, ii) the installation of a new, more flexible TASCA detector chamber, iii) a relocation of the TASCA control room in anticipation of major refurbishment of the SE building, which currently houses the control room, and iv) the design and implementation of a next generation TASCA Control System. Thus, best use was made of the extended shutdown period at GSI.

Selected experiments were performed at other facilities, including the Cyclotron Institute at Texas A&M University, College Station, USA.

'For the superheavy element physics department the activities concentrated on the analysis of data obtained in the past UNILAC beamtime period and preparations of the different experimental setups for the planned experiments in the beamtime period 2018 at GSI.

In parallel, several technical developments were advanced, for example, the completion of the decay spectroscopy system COMPASS, the construction of the single-ion mass measurement setup SHIPTRAP-2, and the design of a novel setup for gas-jet laser spectroscopy.

The specific activities are discussed briefly in the following sections.

Nuclear reaction studies

The drastic reduction of fusion-evaporation cross sections for reactions that form the heaviest elements cannot be understood without knowledge of the competing quasifission (QF) process, which hinders the fusion. Generally, this competition is studied by measuring fission fragments originating from QF and fusion-fission (FF). However, quantitative descriptions of experimental results become complex as many degrees of freedoms are involved and observables for FF and QF can overlap significantly. In collaboration with the Australian National University (ANU), Canberra, Australia, several experiments have been carried out in recent years at ANU's Heavy Ion Accelerator Facility (HIAF). Here, a large range of beam-target configurations was examined in order to investigate how QF/FF competition evolves with changes in entrance channels, taking advantage of the wide angular range available for fission-fragment detection with the CUBE detector setup. These data, together with data on fusion-evaporation reactions (e.g., measured at TASCA and SHIP), provide a comprehensive dataset for describing the QF and FF [Khu17]. In particular, measurements of varying QF probabilities in the ^{48}Ti+^{204,208}Pb and ^{50}Ti+^{206,208}Pb reactions have shed light on the strong influence of nuclear structure on the fusion process. Observed differences for ^{48}Ti+^{208}Pb and ^{50}Ti+^{206}Pb, providing distinct experimental evidence that even reactions that form the same compound nucleus and share the same charge product ($Z_p \cdot Z_t$) can exhibit different levels of QF, cannot be explained by current theories. In addition, data collected using beams of ^{48}Ca, ^{50}Ti, ^{54}Cr, ^{58}Fe and ^{64}Ni incident on actinide targets has yielded a clear systematic picture of a strong dynamical evolution when moving from ^{48}Ca to heavier beams. The data are currently under final analysis. To obtain a conclusive picture concerning the choice of the most preferable beam-target combination for the synthesis of new elements beyond Z=118, fusion-evaporation cross-section measurements of ^{50}Ti-induced reactions on any actinide is suggested. Such measurements are planned to be performed, e.g., at RIKEN, Japan and Dubna, Russia.

Nuclear Structure

Construction of the novel ALpha-BEta-GAmma (ALBEGA) multi-coincidence spectroscopy setup for chemically separated samples [DiN15] continued. Advanced prototypes of the two ALBEGA core detectors, whose inner surfaces are covered with a thin Al and SiO_2 layer, respectively, have been tested. They were developed to provide i) improved energy resolution and sensitivity to low energy signals produced by electrons, ii) higher photon detection efficiency, and iii) better mechanical stability against pressure differences. The tests performed with several radioactive sources including ^{241}Am (α particles) and ^{133}Ba (conversion electrons) confirmed performance according to specifications, including the uniformity and desired very thin thickness of the dead layers, as well as the sensitivity to the low energy signals. In a next step, the detectors will be mounted in a sandwich configuration to produce the final version of the ALBEGA core detector that will be characterized in 2018.

Nuclear decay spectroscopy data collected in parasitic ^{48}Ca beamtime was examined as part of the commissioning of the new Compact Decay Spectroscopy Setup (COMPASS) [Ack18] detection system at SHIP. Initially, the upgrade of using a higher granularity implantation

detector in the form of a double-sided silicon strip detector was assessed, with long correlation times from the decay ^{254}No→^{250}Fm (~30 min) →^{246}Cf measured [Mis18]. In addition, the ability to perform α-γ coincidences was successful, with excited states in ^{249}Fm populated following the decay of ^{253}No. Secondly, with the use of new digital electronics (FEBEX3A) [Hof12], the heavy neutron deficient region around *Z*=92-94 was explored. The use of such a fast timing system (20 ns time resolution) enables full chains to be acquired from a region of fast decaying nuclei, where with a conventional analogue system chain members could not be recorded due to dead time of the electronics system. A successful product of this investigation was synthesis of the previously unconfirmed isotope ^{225}Np. Development work on improvements to the detector system included upgrading to FEBEX4A (10 ns timing resolution) and enhancements to the escape 'box' detectors to maximize efficiency.

Mass measurements for nuclear structure studies

The nuclear structure studies by direct mass spectrometry with SHIPTRAP will be further extended to heavier and more exotic nuclides in the next beamtime period at GSI in 2018. Facing the challenge of ever-lower production rates, it has been worked on measures for a further increase in efficiency and sensitivity. To this end in the recent years, a cryogenic gas cell for SHIPTRAP has recently been built. In the commissioning beamtime in 2015 an increase of the overall efficiency by almost one order of magnitude was achieved [Kal15]. In 2017, additional offline studies were performed with radioactive sources. We studied the extraction of different elements from the gas cell and to optimize the transport of ions to the SHIPTRAP Penning traps following the 2016 relocation of the complete setup [Gia17]. The phase imaging (PI-ICR) measurement technique [Eli13] was further optimized at SHIPTRAP studying systematic uncertainties, exploring the achievable mass resolving power and improving the long-term stability for measurements with lowest yield. The PI-ICR technique has become the new standard for on-line mass measurements of radionuclides worldwide. However, challenges for direct mass spectrometry of the heaviest elements remain. In the next measurement campaign at GSI the identification of low-lying isomeric states in No-, Lr-, and Rf-isotopes is planned. In this mass region the various types of isomeric states are known, many of which have low excitation energies and similar half-lives to the ground state rendering their identification by means of conventional nuclear spectroscopy difficult. The high mass resolving power of the PI-ICR method makes it an ideal choice for this. A mass resolving power of about 100,000 for only 100 ms measurement time has also been reached for heavy ions.

Atomic Physics

The pioneering laser spectroscopy work on nobelium performed at the GSI in recent years led to the observation of more than 30 atomic states in the nobelium atom, among them several Rydberg states [Laa16]. From the convergence of the observed Rydberg series, we eventually obtained the ionization potential based on a two-step laser ionization scheme with high accuracy. However, the presence of buffer gas collisions led to the population of long-lived metastable states below the $^1P_1$ state that was directly excited by the first-step laser. The second laser excitation had sufficient energy to ionize the nobelium atoms from either of the two states. Thus, the identification of the different series was crucial for the IP determination. This was accomplished based on the delayed ionization signal obtained when the second step laser was delayed compared to the first one. In the case of the $^1P_1$ state that features a lifetime of only about 2 ns this signal decayed rapidly, whereas a longer-lived component with a lifetime of tens of ns was observed indicating the population of the lower-lying metastable state. In 2017, the data analysis was completed, and a rate equation model was developed that allowed us to describe the experimental data for nobelium as well as corresponding data for the homolog ytterbium perfectly [Chh17]. Consequently, the first ionization potential of nobelium was determined two orders of magnitude more accurately than before [Chh18].

The analysis of the hyperfine spectroscopy data for ^{253}No was supported by three different sets of atomic structure calculations that provided the mass shift and field shift constants as well as the hyperfine parameters. The results support the ground state spin and parity assignment of $9/2^-$, previously derived from in-beam gamma spectroscopy, and furthermore provide the magnetic and quadrupole moment of this odd-*A* nucleus accurately. Recently, state-of-the-art density functional calculations reproduced the differential charge radii of lighter actinides [Mar14, Rei17]. These calculations are also in excellent agreement with the nobelium data on differential charge radii. This confirms the theoretical prediction of maximum deformation in the nobelium isotopic chain around neutron number N = 152. It also substantiates the claim of a sizeable central depression in the proton distribution of ^{254}No, a feature that is only found in superheavy nuclei and originates from their strong Coulomb repulsion. The hyperfine spectroscopy results have been submitted for publication [Rae18].

Chemistry

In the past beamtime periods, experiments to study the chemical behavior of Fl and Nh in comparison with Hg, Tl, Pb, and Rn were performed at TASCA [Blo16]. In addition, the volatility and reactivity of these elements towards surfaces like SiO_2 and Au were measured. The comprehensive analysis of these results was continued. For Nh, experimental results [Blo16, Aks17] indicate a reduced volatility and enhanced reactivity compared to Cn and Fl. To render assistance to these gas-phase experiments, calculations of the adsorption energies of these elements and their lighter homologs on a Au(111) surface have been performed using a periodic ADF BAND code. Such periodic calculations of adsorption energies have been performed for the first time for superheavy element systems adsorbing on gold. The results have shown that Cn should indeed be the most volatile element out of

 DOI:10.15120/GR-2018-1

those under consideration. In addition, Fl should interact with gold at room temperature. Nh, should very strongly interact with gold. Such a different adsorption behavior allows for a good separation between all of these elements using a combination of quartz and gold surfaces [Per17a]. In addition, molecular properties of group-13 hydroxyls (of Tl and Nh) needed for predictions of their reactivity with quartz and gold have been calculated with the use of most advanced relativistic methods. In difference to the conclusion from the earlier predictions, NhOH is expected to be less volatile than TlOH [Per18]. To study Nh under improved conditions, advanced setups for optimized transport of the element under study to the detection setup are under development also allowing investigation of less volatile species. One such approach involves the direct connection of the existing COMPACT detection array [Yak14] to the TASCA Recoil Transfer Chamber (RTC). Another possibility involves the coupling of COMPACT to a recoil separator by employing a buffer-gas stopping cell instead of a classical RTC. First studies of the extraction efficiency of ^{219}Rn ions obtained from a ^{223}Ra recoil ion source installed in the SHIPTRAP buffer gas stopping cell [Neu06] into a COMPACT detector array were measured in off-line experiments at GSI. A first on-line experiment with such a setup was performed at the Cyclotron Institute, Texas A&M University, College Station, USA. The buffer gas stopping cell was coupled to the Momentum Achromat Recoil Spectrometer (MARS) [Fol12]. The isotopes ^{182,183}Hg and ^{199,200}At were produced in the reactions ^{40}Ar + ^{147}Sm and ^{40}Ar + ^{165}Ho, isolated in MARS, thermalized in the buffer gas stopping cell, and extracted into the COMPACT by using electric fields. The final analysis of the obtained extraction efficiencies and transport times is currently ongoing.

The studies related to volatile transition metal carbonyl complexes with short-lived isotopes have been continued. Currently, the method of choice is the isolation of the studied isotopes in a recoil separator, followed by their thermalization in an RTC that is flushed with CO-containing carrier gas [Eve14]. As the fusion-evaporation products of asymmetric fusion reactions needed for the productions of sufficiently long-lived isotopes of the elements of interest like Sg, Bh, and Hs, have a relatively large angular and energy spread, transmission efficiencies through a recoil separator like TASCA or GARIS at RIKEN are rather moderate, around 10-15%. Thus, the overall efficiency for the synthesis of carbonyl complexes in combination with physical preseparation is rather low. Therefore, possibilities for the chemical investigation of these compounds without a physical preseparator are currently explored. First experiments performed at the Tandem accelerator at JAEA Tokai, Japan, suggested that the successful synthesis of Os and W carbonyl complexes is feasible if the thermalization of the evaporation residues is spatially decoupled from the chemical synthesis. In that way it is needed, that the formation of the carbonyl complexes takes place in the absence of the beam, which is a strict requirement [Wan14]. In experiments with fission products at the research reactor TRIGA Mainz, the partial efficiencies for the flush-out transfer of non-volatile products from the thermalization chamber into the chemical synthesis chamber were measured and confirm that such an approach allows obtaining higher efficiencies than with preseparation. To support gas-phase experiments on studies of the stability and volatility of carbonyls of the heaviest elements, calculations of the electronic structures and properties of group-6 carbonyls [Ili17] and group-7 carbonyls, including those of Bh, were performed using the most advanced relativistic quantum-chemical methods (ADF BAND, X2c-DFT, DIRAC). The work considers all possible formation reaction scenarios of the single species that do not exist in macrochemistry. The formation mechanisms have been found and the volatile species that should form at the experimental conditions are suggested. Accordingly, the detailed properties of the $M(CO)_5H$ species (M= Tc, Re and Bh) have been calculated, including radicals $M(CO)_5$. Volatilities of these species and first bond dissociation energies have been predicted [Per17b].

Further activities, including those centered at the Helmholtz Institute Mainz, are described in more detail in the contribution to the Annual Report 2018 of the Helmholtz Institute Mainz [HIM18].

References

[Ack18] D. Ackermann, A.K. Mistry, F.P. Hessberger et al., Nucl. Instrum. Meth. A, accepted, in publication (2018).
[Aks17] N.V. Aksenov et al., Eur. Phys. J. A 53, 158 (2017).
[Blo16] M. Block et al., GSI Sci. Rep. 2016, p. 197-199, RESEARCH-NUSTAR-SHEP-1.
[Chh17] P. Chhetri et al., Eur. Phys. J. D 71,195 (2017).
[Chh18] P. Chhetri et al., in preparation (2018).
[DiN15] A. Di Nitto et al., GSI Sci. Rep. 2014, p. 184, MU-NUSTAR-SHE-C-06 (2015).
[Eli13] S. Eliseev et al., Phys. Rev. Lett. 100, 082501 (2013)
[Eve14] J. Even et al., Science 345, 1491 (2014).
[Fol12] C.M. Folden III et al., NIMA 678, 1 (2012).
[Gia17] F. Giacoppo et al., Acta Phys. Pol. B 48, 423 (2017).
[HIM18] SHE section of the 2017 HIM Annual Report (2018).
[Hof12] J. Hoffmann et al., GSI Scientific Report 2011, 253, (2012).
[Ili17] M. Iliaš and V. Pershina, Inorg. Chem. 56, 1638 (2017).
[Kal15] O. Kaleja et al., xxx
[Khu17] J. Khuyagbaatar, EPJ Web Conf., 163, 00030 (2017).
[Laa18] M. Laatiaoui et al., Nature 538, 495 (2016).
[Mar14] J. A. Maruhn et al., Comput. Phys. Commun. 185, 2195 (2014).
[Mis18] A. K. Mistry et al., Acta Phys. Pol., accepted, in publication (2018).
[Neu06] J.B. Neumayr et al., NIMB 244, 489 (2006).
[Per17a] V. Pershina, Relativistic Quantum Chemistry for Chemical Identification of the Superheavy Elements, In: Handbook of Relativistic Quantum Chemistry, Ed. W. Liu, Springer, (2017) pp. 857-899.

[Per17b] V. Pershina and M. Iliaš, J. Chem. Phys. 146, 184306 (2017).
[Per18] V. Pershina and M. Ilias, Chem. Phys. Lett. 694, 107 (2018).
[Rae18] S. Raeder et al., in publication (2018).
[Rei17] P.-G. Reinhard and W. Nazarewicz, Phys. Rev. C 95, 064328 (2017).
[Wan14] Y. Wang et al., Radiochim. Acta 102, 69 (2014).
[Yak14] A. Yakushev et al., Inorg. Chem. 53, 1624 (2014).

Experiment beamline: SHIP-SHIPTRAP / TASCA
Experiment collaboration: NUSTAR-SHE / NUSTAR-LASPEC / NUSTAR-MATS
Experiment proposal:
[U259,U288,U295,U308,U312,U313,U314]
Accelerator infrastructure: UNILAC
Grants: [EU H2020 contract No. 654002 / TNA]
Strategic university co-operation with: JGU Mainz

 DOI:10.15120/GR-2018-1

Comparison of nuclear and electromagnetic breakup of ^{17}Ne

F. Wamers[1,2], J. Marganiec[1,2,3], T. Aumann[2,1], L.V. Chulkov[4,1], M. Heil[1], B. Jonson[5], R. Plag[1], H. Simon[1], and the R^{3}B collaboration

[1]GSI, Darmstadt, Germany; [2]TU Darmstadt, Darmstadt, Germany; [3]EMMI@GSI, Darmstadt, Germany; [4]NRC Kurchatov Institute, Moscow, Russia; [5]Chalmers Tekniska Högskola, Göteborg, Sweden

In previous years we have reported on various aspects of the structure of and reactions with the proton dripline nucleus ^{17}Ne, as observed in the S318 experiment [1-4].

Here we highlight our recent study of ~500 MeV/u ^{17}Ne reactions on light (carbon and CH_2) vs. heavy (lead) targets, with a focus on electromagnetic breakup to the ^{15}O+2p continuum [5].

Momentum Distributions

We have analysed channels with one heavy fragment, ^{15}O or ^{14}O, and one or two coincident beam-like protons as forward-focused reaction residues. While, e.g., ^{15}O+1p produced from light targets (H, C) show a narrow fragment momentum distributions (142 MeV/c, 152 MeV/c), produced mainly via *1p knockout* on ^{17}Ne, on the Pb target such a 1p knockout is taking place inside the target's strong Coulomb field causing the ^{15}O momentum distribution is about 3 times wider (430 MeV/c). The fragment momentum distributions in the ^{15}O+2p channels are generally wider (C: 301 MeV/c, Pb: 285 MeV/c), since the reaction mechanisms at work here are mainly *inelastic scattering* and *diffraction dissociation* (plus *electromagnetic dissociation* for Pb), which typically transfer momentum to more than just one nucleon in the projectile nucleus. For the H target and the ^{15}O+2p channel, however, the observed ^{15}O momentum distribution exhibits an even larger width (365 MeV/c); the reaction mechanism here is still unclear, since the three mentioned above should typically be negligible for a proton target.

Electromagnetic Dissociation

Because of the nuclear astrophysics interest for the ^{15}O(2p,g)^{17}Ne reaction rate, we have distilled the pure electromagnetic fraction of the Pb-target based ^{15}O+2p differential cross section, by subtracting the equivalent C-target distribution (scaled by 1.84). Figure 1 shows a comparison of this E_{f2p}-differential cross section (blue filled diamonds) with three theoretical calculations (solid lines = raw, dashed lines = broadened by the experiment resolution). First, the blue line represents a calculation based on a ^{15}O+2p three-body model [6] in which the weight s^2 configuration of the ^{17}Ne g.s. was at P(s^2) = 5%. The calculation result was scaled by 0.5 in order to get a better agreement with the experimental data. Results obtained for larger P(s^2) within this model require an even stronger downscaling; e.g., for P(s^2) = 48% the required scaling is 0.25. Second, the red curve stems from a different three-body model, with P(s^2) = 16%, [7]. Third, the magenta curve shows an RQPRPA based Hartree-Bogoliubov calculation [8]. Generally, the three models produce ^{15}O+2p internal energy spectra that strongly differ between each other. We observe that the calculation resulting from the model of [7] matches the experimental data better than the others, in particular in absolute numbers, and at energies E_{fpp} > 5 MeV. It is interesting to note in particular the difference between [6] and [7], since they are both based on a ^{15}O+2p three-body model. Furthermore, all three calculations feature E1-only dissociation, whereas the experimentally observed population of the $5/2_1^-$ excited state at 830 keV above threshold suggests a non-negligible contribution of E2 strength to the electromagnetic dissociation of ^{17}Ne. We find that yet none of the theoretical models on the market match the entire experimental spectrum in a satisfactory way. However, our data may help to validate models of the ^{17}Ne structure and of dissociation processes in the future.

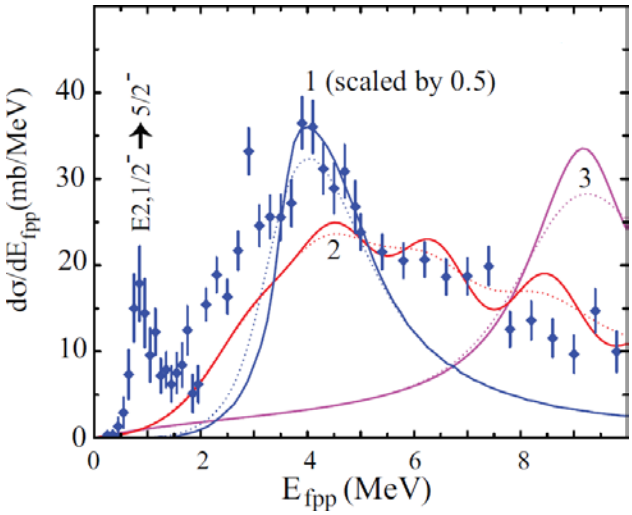

Figure 1: Comparison of our experimental Pb-target electromagnetic dissociation cross section (blue filled diamonds) with theoretical models (solid lines - raw; dotted lines - broadened by experimental resolution). Lines "1": blue [6]; lines "2": red [7]; lines "3": magenta [8].

References

[1] J. Marganiec et al., GSI Scientific Report 2013
[2] J. Marganiec et al., GSI Scientific Report 2014
[3] F. Wamers et al., GSI Scientific Report 2014
[4] J. Marganiec et al., GSI Scientific Report 2015
[5] F. Wamers et al., PRC 97, 034612 (2018)
[6] L. Grigorenko et al., PLB 641, 254 (2006)
[7] T. Oishi et al., PRC 84, 057301 (2011)
[8] Z.Y. Ma, Y. Tian, Sc. Ch. Ph., M. Astr. 54, 49 (2011)

Experiment beamline: R3B
Experiment collaboration: NUSTAR-R3B
Experiment proposal: S318
Accelerator infrastructure: UNILAC / SIS18 / FRS
PSP codes: none
Grants: NAVI, GSI-TU Darmstadt cooperation, HIC for FAIR, EMMI, BMBF, DFG (through grant SFB1245)
Strategic university co-operation with: Darmstadt

Hypernuclei production within the new intranuclear cascade code INCL

J. L. Rodríguez-Sánchez[1,2], J.-C. David[3], J. Cugnon[4], J. Hirtz[3], A. Kelic-Heil[2], S. Leray[3], and D. Mancusi[3].

[1]GSI, Darmstadt, Germany; [2]USC, Santiago de Compostela, Spain; [3]CEA, Saclay, France; [4]Univ. of Liège, Belgium.

In this work, we study the production of hypernuclei in spallation reactions using intranuclear-cascade models (INC) coupled to de-excitation codes by means of a two-step process [1]: the collision itself, where part of the nucleons contained in the target nucleus are removed or modi ed and some excitation energy and angular momenta are gained by the remnant; and subsequent de-excitation processes by evaporation of particles or, if applicable, by ssion. Here, INC models are considered as a Monte Carlo method to solve numerically the dynamic transport equations describing the hadron-nucleus collision. The nature of INC models is essentially classical, being assumed that nucleons are perfectly localised in phase space and that they are bound by a potential. In this approach, the nuclear collision is treated as successive relativistic binary hadron-hadron collisions separated in time, where the positions and momenta of hadrons are followed as time evolves. It is also assumed that hadrons move along straight trajectories until they undergo a collision with another hadron or until they reach the surface, where they could eventually escape. Cross sections are determined from a set of collision events taken at di erent impact parameters and for which nucleon positions and momenta are initially sampled for each participant nucleus.

Recently, the Liege intranuclear-cascade model (INCL) [2,3] has been extended towards high energies (~15 GeV) including multipion production [4], production of η and ω mesons [5], and strange particles like kaons and hyperons [6]. This new version permits us to predict the formation of hyperremnants and their characterization in atomic, mass, and strange numbers together with their excitation energies and angular momenta.

In the new version of INCL, elementary cross sections related with the production and interaction of strange particles (such as K, $\overline{\text{K}}$, Σ, and Λ) were implemented using sophisticated parametrizations of available experimental data as well as their characteristics: angular distributions, momenta, and charge repartition of the particles in the associated nal states. These new ingredients made INCL become in a powerful tool to study the production of strange particles in nuclear matter and to go further in the understanding of hypernuclei formation.

For modeling the de-excitation stage, we use the ABLA07 code [7] developed at GSI, which describes the de-excitation of a nucleus emitting γ-rays, neutrons, light-charged particles, and intermediate-mass fragments according to Weisskopf's formalism. For a more realistic description of this process, the separation energies are taken from the atomic mass evaluation of 2003 and the emission barriers for charged particles are determined with the Bass potential. Fission is also considered according to Ref. [8]. This model has been also extended by us to account for the emission of Λ particles and the production of cold Λ-hypernuclei following Ref. [9].

The coupling of these codes allows us to predict the production of Λ-hypernuclei in spallation reactions, as shown in Fig. 1. In addition, both codes are available in GEANT4 after an important e ort, which will provide a reliable input to design and optimize new experimental setups for the investigation of hypernuclei and strange particles. The benchmark of these models with available experimental data on the production of strange particles will be published soon with promising results.

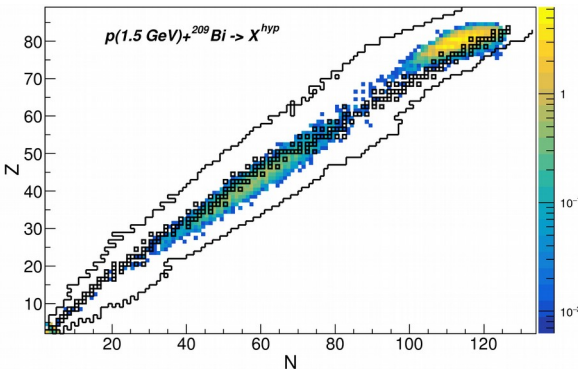

Figure 1: Cross section (in b) of cold Λ-hypernuclei produced in the spallation reaction ^{209}Bi + p at 1.5A GeV.

References

[1] J.-C. David, Eur. Phys. J. A 51 (2015) 68.
[2] D. Mancusi et al., Phys. Rev. C 90 (2014) 054602.
[3] J.L. Rodríguez et al., Phys. Rev. C 96 (2017) 054602.
[4] D. Mancusi et al., Eur. Phys. J. A 53 (2017) 80.
[5] J.-C. David et al., submitted to Eur. Phys. J. Plus.
[6] J. Hirtz et al., submitted to Eur. Phys. J. Plus.
[7] A. Kelic et al., arXiv:0906.4193v1.
[8] B. Jurado et al., Nucl. Phys. A 747 (2005) 14.
[9] A.S. Botvina et al., Phys. Rev. C 94 (2016) 054615.

Grants: This work has been supported by the Department of Education, Culture and University Organization of the Regional Government of Galicia under the program of postdoctoral fellowships

 DOI:10.15120/GR-2018-1

Experimental campaign using the NeuLAND demonstrator at SAMURAI

J. Kahlbow[1], K. Boretzky[2], N.L. Achouri[3], D.S. Ahn[4], H. Al Falou[5], G. Alkhazov[6], M. Assie[7], L. Atar[1], T. Aumann[1,2], H. Baba[4], D. Beaumel[7], D. Bemmerer[8], M. Böhmer[9], M. Caamano[3], C. Caesar[2], D. Calvet[10], H. Chae[11], S. Chen[4], M.I. Cherciu[12], N. Chiga[4], L. Chulkov[13], A. Corsi[10], M.L. Cortes[4], D. Cortina[14], T.E. Cowan[8,15], H.L. Crawford[16], F. de Oliveira Santos[17], F. Delaunay[3], A. Delbart[10], G. Dentinger[1], Q. Deshayes[3], Z. Dombradi[18], P. Doornenbal[4], C.A. Douma[19], F. Dufter[9], Z. Elekes[18], J. Enders[1], P. Fallon[16], J. Feng[20], B. Fernandez[14], F. Flavigny[7], U. Forsberg[21], N. Fukuda[4], Z. Fülöp[18], D. Galaviz Redondo[22], I. Gasparic[23], Z. Ge[4], R. Gernhäuser[9], J.-M. Gheller[10], J. Gibelin[3], A. Gilibert[10], K. Göbel[24], N. Gruzinsky[6], Z. Halasz[18], F. Hammache[7], M.N. Harakeh[19], T. Heftrich[24], M. Heil[2], A. Heinz[25], A. Hirayama[26], C.R. Hoffman[27], M. Holl[1], A. Horvat[1], A. Horvath[28], J.W. Hwang[29], N. Inabe[4], T. Isobe[4], H.T. Johansson[25], B. Jonson[25], N. Kalantar-Nayestanaki[19], S. Kawase[30], A. Kelic-Heil[2], S. Kim[29], D. Kim[31], K. Kisamori[4], R. Kissel[1], M. Knösel[1], T. Kobayashi[32], Y. Kondo[26], D. Körper[2], P. Koseoglou[1,2], S. Koyama[33], N.G. Kozlenko[6], D. Kresan[2], T. Kubo[4], Y. Kubota[4], I. Kuti[18], V. Kuznetsov[6], C. Langer[24,2], V. Lapoux[10], C.S. Lee[34], C. Lehr[1], P.J. Li[35], S. Lindberg[25], Y. Liu[20], B. Löher[1], Y. Maeda[36], F.M. Marques[3], S. Masuoka[34], Y. Matsuda[32], M. Matsumoto[26], A. Matta[3], J. Mayer[37], K. Miki[38], M. Miwa[4], B. Monteagudo[3], T. Murakami[39], I. Murray[4], M.A. Najafi[19], T. Nakamura[26], K. Nakano[30], N. Nakatsuka[39], T. Nilsson[25], G.H. Nyman[25], A. Obertelli[10], N.A. Orr[3], H. Otsu[4], T. Ozaki[26], V. Panin[4], S. Park[31], M. Parlog[3], S. Paschalis[1,21], N. Paul[10], M. Petri[21], S.G. Pickstone[37], M. Pohl[24], P.-M. Potlog[12], S. Reichert[9], R. Reifarth[24], S. Reinicke[8], A. Revel[3,17], C. Rigollet[19], D.M. Rossi[1], A.T. Saito[26], T. Saito[33], S. Sakaguchi[30], M. Sako[4], H. Sakurai[4], M. Sasano[4], H. Sato[4], Y. Satou[29], D. Savran[40], H. Scheit[1], F. Schindler[1], P. Schrock[34], M. Shikata[26], Y. Shimizu[4], S. Shimoura[34], H. Simon[2], D. Sohler[18], O. Sorlin[17], E. Stan[12], S. Storck[1], L. Stuhl[4,34], T. Sumikama[4], Y.L. Sun[10], H. Suzuki[4], D. Symochko[1], I. Syndikus[1], H. Takeda[4], S. Takeuchi[26], J. Tanaka[1], M. Tanaka[41], M. Thoennessen[38], Y. Togano[26], T. Tomai[26], H.T. Törnqvist[1], J. Tscheuschner[1], J. Tsubota[26], T. Uesaka[4], L. Uvarov[6], S. Volkov[6], V. Wagner[1], A. Wagner[8], H. Wang[4], K. Wimmer[33], H. Yamada[26], Z. Yang[4], B. Yang[20], L. Yang[34], M.Yasuda[26], K. Yoneda[4], L. Zanetti[1], J. Zenihiro[4], A. Zilges[37], K. Zuber[15]

(R^3B-NeuLAND-SAMURAI Collaboration)

[1]Technische Universität Darmstadt, Institut für Kernphysik, Darmstadt, Germany; [2]GSI Helmholtzzentrum für Schwerionenforschung, Darmstadt, Germany; [3]LPC Caen, Caen, France; [4]RIKEN Nishina Center for Accelerator-Based Science, Wako, Saitama, Japan; [5]Lebanese-French University, Deddeh, Lebanon; [6]Petersburg Nuclear Physics Institute Gatchina, Leningrad district, Gatchina, Russia; [7]IPN Orsay, Orsay, France; [8]Helmholtz-Zentrum Dresden-Rossendorf, Institute of Radiation Physics, Dresden, Germany; [9]Technische Universität München, Garching, Germany; [10]CEA Saclay, Gif-sur-Yvette, France; [11]IBS, South Korea; [12]Institute of Space Sciences, Magurele, Romania; [13]NRC Kurchatov Institute pl. Akademika Kurchatova, Moscow, Russia; [14]Universidade de Santiago de Compostela, Santiago de Compostela, Spain; [15]Technische Universität Dresden, Institut für Kern- und Teilchenphysik, Dresden, Germany; [16]Lawrence Berkeley National Laboratory, Berkeley, United States of America; [17]GANIL, Caen, France; [18]MTA Atomki, Debrecen, Hungary; [19]KVI - Center for Advanced Radiation Technology, Groningen, Netherlands; [20]Peking University, Beijing, China; [21]Department of Physics, University of York, United Kingdom; [22]Laboratory for Instrumentation and Experimental Particle Physics, Lisbon, Portugal; [23]RBI Zagreb, Zagreb, Croatia; [24]Johann Wolfgang Goethe-Universität Frankfurt, Frankfurt am Main, Germany; [25]Chalmers University of Technology, Göteborg, Sweden; [26]Tokyo Institute of Technology, Tokyo, Japan; [27]Argonne National Laboratory, Lemont, United States of America; [28]Eötvös Lorand University, Budapest, Hungary; [29]Seoul National University, Seoul, South Korea; [30]Kyushu University, Fukuoka, Japan; [31]Ewha Womans University, Seoul, South Korea; [32]Tohoku University, Sendai, Japan; [33]University of Tokyo, Tokyo, Japan; [34]Center for Nuclear Study, Tokyo, Japan; [35]Hongkong University, Hongkong; [36]Miyazaki University, Miyazaki, Japan; [37]Universität zu Köln, Institut für Kernphysik, Köln, Germany; [38]Michigan State University, East Lansing, United States of America; [39]Kyoto University, Kyoto, Japan; [40]Extreme Matter Institute, Darmstadt, Germany; [41]Osaka University, Osaka, Japan

NeuLAND – an introduction

The Large Area Neutron Detector NeuLAND [1] as part of the R^3B setup at FAIR is a neutron time-of-flight spectrometer aiming at detecting fast neutrons (0.2 to 1 GeV) from nuclear reactions. The detector concept is based on detection of hadronic interactions within the fully-active detector volume, made from organic scintillator material. The design goals comprise a spatial

Year	*Experiment*	*Spokespersons*
2015	ImPACT campaign (transmutation studies)	H. Sakurai (RIBF)
	1n efficiency measurement at 110 MeV & 250 MeV	H. Otsu (RIBF)
	^{28}O & ^{27}O spectroscopy	Y. Kondo (TITech)
2016	Sπrit TPC – EOS experiment	T. Isobe (RIBF) / W. Lynch (NSCL) / T. Murakami (U Kyoto) / B. Tsang (NSCL)
	^{31}Ne Coulomb breakup & knockout	N. Kobayashi (RCNP) / Y. Togano (TITech)
	Search for ^{22}C (2^+) and ^{21}B: Structure at and beyond the N=16 subshell closure	N.A. Orr (LPC)
	Lifetime of ^{26}O ground state	C. Caesar (TU Darmstadt/GSI)
2017	Dipole response of n-rich Ca isotopes	Y. Togano (TITech) / T. Kobayashi (U Tohoku)
	SEASTAR-3 (n-rich isotopes in K – V region)	P. Doornenbal (RIBF) / A. Obertelli (CEA)
	Dipole response of light, dripline nuclei (^{6,8}He)	T. Aumann (TU Darmstadt)
	Study of tetraneutron system using ^{8}He(p,pα)4n	D. Rossi (TU Darmstadt) / S. Paschalis (U York) / S. Shimoura (CNS)
	Study of tetraneutron system using ^{8}He(p,2p)^{7}H	F.M. Marques (LPC) / Z. Yang (RIBF)

Table 1: Overview over the experiments using the NeuLAND demonstrator at the SAMURAI setup at RIKEN during 2015-2017.

resolution of $\sigma_{x,y,z} \approx 1$ cm and a time resolution of $\sigma_t < 150$ ps. The once finished detector will have a front size of 250x250 cm^2 and a depth of 3 m, thus enabling a high neutron-detection efficiency of more than 90%. Due to its calorimetric properties, NeuLAND has also a large multi-neutron recognition capability, aiming for the unambiguous detection of up to 5 neutrons simultaneously. Together with the long flight path of about 35 m between target and detector, available in the high-energy cave at FAIR, a resolution of about $\sigma_E \approx 20$ keV at 100 keV above threshold will be obtained. NeuLAND consists of scintillator bars arranged in double planes. Each double plane comprises one horizontal and one vertical layer of 50 scintillator bars (250x5x5 cm^3). The production of double-planes is underway at GSI, and 13 out of the final 30 double-planes will be used in the phase-0 campaign at GSI, starting from 2018.

Experimental campaign at RIKEN

After successful tests of the first 4 double-planes, the so-called NeuLAND demonstrator, with beams at GSI in 2014, this demonstrator was transported to the RI Beam Factory (RIBF) at the RIKEN Nishina Center (Japan) in the beginning of 2015. There it complemented the neutron detection system NEBULA [2,3] at the SAMURAI setup [4] for a two-year experimental campaign [5].

Figure 1 displays a schematic view of the SAMURAI experimental setup including the NeuLAND demonstrator. At SAMURAI, experiments with radioactive beams with a large-acceptance spectrometer are performed. In a kinematically complete measurement also the fast neutrons need to be detected.

The combination of the neutron detection systems leads to a significant increase in total efficiency and invariant-mass resolution, thus allowing for the detection of four simultaneously emitted neutrons, their tracking and the determination of their individual four-momenta.

In total, 12 experiments were performed, covering a wide spectrum of nuclear physics from nuclear breakup reactions with very exotic light systems, and the dipole response of neutron-rich nuclei to the study of the

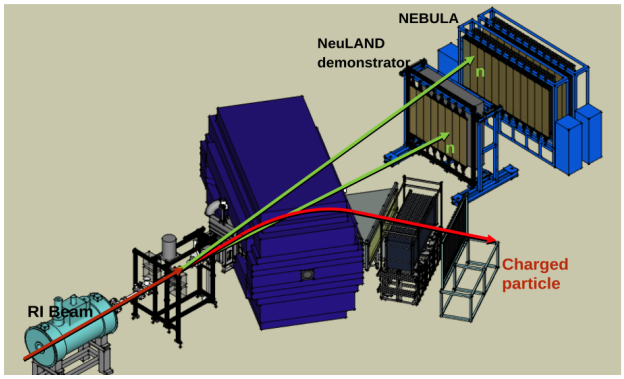

Figure 1: Schematic view of the SAMURAI experimental setup with its target region at the left hand side, the SAMURAI large-acceptance superconducting dipole magnet in the center and at the zero degree line the NeuLAND demonstrator, complemented with a VETO wall, in front of the NEBULA arrays. At deflection angles around 60 degrees a charged particle detection system is located.

equation-of-state (EOS) of nuclear matter in central collisions. These are summarized in Table 1. In the

 DOI:10.15120/GR-2018-1

following, we give an overview about the experiments in this campaign and highlight selected experiments.

One-neutron detection efficiency study

In one of the first experiments a key quantity of the NeuLAND demonstrator, namely the one-neutron detection efficiency, was determined. In the charge-exchange reaction ^{7}Li(p,n)^{7}Be(g.s.+430 keV) quasi-monoenergetic neutrons at 106.8 MeV and 250.5 MeV were produced from a high-intensity proton beam and detected by NeuLAND [6,7]. Preliminary results for the 1n-detection efficiency give (27.8±1.2)% and (26.6±1.1)% for neutrons at energies of 106.8 MeV and 250.5 MeV, respectively. These results are essential to extract cross sections from experiments using NeuLAND at SAMURAI.

Once NeuLAND was successfully commissioned at SAMURAI, the physics program started. We describe the experiments in the following, starting with experiments focussing on multi-neutron decays beyond the dripline.

Spectroscopy of ^{28}O

The combined neutron detection system of NeuLAND and NEBULA allows for the first time the detection and tracking of four coincident neutrons, in particular the spectroscopy of the neutron-unbound nuclei ^{28}O and ^{27}O. The neutron dripline is established at mass number 24 for the oxygen isotopic chain; heavier oxygen isotopes are not bound. A sudden change in the binding is observed by adding one more proton to oxygen – fluorine can bind at least six more neutrons. It is crucial to understand the shell evolution for these most neutron-rich isotopes. The spectroscopy of the one- and two-neutron decay channels ^{25}O and ^{26}O has already been performed in a previous experiment at SAMURAI [8].

The unbound system ^{28}O was populated by a proton knockout reaction on a ^{29}F beam at 235 MeV/u (before target). Since the neutron-reconstruction efficiency is still low for three and four neutrons a liquid hydrogen target of 15 cm length was used to increase the luminosity. The target was surrounded by a time-projection chamber to reconstruct the reaction-vertex position. Including this information the invariant mass can be determined precisely. For details on the setup see [9]. After the reaction, the ^{28}O system decays in-flight into the heavy fragment ^{24}O and four neutrons. The challenge is the unambiguous identification of the four neutrons in NeuLAND and NEBULA to reconstruct the invariant-mass of the decaying system.

In this experiment also other reaction channels were investigated, in particular proton-knockout reactions on neon isotopes. Thus, also spectroscopy of the heaviest fluorine can be performed. Here, γ-rays are measured in addition to neutrons. With this information, excitation energies are obtained, which provide insight into the shell structure and its evolution.

In order to benchmark the performance of the detection system a reference channel, the invariant-mass of the ^{24}O fragment, and only one neutron from the 4n decay channel is investigated, see Figure 2. Known intermediate resonances from sequential decays are identified, in particular the broad ground-state resonance of ^{25}O at 749 keV and the ground state of ^{26}O which is located at only 18 keV above threshold [8]. The sharp peak close to the decay threshold in this preliminary analysis indicates the good resolution of the detection system where the narrow ^{26}O(g.s.) resonance is well resolved.

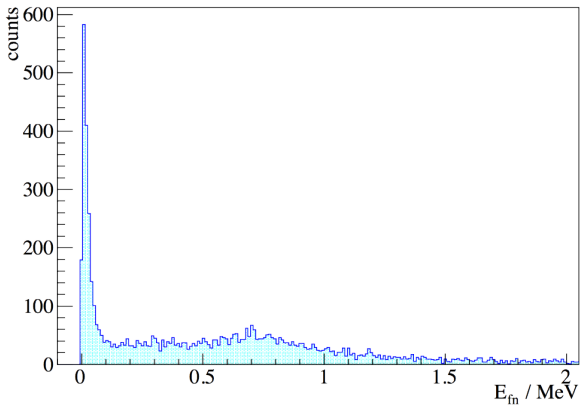

Figure 2: Preliminary invariant-mass spectrum of ^{24}O+1n from the reaction ^{29}F(p,2p). The narrow ^{26}O(g.s.) resonance at 18 keV is clearly seen.

Lifetime of the ^{26}O ground state

Another experiment along the oxygen-chain aimed specifically at investigating the properties of ^{26}O. Besides the spectroscopic information of ^{26}O, the ground state of this nucleus might have an unusually long lifetime [10] where the two-neutron decay is hindered by the angular momentum barrier for *d*-wave valence neutrons. We have developed a new method to determine lifetimes in the (sub-)picosecond range of systems which decay via neutron emission [11]. The method is based on the idea that the ^{26}O nuclei, which are produced by proton removal on a ^{27}F beam, decay with a larger fraction outside the reaction target the longer their lifetime is. This can be observed in the velocity difference between the decay-neutrons and the ^{24}O fragment. The characteristic shape of this velocity-difference spectrum allows to extract the lifetime. A stack of targets of dense material and of high nuclear charge was used to decelerate the ^{26}O ions and thereby increase the sensitivity of the method. The neutron velocity is determined from the time-of-flight and position measured with NeuLAND and NEBULA. For further details on the setup see [12].

Search for a tetraneutron system

The possible existence of a four-neutron system as well as its properties has been a long lasting question in nuclear physics starting in the mid-1960s [13]. A recent experiment carried out at the SHARAQ spectrometer at RIKEN uncovered four candidate events for a low-lying four-neutron ground-state resonance with a 4.9σ significance level, generated in a ^{4}He(^{8}He,^{8}Be) reaction

[14]. This measurement triggered new efforts to finally uncover direct evidence for the existence of this system.

To this end, we have performed an experiment to investigate the four-neutron system via a new method, i.e., the measurement of ^{8}He(p,pα)4n at large momentum transfer, using a secondary ^{8}He beam at an energy of 156 MeV/u, impinging on a liquid-hydrogen target of 5 cm thickness [15]. The ^{8}He nucleus is expected to be a suitable environment to form the four-neutron system in a ground-state resonance. The reaction process described above allows for a very clean investigation of its properties due to the fact that final-state interactions between the tetraneutron and the outgoing charged particles are basically absent.

The four-neutron energy-spectrum will be deduced from the momenta of all charged particles, i.e. the ^{8}He projectile, the knocked-out ^{4}He, and the target proton via the missing-mass technique to identify the possible resonance and to determine its energy and width. The neutron measurement will allow for a kinematically complete investigation of the reaction and the study of the four-neutron decay properties with lower but sufficient statistics in addition.

Complementary insight into the system of interest will be achieved by a ^{8}He(p,2p)^{7}H measurement, namely the investigation of the ^{7}H ground state and its decay into a triton and four neutrons, performed within the same experimental campaign [16].

Dipole response of n-rich nuclei

In 2017, two experiments were carried out, using Coulomb excitation in inverse kinematics to investigate the dipole response of neutron-rich nuclei. One experiment focused on the low-lying dipole strength of the two- and four-neutron halo nuclei ^{6}He and ^{8}He [17]. After electromagnetic excitation these nuclei mainly decay via two- and four-neutron emission. The ^{6}He breakup has been measured previously at GSI up to around 7 MeV excitation energy [18], while nothing is known so far about the ^{8}He 4n-breakup channel. In this experiment the multi-neutron decay of ^{6}He and ^{8}He, after heavy-ion induced electromagnetic excitation up to increased excitation energies of approx. 15 MeV, has been measured in complete kinematics. The unique combination of the neutron detector NEBULA, the NeuLAND demonstrator, and the high beam intensities available at RIBF made the measurement of the 4n-breakup channel of ^{8}He possible for the first time. A primary ^{18}O beam with an energy of 220 MeV/u was used to produce secondary beams of ^{6}He and ^{8}He with 180 MeV/u. The dipole-strength distribution dB(E1)/dE and the photo-absorption cross section will be obtained from the differential cross section for the E1 excitation dσ(E1)/dE where the excitation energy is reconstructed from the invariant mass. To excite ^{6}He and ^{8}He electromagnetically, a Pb target was used. Additionally, a series of targets covering a wide range of nuclear charges, namely CH_2, C, Ti and Sn, was used to enable a precise study of the nuclear contribution to the cross section. This is especially important for high excitation energies, where the contribution of electromagnetic excitation might not be dominant.

The Coulomb excitation method to study the dipole response of neutron-rich nuclei was also utilized to study ^{50}Ca and ^{52}Ca [19] in an experiment carried out during spring 2017. This experiment is motivated by theoretical predictions, indicating a strong rise of the pygmy dipole resonance strength from ^{48}Ca to ^{54}Ca and its firm correlation with the density dependence of the symmetry energy term of the EOS of neutron matter.

Sπrit TPC – EOS experiment

During 2016, NeuLAND was moved from 0° to 30° with respect to the beamline to measure light charged particles, neutrons and γ-rays from central collisions of neutron-rich and neutron-deficient Sn-isotope systems in experiments studying the nuclear EOS by its proton/neutron and triton/^{3}He yield ratios and flows. The VETO detector in front of NeuLAND played an essential role for distinguishing charged and neutral particles in contrast to other experiments, where neutrons are expected to be dominant and the VETO serves for background discrimination only [5,20].

Structure of n-rich nuclei

It is known that shell structure evolves substantially for nuclear systems with large isospin asymmetry. For bound and unbound systems well known shell closures disappear and new sub-shell closures may appear.

One of the experiments aimed to study the most neutron-rich B and C isotopes, namely ^{21}B and ^{22}C, to establish their level scheme. It is predicted that the sub-shell closure at N=14, which is confirmed in case of the oxygen isotopes, disappears but the increased energy gap at N=16 remains. This can be seen as the origin of the halo character of ^{22}C. In the experiment, the one- and two-proton removal reactions of ^{23}N on a carbon target are analysed. Excitation energies of excited states in both, ^{22}C and ^{21}B, will be reconstructed from the 2n-decay channels to ^{19}B and ^{20}C. Further details about the experiment can be found in [21].

Another experiment from the same campaign investigates neutron-rich neon isotopes. ^{31}Ne is a strongly deformed nucleus located in the so-called island of inversion. In addition, it is also seen as one of the heaviest halo nuclei, which is in particular formed by a dominant p-wave neutron orbiting around the core. Here, ^{31}Ne was studied with exclusive methods at the SAMURAI setup, for details see [22]. The inelastic scattering reaction on a C target, ^{31}Ne(C,X)^{30}Ne+n, and the one-neutron removal reaction on ^{32}Ne were employed to study the neutron-unbound excited states. In addition, the Coulomb breakup reaction was studied in terms of the invariant-mass analysis.

Nuclear shell-structure information is also deduced from spectroscopy of bound excited states. The “Shell Evolution And Search for Two-plus energies At RIBF”

 DOI:10.15120/GR-2018-1

(SEASTAR) project studies new 2^+ excitation energies in a wide range of the neutron-rich nuclei. The 3rd campaign in 2017 focused on the medium-mass nuclei around neutron-rich Ca isotopes and many reaction channels were observed. The combination of the NeuLAND demonstrator and NEBULA allows to construct the invariant-mass above the neutron-decay thresholds.

Figure 3: The NeuLAND demonstrator (oversize silver box) and its electronics (blue box) arriving at GSI after being transported back from RIKEN, Japan.

Summary

During this very fruitful experimental campaign the NeuLAND demonstrator with its 800 read-out channels showed a very good reliability in operation and excellent performance, exhibiting its design goals. While the analysis of the data is underway, the demonstrator was delivered back to GSI in autumn of 2017, see Figure 3. It is now being integrated into the NeuLAND startup version for the experimental campaign at GSI in 2018/19.

Acknowledgments

We would like to thank the RIBF accelerator and BigRIPS teams for the excellent beam-preparation work.

References

[1] NeuLAND@R3B: A Fully-Active Detector for Time of Flight and Calorimetry of Fast Neutrons, NeuLAND Technical Design Report, https://edms.cern.ch/document/1865739/1
[2] T. Nakamura and Y. Kondo, Large acceptance spectrometers for invariant mass spectroscopy of exotic nuclei and future developments, NIM B 376 (2016) 156–161
[3] Y. Kondo et al., Calibration methods of the neutron detector array NEBULA, RIKEN Accel. Prog. Rep. 45, 131 (2012)
[4] T. Kobayashi et al., SAMURAI spectrometer for RI beam experiments, NIM B 317, 294 (2013)
[5] K. Boretzky et al., NeuLAND – from the demonstrator to the start version, GSI Scientific Report 2016 (2017) p.207-210, 10.15120/GR-2017-1
[6] J. Kahlbow et al., RIKEN Accel. Prog. Rep. 49 (2017)
[7] J. Kahlbow et al., Efficiency study of the NeuLAND demonstrator, GSI Scientific Report 2016 (2017) p.211, 10.15120/GR-2017-1
[8] Y. Kondo et al., Phys. Rev. Lett. 116, 102503 (2016)
[9] Y. Kondo et al., RIKEN Accel. Prog. Rep. 49 (2017)
[10] Z. Kohley et al., Phys. Rev. Lett. 110, 152501 (2013)
[11] J. Kahlbow et al., NIM A 866 (2017) 265-271
[12] C. Caesar et al., RIKEN Accel. Prog. Rep. 50 (2017)
[13] D.R. Tilley et al., Nucl. Phys. A 541, 1104 (1992)
[14] K. Kisamori et al., Phys. Rev. Lett. 116, 052501 (2016)
[15] F. Schindler et al., Investigation of the tetraneutron by quasi-free α-knockout from ^{8}He, submitted to RIKEN Accel. Prog. Rep. 51 (2018)
[16] F. M. Marqués, Z. Yang et al., Many-neutron systems: search for superheavy ^{7}H and its tetraneutron decay, submitted to RIKEN Accel. Prog. Rep. 51 (2018)
[17] C. Lehr et al., Low-energy dipole response of the halo nuclei ^{6,8}He, submitted to RIKEN Accel. Prog. Rep. 51 (2018)
[18] T. Aumann et al., Phys. Rev. C 59, 1252 (1999)
[19] Y. Togano et al., Electric dipole responses of ^{50}Ca and ^{52}Ca, submitted to RIKEN Accel. Prog. Rep. 51 (2018) and references therein
[20] I. Gasparic et al., RIKEN Accel. Prog. Rep. 50 (2017)
[21] N. Orr et al., RIKEN Accel. Prog. Rep. 50 (2017)
[22] T. Tomai et al., RIKEN Accel. Prog. Rep. 50 (2017)

Experiment beamline: other: RIBF, RIKEN
Experiment collaboration: other: R3B-NeuLAND-SAMURAI
Experiment proposal: none at GSI
Accelerator infrastructure: other: RIBF, RIKEN
PSP codes: 1.2.5.1.2.5
Grants: This work was supported by the Deutsche Forschungsgemeinschaft through Grant No. SFB 1245, the BMBF Verbundforschung contracts NuSTAR.DA 05P15RDFN1, 05P15PKFNA and 05P15RFFN1, the Croatian Science Foundation (CSF) project SR-ETNo, HIC for FAIR, and NN114454 (NKFIH)
Strategic university co-operation with: Darmstadt, Frankfurt-M

A silicon vertex tracker for the SAMURAI19 experiment at RIKEN

F. Dufter[1], T. Aumann[2], M. Böhmer[1], R. Gernhäuser[1], S. Paschalis[2,3], S. Reichert[1], D. Rossi[3], M. Sasano[4] for the R³B-NeuLAND-SAMURAI collaboration

[1]Physik-Dept., Technische Universität München, Germany; [2]Physics-Dept., Technische Universität Darmstadt, Germany;[3]University of York, United Kingdom;[4]RIKEN, Nishina Center for Accelerator-Based Science, Japan

The SAMURAI19 [1,2] experiment at the RIKEN RIBF aims for producing *4n* ground-state resonances with the ^{8}He(p,pα)4n quasi-free scattering reaction at large momentum transfers at beam energies of 156 *A*MeV. A 5 cm long liquid-hydrogen target (MINOS) with a diameter of 4 cm was used to achieve a luminosity of ~ 10^{28} cm^{-2}s^{-1}. For missing-energy reconstruction, the momenta of all particles are measured with high accuracy.

To get the best energy and track reconstruction using such a thick target, a silicon vertex tracker was developed by TUM and RIKEN. The tracker is placed in a vacuum chamber (49 cm x 36 cm x 29 cm) and records the hits of charged particles in six layers of silicon detectors, allowing to track the produced particles, their opening angle and the position of the vertex. The chamber was drilled from a single aluminium block to reach a vacuum of 10^{-4} Pa. It features in total six data feedthroughs, a newly designed connection to the LH_2 target and a 125 µm thick kapton window for the beam exit. The chamber is mounted on a rail system for fast and easy setup.

The detector system with X and Y readout capabilities consists of six single sided silicon strip detectors (AC coupled) with an active area of 5x8 cm^2 each and a thickness and pitch size of 100 µm developed in a RIKEN cooperation with Hamamatsu. Two SSD's each were combined in three water-cooled stations at distances of 0.6 cm, 12.6 cm and 24.6 cm with respect to the end of the target cell. A detector station is depicted in Fig. 1. The Y and X sectors are closely placed with a distance of 3 mm only on top of each other to optimize the spatial resolution.

The 3708 detector segments are all individually read out by 60 ASIC APV25S1 chips [3]. The multiplexed analog data are then digitalized by an ADCM module developed at TUM. The digital data are collected through a single TRB3 board developed at GSI [4]. Synchronization with the BABIRL-DAQ is done with a 40 MHz time stamp distribution, which is used for other parts of the experiment.

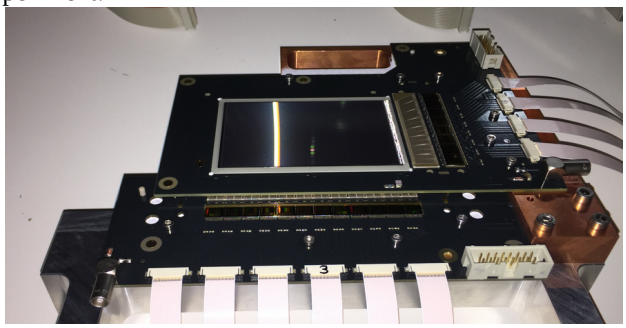

Figure 1: One detector station with attached data cables. The Y layer is placed on top of the X layer, both are mounted on the same cooling frame.

As a first step in the analysis, the detectors are calibrated with proton and ^{6}He calibration beams. Due to the typical electronics-noise figure of ENC ~ 7 keV a single-channel energy threshold of 38 keV was used to reduce event multiplicities. The average energy loss of a proton from the reaction of interest in the detector is in the order of 60 keV per silicon layer only while signals from α-particles may exceed the ASIC's analogue range, which is limited to about 8 MIPs (Minimum ionizing particle) only. To separate α-particles from the reaction from ^{8}He projectiles, which pass all detector planes at a high rate, a sophisticated pulse-shape algorithm is applied.

The ADCM samples the shaper signals of triggered events with three samples in 150 ns and allows therefore to improve the data purity [5]. In Fig. 2 the relations among the three consecutive samples are compared with each other. Unaffected events should appear on the lower right quadrant.

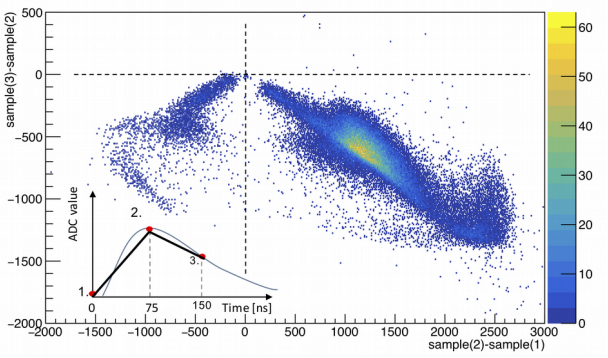

Figure 2: Comparison between the sample differences from shaper signals. Events with an ADC-value < 30 channels are neglected. Events in the lower left quadrant are influenced by beam particles. The inset depicts a shaper signal while the marked points resemble points of sampling schematically.

Hits in all three detector stations are sorted by their energy and combined to identify particles and their tracks. Events with two particle tracks are used to determine a reaction vertex. We deduced an average transverse vertex resolution of $\sigma_{x,y}$ ~ 60 µm. The resolution along the beam direction is σ_z ~ 1 mm due to the small opening angle of the reaction residues.

As a next step, we will further investigate the detection efficiency, hit multiplicities, transverse momenta and the tracking towards the SAMURAI detectors.

We especially thank Michael Traxler and Jan Michel from the TRB3 team of GSI for their continuous help and support of this work.

 DOI:10.15120/GR-2018-1

References

[1] S. Paschalis, S. Shimoura et al.: RIBF Proposal NP1406-SAMURAI19
[2] F. Schindler et al. RIKEN Accel. Prog. Rep. 50, 2017
[3] M.J. French et al. NIM A 466/2 359-365, 2001
[4] M. Traxler et al.: TRB3 Documentation, "https://hades-wiki.gsi.de/cgi-bin/view/DaqSlowControl/TDCReadoutBoardV3"
[5] F. Dufter et al. RIKEN Accel. Prog. Rep. 50, 2017

Experiment beamline: other, RIBF, RIKEN
Experiment collaboration: other: R3B-NeuLAND-SAMURAI
Experiment proposal: none at GSI, RIBF Proposal NP1406-SAMURAI19
Accelerator infrastructure: other: RIBF, RIKEN
PSP codes:
Grants: DFB grant SFB 1245, BMBF 05P15WOFNA
Strategic university co-operation with: contract Nr. TMLFRG1316

Tests of CALIFA Barrel modules at CCB in Kraków

J. Park[1], B. Heiss[2], A.-L. Hartig[3], H. Alvarez-Pol[4], G. Bruni[5], E. Casarejos[6], J. Cederkäll[1], D. Cortina-Gil[4], P. Díaz Fernández[5], D. Galaviz[7], R. Gernhäuser[2], P. Golubev[1], A. Heinz[5], H. T. Johansson[5], P. Klenze[2], A. Knyazev[1], T. Kröll[3], T. Nilsson[5], A. Perea[8], H.-B. Rhee[3], O. Tengblad[8], P. Teubig[7], M. Zieblinski[9], for the CALIFA working group of the R[3]B collaboration

[1]Lund University, [2]TU München, [3]TU Darmstadt, [4]University of Santiago de Compostela, [5]Chalmers University of Technology, [6]Universidade de Vigo, [7]LIP Lisbon, [8]CSIC Madrid, [9]IFJ PAN Kraków

CALIFA (CALorimeter for In-Flight gamma-ray and pArticle detection) [1] is dedicated to the detection, tracking and energy determination of light charged particles and γ rays emerging from R^{3}B experiments. Significant progress has been made on the Barrel section [2] of CALIFA, which consists of ~2000 CsI(Tl) scintillator crystals that provide a high angular resolution needed for effective Doppler corrections.

For the Phase-0 experiments at GSI in 2018, a substantial part of the CALIFA Barrel detectors will be installed and operated in the Demonstrator [3] configuration. An extensive preparatory work in detector performance, stability and data acquisition is required to provide a sound and effective experimental campaign at GSI. To that end, in-beam tests at the Bronowice Cyclotron Center (CCB) at IFJ PAN in Kraków were carried out. The cyclotron at CCB provided proton beams with energies up to 225 MeV, which enabled experiments for (p,2p) quasifree scattering (QFS) reactions on stable targets.

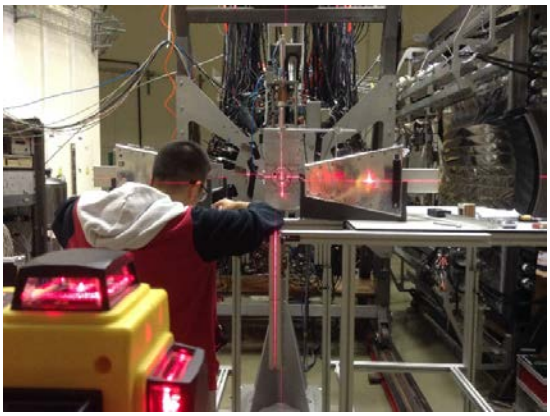

Figure 1: Detectors seen during mounting at CCB for the (p,2p) experiment. Three CALIFA Barrel petals (one placed below the target later), two DSSSD tracking detectors, and one CEPA4 detector were tested.

The experimental setup at CCB is shown in Fig. 1. Two petals were positioned on a horizontal plane with a polar angular coverage of 25° < θ < 58° to detect the scattered particles. One petal was deployed at its nominal CALIFA position (43° < θ < 82°) to detect γ rays. Two double-sided silicon strip detectors (DSSSDs) were also employed as particle trackers. A CEPA4 [4] prototype detector for the CALIFA Forward Endcap was placed at θ ~ 11° for its performance test. Data from the petals and the DSSSD trackers were read out with the MBS system featuring FEBEX3B cards [5]. The calibration data from a ^{60}Co γ-ray source was analysed with the UCESB/R^{3}BRoot software [6].

A laminar water jet, with a small diameter of 0.46 mm was used to provide well-defined tracking correlations for the reactions at the target, and give an energy straggling below the expected resolution limit for the total energy reconstruction of the scattered protons with CALIFA. Other targets such as graphite, polypropylene, ^{112,124}Sn and ^{208}Pb were also irradiated. The proton beam energy was 200 MeV for over 95% of the total beam time. Other beam energies ranged from 70 to 225 MeV.

A preliminary analysis of (p,2p) data from the water target revealed a γ-ray peak at 6.3 MeV (see Fig. 2), corresponding to the known transition from the first excited 3/2$^-$ state to the 1/2$^-$ ground state in ^{15}N. More sophisticated energy calibration, event selection cuts and simulations are being developed to refine and extend the analysis to the data from other targets. We acknowledge the local support at CCB with logistics and beam delivery.

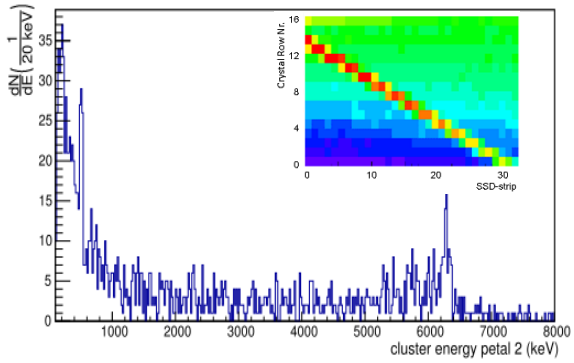

Figure 2: γ-ray energy spectrum following (p,2p) reactions on the water target. The 6.3-MeV transition in ^{15}N is clearly visible. The inset shows the proton tracking data from a DSSSD-petal pair used in the event selection cut.

References

[1] D. Cortina-Gil et al., NDS 120 (2014) 99.
[2] H. Alvarez-Pol et al., NIM A 767 (2014) 453.
[3] B. Pietras et al., NIM A 814 (2016) 56.
[4] E. Nacher et al., NIM A 769 (2015) 105.
[5] T. Le Bleis et al., GSI Scientific Report (2013) 201.
[6] D. Bertini, J. Phys. Conf. Ser. 331 (2011) 032036.

Experiment beamline: none
Experiment collaboration: NUSTAR-R3B
Experiment proposal: none
Accelerator infrastructure: CCB at IFJ PAN in Kraków
PSP codes: none
Grants: EU H2020 contract No. 654002, BMBF 05P15WOFNA
Strategic university co-operation with: none

 DOI:10.15120/GR-2018-1

Response and resolution measurements of CALIFA CsI(Tl) detectors

A. Knyazev[1], J. Park[1], H. Alvarez-Pol[2], G. Bruni[3], E. Casarejos[4], J. Cederkäll[1], D. Cortina-Gil[2], P. Díaz Fernández[3], D. Galaviz[5], R. Gernhäuser[6], P. Golubev[1], A.-L. Hartig[7], A. Heinz[3], B. Heiss[6], H. T. Johansson[3], P. Klenze[6], T. Kröll[7], T. Nilsson[3], A. Perea[8], H.-B. Rhee[7], O. Tengblad[8] and P. Teubig[5] for the CALIFA working group of the R3B collaboration

[1]Lund University, [2]University of Santiago de Compostela, [3]Chalmers University of Technology, [4]Universidade de Vigo, [5]LIP Lisbon, [6]TU München, [7]TU Darmstadt, [8]CSIC Madrid

A test bench has been constructed for acceptance test of CsI(Tl) detector elements for the CALIFA calorimeter [1] for R^{3}B. A detector module consists of an APD and a long tapered CsI(Tl) crystal wrapped in ESR foil. The geometry is a consequence of the requirement to have high granularity, to achieve the necessary angular resolution for Doppler correction, and the need to be able to register high-energy charged particles that emerge from the reactions.

Figure 1: The test bench for CALIFA Barrel crystals in the Lund university detector laboratory. Batches of up to 32 crystals can be scanned per test with a rate of 5.2 detectors per hour.

An inherent challenge with such a geometry is that the combined effects of absorption and focusing of optical photons influence the scintillation light output, and thus the signal amplitude for events occurring at different depths in the crystal. In order to ensure that these effects do not influence the overall resolution of the detector module, it is necessary to measure the response to ionizing radiation along the crystal axis.

To accomplish this, a test stand consisting of an insulated dark box, in which up to 32 crystals can be mounted for performance tests, has been constructed. The temperature in the enclosed volume of the setup can be regulated with the help of a Peltier element and a temperature sensor feedback loop. The crystals are scanned using two separate scanning heads mounted on a commercial XY-table using a collimated ^{137}Cs source for light output non-linearity tests, or alternatively an uncollimated ^{22}Na source for energy resolution measurements. Dedicated software has been developed to operate the XY-table, the temperature regulation, the bias supply and to automatically analyse the registered spectra to extract the resolution and light output nonlinearity (LON) along the crystal axis.

Readout of the signals from the modules is done using the standard readout chain planned for CALIFA. The chain comprises a Mesytec MPRB-32 preamplifier, with integrated detector bias supply, and a FEBEX3B sampling digitizer [2]. The data from from the digitizer is fed to an acquisition system based on the Multi Branch System (MBS).

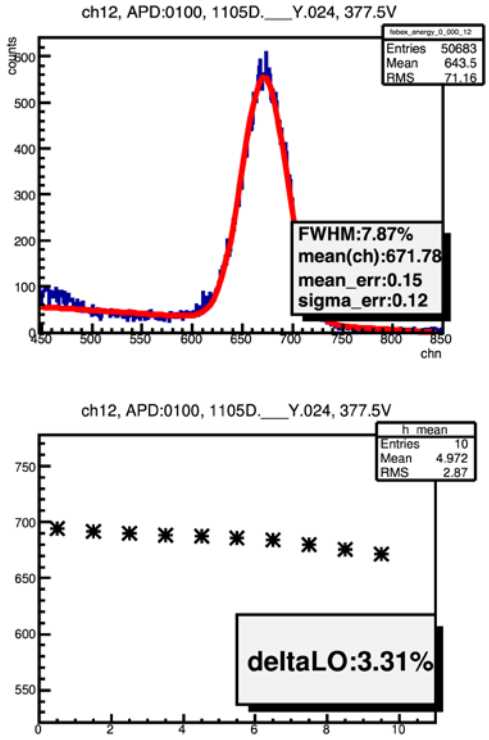

Figure 2: Typical response of a test scan showing, in the top panel, an automatically fitted response of the 662 keV gamma ray from ^{137}Cs source and the change in position of the centroid of this peak as a function of the source position.

The typical crystal scanning rate is 5.2 detectors per hour for a non-linearity test, using 10 points along the crystal axis and 2 minutes per measurement point; and 13.8 detectors per hour for resolution measurements. To date ca 600 crystals have been tested using the test bench, corresponding to nine CALIFA petals of 64 crystals, that can be used in Phase-0 experiments in the fall of 2018.

References

[1] D. Cortina-Gil et al., NDS 120 (2014) 99.
[2] Bendel, M., Gernhäuser, R., Henning, W.F. et al. Eur. Phys. J. A (2013) 49: 69.

Experiment beamline: R3B
Experiment collaboration: NUSTAR-R3B
Experiment proposal: none
Accelerator infrastructure: FRS
PSP codes: 1.2.5.1.2.3.1.1.5.
Grants: VR-822-2012-4550**,** BMBF 05P15WOFNA
Strategic university co-operation with: none

 DOI:10.15120/GR-2018-1

PMT saturation due to large dynamic range

G. Bruni[1], P. Díaz Fernández[1], H.T. Johansson[1], A. Heinz[1], T. Nilsson[1], O. Tengblad[2], H. Alvarez-Pol[3], J. Cederkäll[5], E. Casarejos[6], D. Cortina Gil[3], D. Galaviz Redondo[7], R. Gernhäuser[4], B. Heiss[4], P. Klenze[4], P. Golubev[5], A.-L. Hartig[8], A. Knyazev[5], T. Kröll[8], J. Park[5], A. Perea[2], H.-B. Rhee[4], P. Teubig[7], M. Zieblinski[9], for the CALIFA /R³B working group.

[1]Chalmers Tekniska Högskola, Göteborg, Sweden; [2]Instituto de Estructura de la Materia, CSIC, Madrid, Spain, [3]University of Santiago de Compostela, Santiago de Compostela, Spain;[4]Technische Universität München, Garching, Germany;[5]Lund University, Lund, Sweden; [6]University of Vigo, Vigo, Spain;[7]FCU Lisbon, Lisbon, Portugal;[8]Technische Universität Darmstadt, Darmstadt, Germany;[9]Institute of Nuclear Physics, Kraków, Poland.

Phoswich detectors, composed of optically coupled $LaBr_3$ and $LaCl_3$ scintillating crystals will be used at the most forward angles in the CALIFA calorimeter at the R³B setup [1]. These crystals offer ideal conditions for detection of gamma radiation, as well as for charged particles at relativistic energies, with high efficiency, and excellent energy and time resolution [2-5].

The goal of this study is to verify the performance of the CEPA4 prototype, consisting of four phoswich crystals with individual photo-multiplier tubes (PMTs) for readout, attached to the $LaCl_3$. A particular challenge, especially for the PMTs and read-out electronics, is the large dynamic range needed to cope with signals from gamma radiation (up to 20 MeV) and charged particles (up to 270 MeV). The TDR [5] specifies the use of the Hamamatsu R7600U-200 PMTs. These tests have been performed using the commercial digitisers CAEN DT5751 and DT5730.

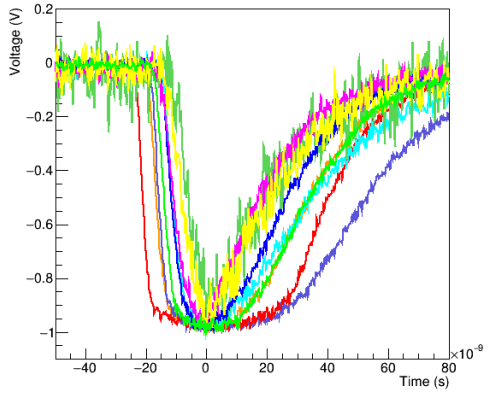

Figure 1: Photomultiplier tube signals of cosmic muons, normalized to the maximum amplitude, showing saturation.

The investigations performed with the crystals revealed a good energy and time resolution for both gammas and muons. While it is relatively easy to obtain good energy resolution for either gamma rays or protons by selecting an appropriate bias voltage, it was not possible to find a bias voltage, which allowed for a good resolution for both, because the PMTs displayed clear signs of saturation already around 20 MeV of deposited energy (see Figure 1). As a first attempt at improving this situation, a new base was used for the R7600U-200 PMTs, providing also a second lower-gain signal from the last dynode in addition to the anode readout (with a gain ratio of ~2.5). This was not sufficient. Therefore, a new PMT, R11187, has been tested. Results are shown in Figure 2, where the saturation starts at the same pulse amplitude independently of the applied bias voltage. This indicates that saturation occurs in the final stages of the PMT.

Figure 2: Energy versus pulse amplitude for two high voltages. The degradation of the signals starts at about the same signal amplitude, indicating that saturation occurs in the final stages of the PMT.

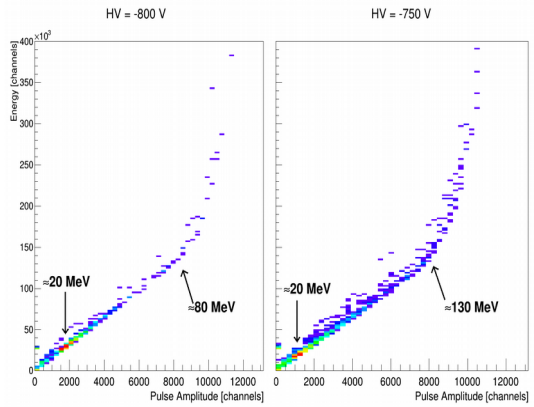

To cope with the large dynamic range we want to implement an improved double read-out with a higher gain ratio between the two branches [6].

References

[1] Technical Design Report for the Design, Construction and Comissioning of the CALIFA Endcap, (2015).
[2] O. Tengblad et al., Nucl. Instr. Meth. Phys. Res. A 704, 19 (2013).
[3] E. Nácher et al., Nucl. Instr. Meth. Phys. Res. A 709, 105 (2015).
[4] M. Mårtensson, Master thesis, Chalmers Univ. Tech. (2013).
[5] G. Bruni, Master thesis, Chalmers Univ. Tech. (2017).
[6] Hongkui Lv et al., Nucl. Instr. Meth. Phys. Res. A 781, 34-38 (2015).

Experiment collaboration: NUSTAR-R3B.
PSP codes: 1.2.5.1.2.3.2
Grants: supported by the Swedish Research Council, ENSAR2 (project Nr. 654002) and BMBF (contract Nr. 05P15WOFNA)
Strategic university co-operation with: contract Nr. TMLFRG1316

The quality assurance test stand for CALIFA APDs

H.-B. Rhee[1], A.-L. Hartig[1], H. Alvarez-Pol[2], G. Bruni[3], E. Casarejos[4], J. Cederkäll[5], D. Cortina-Gil[2], P. Díaz Fernández[3], D. Galaviz[6], R. Gernhäuser[7], P. Golubev[5], A.Heinz[3], B. Heiss[7], H. Johansson[3], P. Klenze[5],A. Knyazev[5], T. Kröll[1], T. Nilsson[3], J. Park[5], A. Perea[8], O. Tengblad[8], P. Teubig[6] , for the CALIFA working group of the R3B collaboration

[1]TU Darmstadt,[2]University of Santiago de Compostela, [3]Chalmers University of Technology, [4]Universidade de Vigo, [5]Lund University, [6]FCU Lisbon,[7]TU München, [8]CSIC Madrid

The quality assurance test stand for the CALIFA APDs aims to prove the functionality of the APDs and to characterize them. It ensures controlled temperature and bias voltage for the APDs during the test [1].
Particularly, the bias voltage of the APDs is readjusted with respect to the temperature to keep the gain constant during the experiment. The main goal of this project is to obtain the temperature coefficients of the tested APDs.

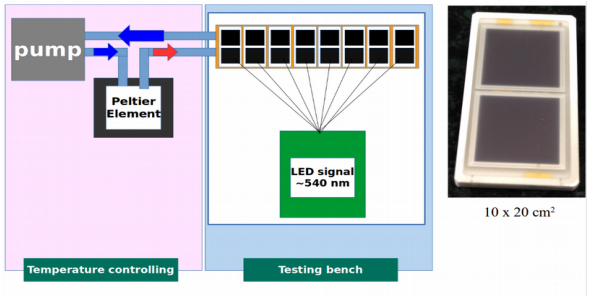

Figure 1: Left: Schematic view of the quality assurance test stand. Right: CALIFA APD (Hamamatsu S8664 series).

Fig. 1 shows a schematic view of the quality assurance test stand. It is divided into two parts: temperature controlling (left) and testing bench (middle). The Mesytec MPRB-16, which is a preamplifier and bias voltage supply for APDs, is chosen to maintain consistency with the electronics of CALIFA. The output of the APDs and the temperature are read by FEBEX3b.
The temperature of the test bench is kept constant by circulating water heated or cooled by peltier units. The temperature of the system is monitored with a NTC thermistor. The testing bench can test 8 APDs simultaneously. The APDs were tested with a pulsed green LED signal (λ_{max} = 520 nm), which is chosen to mimic signals of the CsI(Tl) scintillator.
The test temperature spans the range from 15°C to 25°C. This range includes the working condition required for the CALIFA APDs: 18 ± 1°C. For each temperature step, the gain curve of the APDs as a function of bias voltage is obtained. Fig. 2 shows an example of the gain curve and the energy resolution of the APD for the LED wavelength. In addition, a temperature stability check is necessary to confirm for reliability of the measured data (Fig. 3).
The APDs have a reference voltage for a nominal gain 50. It is the bias voltage that corresponds to gain 50 at 25°C.

Experiment collaboration: NUSTAR-R3B
PSP codes: 1.2.5.1.2.3.1
Grants: BMBF(05P15RDFN1), HIC for FAIR

Fig. 4 shows the comparison between the nominal voltage provided by the manufacturer and the measured one.

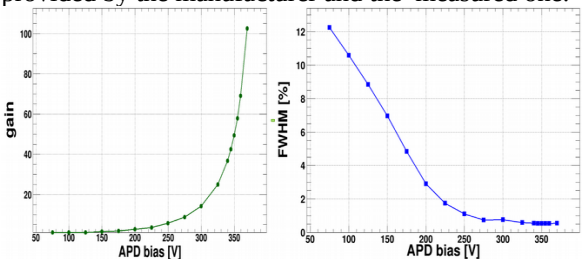

Figure 2: Left: APD gain curve. Right: APD energy resolution for LED signal.

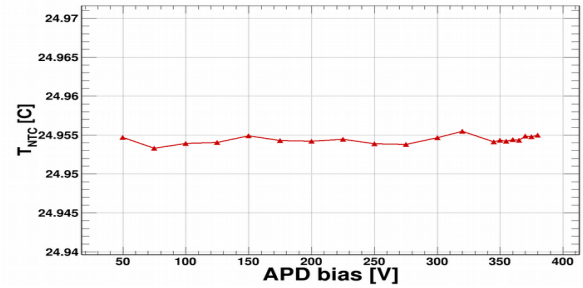

Figure 3: Measured temperature. The temperature of the system is stable within 0.002°C over 20 min. ($T_{peltier}$ = 25°C)

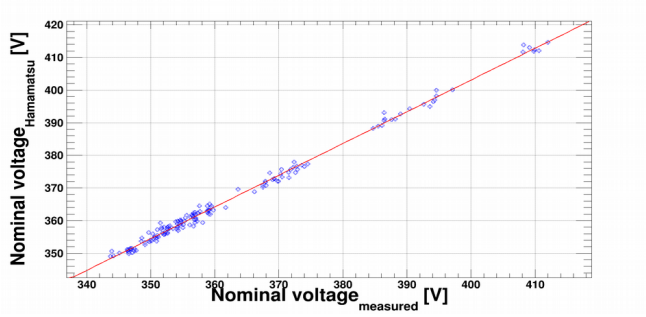

Figure 4: Correlation between the nominal voltage provided by the manufacturer with respect to the measured value.

References

[1] R.S. Gilmore et al., "Avalanche photodiodes as proportional particle detectors", Nucl. Instr. and Meth. A 388, 79 (1997).

Strategic university co-operation with: TU Darmstadt

 DOI:10.15120/GR-2018-1

First measurement of isotopic fission-fragment yields with calorimetric low-temperature detectors

S. Dubey [1,2], A. Echler[1,2], P. Egelhof[1,2], M. Mutterer[1], P. Grabitz[1,2], W. Lauterfeld[2], S. Stolte[2], A. Blanc[3], U. Köster[3], S. Kraft-Bermuth[4], P. Scholz[4], S. Bishop[5], J.M. Gomez-Guzman[5], and F. Gönnenwein[6]

[1]GSI, Darmstadt, Germany; [2]University of Mainz, Germany; [3]Institut Laue-Langevin, Grenoble, France; [4]University of Giessen, Germany; [5]Technical University Munich, Germany; [6]University of Tübingen, Germany

For thermal-neutron induced fission, precise data on fission-fragment yields in terms of mass, nuclear charge, and kinetic energy are of great interest for a better understanding of the fission process, and also required at several stages of the fuel cycle in nuclear reactors. Since more than 3 decades, the recoil mass spectrometer LOHENGRIN at the ILL Grenoble has been a leading instrument for fission fragment studies. Fission fragments emerging from a thin fissile target located close to the high-flux reactor core are separated according to the ratios of E/q and A/q (A = mass of fragment, q = ionic charge) and registered with silicon detectors or ionization chambers. For determining isotopic fragment yields a fairly universal method is the passive absorber technique exploiting the nuclear charge dependent energy loss of fission fragments in an energy degrader [1]. Due to its perfect mass resolution, LOHENGRIN has contributed more complete data sets on mass, nuclear-charge and energy distributions than any other method, with the resolving power for isotopic yields being restricted to the group of light fragment masses. Hitherto, cumulative yields of specific radioactive isotopes in the heavy fragment group have been tackled with the aid of gamma spectroscopy or, formerly, determined by radiochemical methods.

In the present work we have applied a new experimental approach to determine isotopic yields at LOHENGRIN by the passive absorber method using an array of calorimetric low-temperature detectors (CLTDs) instead of an ionization chamber for the residual energy measurement. Due to their principle of operation, CLTDs provide good energy linearity and resolution for the spectroscopy of heavy ions at low energies [2] and are, thus, predestined for measuring heavy fission fragments after degradation of a large proportion of kinetic energy. Furthermore, for the first time, stacks of commercially available silicon nitride (SiN) membranes were used as degrader material, favourably replacing the previously used Parylene-C plastic foils.

The detector array used in the present experiment is built-up from 25 individual pixels, made of sapphire chips of 430 µm thickness, with a total active area of 15x15 mm^2, operated at 1.5 K temperature in a windowless 4He-bath cryostat. The SiN absorber stacks of 16 x 10 mm^2 area were positioned closely in front of the CLTDs by a rotatable sample changer with six positions for SiN stacks of various thicknesses (Figure 1). This arrangement was intended to optimize the setup with respect to transmission, resolution and flexibility for measurements in different mass and energy ranges.

During a measuring period of about 4 weeks we investigated fragment yields in various fragment mass regions

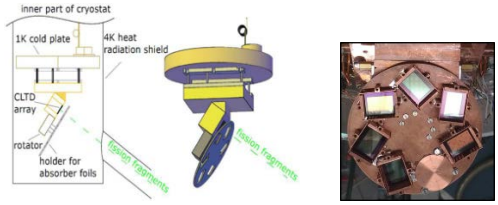

Figure 1: Schematic view of the detector cryostat with CLTD's as residual-energy detector and rotatable sample changer for silicon nitride absorber stacks (right).

for ^{235}U(n$_{th}$,f), ^{239}Pu(n$_{th}$,f) and ^{241}Pu(n$_{th}$,f). As a first topic, we have gained first ever LOHENGRIN data on fractional Z yields in the light-mass group of ^{241}Pu fission. A second topic was the study of light-fragment yields towards mass symmetry, up to A = 112 (113) in $^{241(239)}$Pu(n$_{th}$,f). This permits to elucidate how the local proton odd-even effect develops towards mass symmetry, which is of high interest for the nuclear model description near scission. A further issue was accurately measuring the isotopic fission yields of ^{92}Rb and ^{96}Y from ^{235}U(n$_{th}$,f), ^{239}Pu(n$_{th}$,f) and ^{241}Pu(n$_{th}$,f) since the decay of these isotopes is a main contributor to the integral reactor antineutrino spectra above 4 MeV that are important for the quantification of the so-called antineutrino anomaly and the postulation of sterile neutrinos. A final topical issue was to elaborate our novel technology for an accurate determination of isotopic yields for the first time also in the heavy fragment group, for selected masses in ^{239}Pu(n$_{th}$,f) up to A = 137. For the heavy fragments, the obtained Z-resolution did not permit to fully resolve individual peaks in the residual energy spectra, but to reliably retrieve fractional isotopic yields by constrained fitting of the overlapping peaks. Figure 2 shows, as example, residual energy spectra and fit results for A = 128 to 130 at 88 MeV, assuming up to three Z constituents. The increasing dominance of the magic proton shell Z = 50 towards symmetry is obvious.

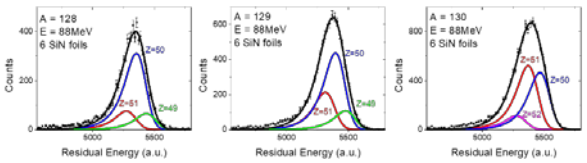

Figure 2: Residual energy spectra of heavy-fragment masses at 88 MeV energy in ^{239}Pu(n$_{th}$,f) from A = 128 to A = 130, with their individual Z constituents.

References

[1] U. Quade et al., Nucl. Phys. A 487, 1 (1988).
[2] S. Kraft-Bermuth, et. al., Rev. Sci. Instr. 80, 103304 (2009).

 DOI:10.15120/GR-2018-1